AD-A048 842 CALIFORNIA UNIV BERKELEY DEPT OF MECHANICAL ENGINEERING F/G 13/8
DUCTILE FRACTURE IN AXISYMMETRIC EXTRUSION AND DRAWING. PART 1.--ETC(U)
JUN 77 C C CHEN, S I OH, S KOBAYASHI F33615-75-C-5151

UNCLASSIFIED AFML-TR-77-96 NL

1 OF 2
AD
A048 842

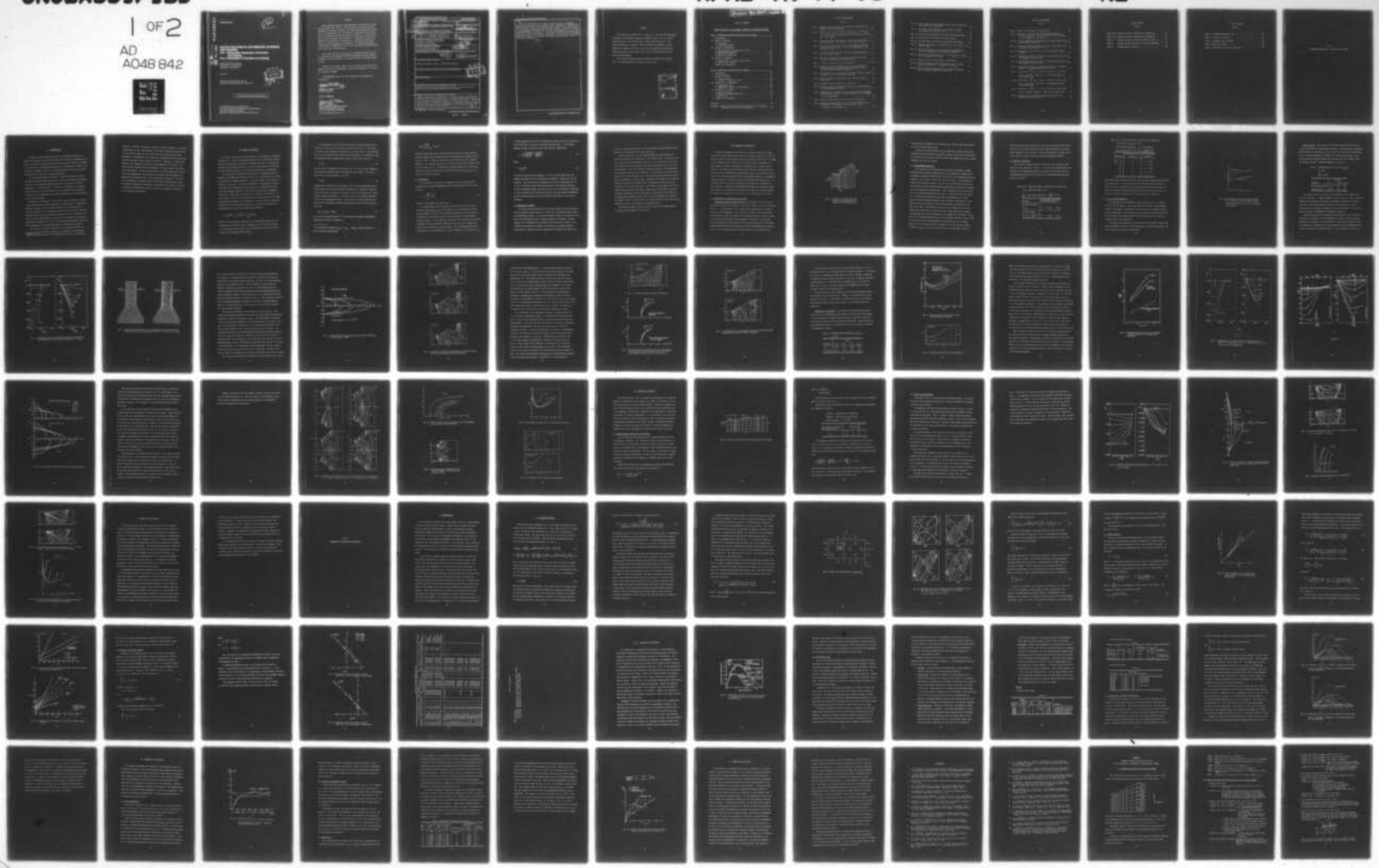

12

AFML-TR-77-96

DUCTILE FRACTURE IN AXISYMMETRIC EXTRUSION AND DRAWING

Part 1 Deformation Mechanics of Extrusion and Drawing

Part 2 Workability in Extrusion and Drawing

MECHANICAL ENGINEERING
UNIVERSITY OF CALIFORNIA
BERKELEY, CALIFORNIA

JUNE 1977

TECHNICAL REPORT AFML-TR-77-96
Final Report for Period March 1976 – March 1977

Approved for public release; distribution unlimited.

AIR FORCE MATERIALS LABORATORY
AIR FORCE WRIGHT AERONAUTICAL LABORATORIES
AIR FORCE SYSTEMS COMMAND
WRIGHT-PATTERSON AIR FORCE BASE, OHIO 45433

NOTICE

When government drawings, specifications, or other data are used for any purpose other than in connection with a definitely related government procurement operation, the United States government thereby incurs no responsibility nor any obligation whatsoever; and the fact that the government may have formulated, furnished, or in any way supplied the said drawings, specifications, or other data, is not to be regarded by implication or otherwise as in any manner licensing the holder or any other person or corporation, or conveying any rights or permission to manufacture, use, or sell any patented invention that may in any way be related thereto.

This report has been reviewed by the Information Office (IO) and is releasable to the National Technical Information Services (NTIS). At NTIS it will be available to the general public, including foreign nations.

Copies of this report should not be returned unless return is required by security considerations, contractual obligations, or notice on a specific document.

This technical report has been reviewed and is approved for publication.

Attwell M Adair for

VINCENT De PIERRE
Project Engineer

FOR THE COMMANDER

Norman M Tallan

NORMAN M. TALLAN
Chief, Processing and
High Temperature Materials Branch
Metals and Ceramics Division
Air Force Materials Laboratory

SECURITY CLASSIFICATION OF THIS PAGE (When Data Entered)

REPORT DOCUMENTATION PAGE

READ INSTRUCTIONS BEFORE COMPLETING FORM

18 19

1. REPORT NUMBER: AFML-TR-77-96
2. GOVT ACCESSION NO.:
3. RECIPIENT'S CATALOG NUMBER: 9
4. TITLE (and Subtitle): 6 DUCTILE FRACTURE IN AXISYMMETRIC EXTRUSION AND DRAWING. Part 1. Mechanics of Extrusion and Drawing Part 2. Workability in Extrusion and Drawing.

 eformation

5. TYPE OF REPORT & PERIOD COVERED: Final Report, Mar[redacted]976-Mar[redacted]977
6. PERFORMING ORG. REPORT NUMBER:
7. AUTHOR(s): 10 C. C. Chen, S. I. Oh [redacted] Shiro Kobayashi
8. CONTRACT OR GRANT NUMBER(s): 15 F33615-75-C-5151
9. PERFORMING ORGANIZATION NAME AND ADDRESS: Department of Mechanical Engineering, University of California, Berkeley, California 94720
10. PROGRAM ELEMENT, PROJECT, TASK AREA & WORK UNIT NUMBERS: 62102F 7351 08-20 16 17
11. CONTROLLING OFFICE NAME AND ADDRESS: Air Force Materials Laboratory, Air Force Systems Command, Wright-Patterson Air Force Base, Ohio 45433
12. REPORT DATE: 11 June [redacted]77
13. NUMBER OF PAGES: 115
14. MONITORING AGENCY NAME & ADDRESS (if different from Controlling Office): 12 126p.
15. SECURITY CLASS. (of this report): Unclassified
15a. DECLASSIFICATION/DOWNGRADING SCHEDULE:
16. DISTRIBUTION STATEMENT (of this Report): Approved for public release: distribution unlimited.
17. DISTRIBUTION STATEMENT (of the abstract entered in Block 20, if different from Report):

18. SUPPLEMENTARY NOTES:
19. KEY WORDS (Continue on reverse side if necessary and identify by block number): Workability, fracture, plastic deformation processes, void growth, matrix method, extrusion, drawing, mechanics, central bursting
20. ABSTRACT (Continue on reverse side if necessary and identify by block number):

This investigation applies theories on flow and fracture in metalworking processes to prediction of workability of materials in axisymmetric bar extrusion and drawing, with special reference to central bursting. Part 1 deals with the determination of deformation mechanics in extrusion and drawing. The matrix method is used as the method of analysis and is shown to be an efficient numerical method which provides useful information on the detailed deformation characteristics for various process variables. (over)

DD FORM 1 JAN 73 1473 EDITION OF 1 NOV 65 IS OBSOLETE

SECURITY CLASSIFICATION OF THIS PAGE (When Data Entered)

400 426

mt

SECURITY CLASSIFICATION OF THIS PAGE(When Data Entered)

In Part 2 the validity of a theory on ductile fracture was examined by experimental data found in the literature. Then, combining the formulation of fracture criteria with the deformation mechanics found in Part 1, the workability of materials in extrusion and drawing was determined. Workability in extrusion was examined for aluminum alloy 2024-T351, using data found in the literature, and experiments of workability in drawing were attempted for SAE 1144 cold-drawn steel to test the prediction. The results of validation were inconclusive. Conclusive validation of the present workability theory in extrusion and drawing awaits more extensive and systematic experimental investigations, as well as theoretical calculations.

SECURITY CLASSIFICATION OF THIS PAGE(When Data Entered)

FOREWORD

This report was prepared by C. C. Chen, S. I. Oh, and Shiro Kobayashi, University of California, Berkeley, California, under U.S.A.F. Contract F33615-75-C-5151. The contract was initiated under Project No. 7351, "Metallic Materials," Task No. 735108, "Processing of Metals," and was administered under the direction of the Air Force Materials Laboratory, Wright-Patterson Air Force Base, Ohio, with Mr. Vincent DePierre as Air Force Project Engineer.

This report discusses research conducted from March 1976 to March 1977. It was submitted by the authors in April 1977.

Preceding Page Blank - Filmed

TABLE OF CONTENTS

DUCTILE FRACTURE IN AXISYMMETRIC EXTRUSION AND DRAWING PROCESSES

LIST OF ILLUSTRATIONS

Part 1

LIST OF ILLUSTRATIONS

Part 2

LIST OF TABLES

Part 1

LIST OF TABLES

Part 2

Part 1

DEFORMATION MECHANICS OF EXTRUSION AND DRAWING

I. INTRODUCTION

In order to apply workability theory to metalworking processes, we must first establish flow and fracture theories. Then, by combining the detailed information on mechanics and the ductile fracture criterion, workability of materials in metalworking processes can be predicted. Based on this prediction, workability control for preventing fracturing can be achieved by selecting the proper set of process parameters.

In the previous report [1]*, theories on flow and fracture in metalworking processes were developed with an emphasis on applying the workability theory to metalworking processes where the occurrence of internal fracturing is a limiting factor. The present investigation is concerned with the application of these theories to the prediction of workability of materials in axisymmetric bar extrusion and drawing, with special reference to center bursting.

Workability of materials is the extent to which materials can deform without forming cracks during a mechanical working process. Workability, therefore, depends on the conditions imposed by the working process. Critical stress and strain conditions involved in the mechanical working processes must be known and should be specified in terms of process variables, such as height reduction, friction at the interface, and workpiece geometries and dimensions. Part I of the present investigation deals with the determination of deformation mechanics in extrusion and drawing.

The role of the detailed mechanics in the workability study is to provide the stress and strain paths at a critical site of a deforming

*Numbers in brackets refer to the references at the end of this report.

material. Therefore, the method of analysis should be capable of accurately determining not only overall quantities involved in metalworking processes, such as forming loads, but also stress and strain distributions during deformation. Furthermore, it is required to determine the stress and strain distributions under various process conditions. Therefore, to justify the approach, the computation involved in the method must be efficient. The matrix method developed by Lee and Kobayashi [2] comes close to fulfilling these requirements. In the previous report, this matrix method was refined and it was demonstrated that the method is effective for the analysis of steady-state processes as well as non-steady-state processes. In the present investigation, the matrix method, with further improvements, is used to determine steady-state deformation characteristics as functions of material property, die-workpiece interface friction, die angle, and reduction in bar extrusion and drawing.

II. METHOD OF ANALYSIS

The basic concepts of the matrix method for rigid-plastic deformation problems are the use of the Lagrange multiplier in a variational formulation and linearization of nonlinear stiffness equations. In the present formulation the dynamic effects, i.e., the inertia effects on the forces and the strain-rate effects on the material properties, are neglected.

For rigid-plastic materials the condition of incompressibility is imposed on the admissible velocity fields. This constraint can be removed by introducing a Lagrange multiplier. Consider a body V whose surface S, consists of S_U and S_T. The body is composed of a rigid-plastic material that obeys the von Mises yield criterion and its associated flow rule, under the boundary conditions, such that the entire body is deforming plastically. Body forces are assumed to be absent in the region V. It can be shown [3] that for the actual solution, the functional (1) becomes stationary with respect to the multiplier λ and the velocity fields that satisfy the velocity boundary conditions on S_U but not necessarily the incompressibility condition (kinematically complete):

$$\Phi = \int_V \bar{\sigma}\dot{\bar{\varepsilon}}\, dV + \int_V \lambda \underset{\sim}{C}^T \dot{\varepsilon}\, dV - \int_{S_T} \underset{\sim}{T}^T \underset{\sim}{U}\, dS, \tag{1}$$

where $\dot{\bar{\varepsilon}}$ is the effective strain-rate; $\bar{\sigma}$, the effective stress; $\underset{\sim}{T}$, the traction vector specified on the boundary S_T; $\underset{\sim}{U}$, the velocity vector; C is the proper vector notation of the Kronecker delta such that $\underset{\sim}{C}^T \underset{\sim}{\dot{\varepsilon}} = 0$ implies the incompressibility condition.

The formulation of the discrete variational problem follows the same procedure as that used in the finite-element method [4], [5]. The body V is divided into M elements interconnected at N nodal points. The approximation of the functional Φ by a function ϕ is performed on the elemental level by replacing U with a kinematically complete distribution, given by

$$\underset{\sim}{U} \simeq \underline{G}\underset{\sim}{u}, \tag{2}$$

where $\underline{G}$ is the interpolation function and $\underset{\sim}{u}$ is the vector whose components are velocities at nodal points associated with the element. The strain-rate vector is then derivable in the form

$$\dot{\underset{\sim}{\varepsilon}} = \underline{B}\underset{\sim}{u}. \tag{3}$$

Assembling the function at the elemental level into an approximate finite-element model over all the elements and applying the stationary condition to the function ϕ, we obtain the stiffness relations consisting of a large system of nonlinear equations. In order to solve the stiffness equations, we adopt the following procedure. The nonlinear stiffness equations were linearized by considering a small perturbation $\Delta\underset{\sim}{u}$ in the velocity vector $\underset{\sim}{u}$, such that

$$\underset{\sim}{u}_{(n)} = \underset{\sim}{u}_{(n-1)} + \Delta\underset{\sim}{u}_{(n)}, \tag{4}$$

for the n-th iteration process.† We then obtain the global perturbation equation for the n-th iteration as

---

†In the actual calculations, $\underset{\sim}{u}_{(n)} = \underset{\sim}{u}_{(n-1)} + \alpha\Delta\underset{\sim}{u}_{(n)}$ is used, where α is the deceleration coefficient.

$$\underset{\sim}{S}_{(n-1)}\left\{\begin{array}{c}\Delta\underset{\sim}{u}\\ \hdashline \underset{\sim}{\lambda}\end{array}\right\}_{(n)} = \underset{\sim}{R}_{(n-1)}. \tag{5}$$

Specific formulations for the matrix $\underset{\sim}{S}$ and the vector $\underset{\sim}{R}$, using a quadrilateral element with a bilinear velocity distribution, are presented elsewhere [1], [6]. It must be noted that, since the method is an iterative process, it is necessary to provide an initial guess for the velocity field $\underset{\sim}{u}_0$ (but no need for λ). The solution of linear equation (5) yields $\Delta\underset{\sim}{u}_{(n)}$ close to zero and a proper value of the mean stresses $\underset{\sim}{\lambda}_{(n)}$, if $\underset{\sim}{u}_{(n-1)}$ is close to the actual solution.

A. Convergence

In the previous studies the convergence of the solution has been measured by the quantity $\|\Delta\underset{\sim}{u}\|/\|\underset{\sim}{u}\|$, where the Euclidean vector norm is defined by

$$\underset{\sim}{u} = \sqrt{\sum_{i=1}^{N} |\underset{\sim}{u}_i|^2}, \tag{6}$$

where N = total number of nodal points.

The convergence criterion requires that the error norm at the n-th iteration ($\|\Delta\underset{\sim}{u}_{(n)}\|/\|\underset{\sim}{u}_{(n-1)}\|$) be less than that at the previous iteration This convergence criterion, with suitable selections of the deceleration coefficient α, has worked out well for the solutions of various metal-working problems. At the same time, however, it was realized that solution divergence has been indicated according to this criterion, although the solution was converging in its true sense. This can apparently be seen, particularly for a function which is not well behaved. In this case, the

criterion resulted in the use of unnecessarily small values of the deceleration coefficient, and thus in increased computing time. In the present program, instead of the error norm, the quantity f defined by

$$f = \sqrt{\sum_m \left\{ \left(\frac{\partial \tilde{\phi}^{(m)}}{\partial \underset{\sim}{u}^{(m)}} \right)^2 + \left(\frac{\partial \tilde{\phi}^{(m)}}{\partial \lambda^{(m)}} \right)^2 \right\}} \tag{7}$$

where

$$\Phi \cong \sum_m \tilde{\phi}^{(m)} \tag{8}$$

is utilized for solution convergence. In Eq. (7), the superscript (m) denotes the values of the m-th element and summation is made over all the elements. The criterion for convergence now is that the magnitude of f at the n-th iteration be less than the magnitude at the previous iteration. In this convergence scheme, the proper value of the deceleration coefficient at each iteration can be selected efficiently from the previous information on the function behavior and the convergence requirement at the current iteration.

B. Rigid-body treatment

The matrix method described in this section applies only if the entire body is deforming plastically and no rigid zone or unloading exists during the deformation process. In practical problems, however, situations do arise where the rigid zone as well as rigid unloading are involved. If these regions of no deformation are contained within the control volume V, the extremum principles do not apply to the problem of obtaining internal distributions. There are several approaches to handling this difficulty,

but a most effective technique is one which involves the approximate determination of the boundary of a nearly rigid zone.

A nearly rigid zone can be characterized by its very low value of effective strain rate in comparison to the deforming body. During the iteration process for an incremental solution over the entire body, the effective strain-rate in the possible rigid region approaches zero as the solution converges. Since the effective strain-rate appears in the denominator of the stiffness matrix S, the component of the normalized stiffness matrix will tend to become infinity if the nodal point associated with this component is contained in the rigid zone. Therefore, the elements for which the effective strain-rate is smaller than a certain value (say, 0.0001) are considered to be in the rigid zone. The effective strain-rates of the elements lying inside the rigid zone are then kept at this value in the perturbation relationship, and the iteration is continued for the solution in the plastically deforming region until a desired convergence is achieved. It should be noted, of course, that the converged solution gives the stress distribution only in the plastically deforming region.

The complete program of this improved version of the matrix method is listed in the appendix of this report.

III. ANALYSIS OF EXTRUSION

Several investigators have analyzed the extrusion process by using the finite-element method, mostly by elastic-plastic analysis [7], [8], [9]. However, almost all the analyses have been performed for the case of loading of the workpiece that fits the die and container and of extruding it a small amount, instead of extruding the workpiece until a steady state is reached. The exceptions are the work by Lee, Mallett, and Yang [10] for the plane-strain extrusion with frictionless curved dies using the elastic-plastic finite-element method and the rigid-plastic analysis of axisymmetric extrusion through frictionless conical dies by Shah and Kobayashi [6]. In the latter work, the authors investigated a possibility of applying the matrix method to steady-state metalworking processes and demonstrated that the analysis of a steady-state extrusion can be made by the matrix method. The analysis of extrusion in this section is an extension of this work.

A. Computational conditions and procedures

Boundary conditions and mesh system The boundary conditions and the mesh system used for the analysis of extrusion through conical dies are shown in Fig. 1. The material in the container moves axially with the uniform velocity of unit magnitude. The container is assumed to be frictionless, and along the conical die surfaces, the tangential traction, which is equal to the frictional stress at the die-workpiece interface, is prescribed. The extruded material moves axially with the uniform velocity of the magnitude determined from the area reduction and the incompressibility relationship. Also, no traction acts along the surfaces of the extruded part.

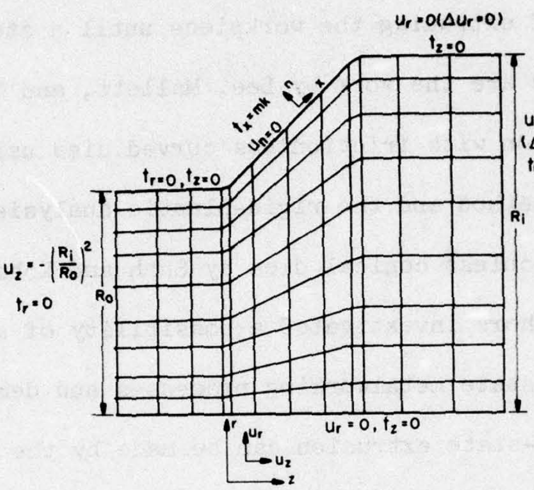

Fig. 1 Boundary conditions and mesh system for steady-state axisymmetric extrusion analysis.

Along the axis of symmetry, the conditions are that the shear traction and the radial velocity must vanish.

It must be noted here that the die corners were slightly modified by connecting the two material nodal points located closest to the die corners. This modification was made in order to avoid high singularity of the velocity components near the die corners.

B. Work-hardening materials

In the analysis of a non-steady-state process, the effect of work-hardening can be readily incorporated into the analysis by computing the incremental strains and modifying the flow stress at each deformation step according to the increase in the total effective strain. In the analysis of steady-state processes, however, the flow stress distribution must be consistent with the final effective strain distribution according to the material's work-hardening characteristics. This requirement can be achieved by using the following computational procedure. During the iteration process for a converging solution, the flow lines corresponding to the latest velocity field are constructed after each iteration. The network of grid distortions and the effective strain distributions are determined from these flow lines. The effective strains for all elements are then interpolated from these values, and using a given stress-strain relationship, corresponding flow stress distributions for elements are determined. Using this new flow stress distribution, the next iteration for the velocity field is carried out and the same procedure is repeated until the converged solution for the velocity field is obtained. Since the solution depends not only on $\underset{\sim}{u}_{(n-1)}$, but also on the flow stress distribution, when the

velocity solution has converged, the flow stress distribution and effective strain distribution also match each other according to the stress-strain behavior of the material. Thus the convergence of velocity solutions gives the correct solution for the work-hardening material.

C. Extrusion conditions

The extrusion process conditions under which the computation was carried out are summarized in Table 1. Since the final solution for the extrusion with nonhardening material was used as the initial guess for work-hardening materials, the results for non-work-hardening materials are also presented.

Table 1(a): Extrusion process conditions for computation.

α (die semi-cone angle) = 30^o

$\frac{R_i}{R_0} = 2.366$, area reduction $1 - (\frac{R_0}{R_i})^2 = 0.82$

Material	Die-workpiece interface frictional stress f		
Non-work-hardening			
$\bar{\sigma} = Y_0$	0,	$0.2Y_0$,	$0.4Y_0$
SAE 1112 steel			
$\bar{\sigma} = Y_0(1 + \frac{\bar{\varepsilon}}{0.3})^{0.25}$	0,	$0.2Y_0$,	$0.4Y_0$

Table 1(b): Extrusion process conditions for computation.

α (die semi-cone angle) = 45°

Work-hardening material: al alloy 2024-T351

$\bar{\sigma} = Y_0 \cdot 2.202(\bar{\varepsilon})^{0.1675}$ or $Y_0(1 + \frac{\bar{\varepsilon}}{0.01021})^{0.171}$

Reduction	Non-work-hardening friction f	Work-hardening friction f
$\frac{R_i}{R_0} = 1.25$	0	0 , $0.4Y_0$
1.6	0	0 , $0.4Y_0$
1.8	-	0 , $0.4Y_0$
2.0	0	0 , $0.4Y_0$
2.4	0	- , -

The stress-strain curves for SAE 1112 steel and for aluminum alloy 2024-T351 are shown in Fig. 2. The calculations for SAE 1112 steels are mainly to find the effect of friction on the deformation characteristics, while the cases for al alloy 2024-T351 emphasized the effect of area reduction, as well as the effect of friction, on the deformation in extrusion.

D. Results and discussion

The computation was performed for each solution until the accuracy of $f^2 = 10^{-5}$ was reached. This corresponds to the error norm of $\|\Delta \underset{\sim}{u}\| / \|\underset{\sim}{u}\|$ = 0.00008. The number of iterations to reach the above convergence depends on the initial guess, but by using the best available initial guess for the velocity field, the average number of iterations required for the final solution was 25 $\sim$ 30 iterations.

The results were obtained for average extrusion pressure, normal pressure distribution on the die, grid distortions, velocity distributions, and stress, strain, strain-rate distributions.

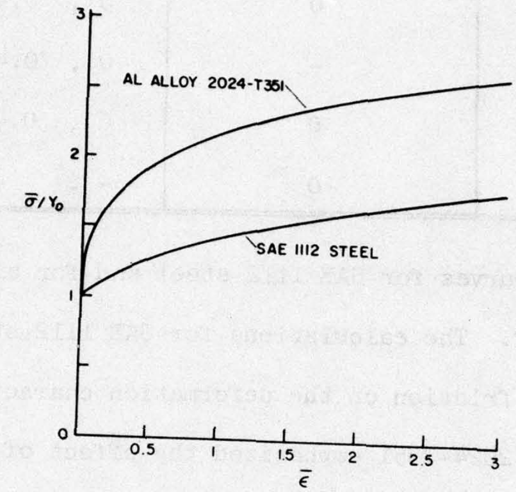

Fig. 2 Stress-strain curves for SAE 1112 steel (Y_0 = 79,800 psi; 550.21 MN/m^2) and for aluminum alloy 2024-T351 (Y_0 = 47,778 psi; 329.42 MN/m^2).

SAE 1112 steel The stress distributions computed differs from the actual distribution by a hydrostatic component. This hydrostatic component was determined by setting the net axial force along the exit boundary equal to zero, and the magnitude of stresses were corrected accordingly. The average extrusion pressures were then determined from the stresses along the entrance boundary. They are summarized in Table 2.

Table 2: Average extrusion pressure, p_{ave}/Y_0.

$\alpha = 30°$

$\frac{R_i}{R_0} = 2.366$

Material	Friction 0	$0.2Y_0$	$0.4Y_0$
Non-work-hardening	1.755	2.292	2.784
SAE 1112 steel	2.425	3.148	3.665

The general trend of the velocity distributions is the same for all friction conditions. A typical example is given in Fig. 3. The two velocity components are plotted as functions of the radial coordinate at various locations in the axial direction within the deformation zone. These distributions are in general agreement with the measurements in the visioplasticity study of axisymmetric extrusion of lead [11].

Detailed differences of deformation characteristics, due to material properties and friction at the die-workpiece interface, are more clearly indicated, for example, in grid distortions. The steady-state grid distortion patterns are compared for non-work-hardening and work-hardening cases for the two friction conditions in Fig. 4. With reference to Fig. 4(a),

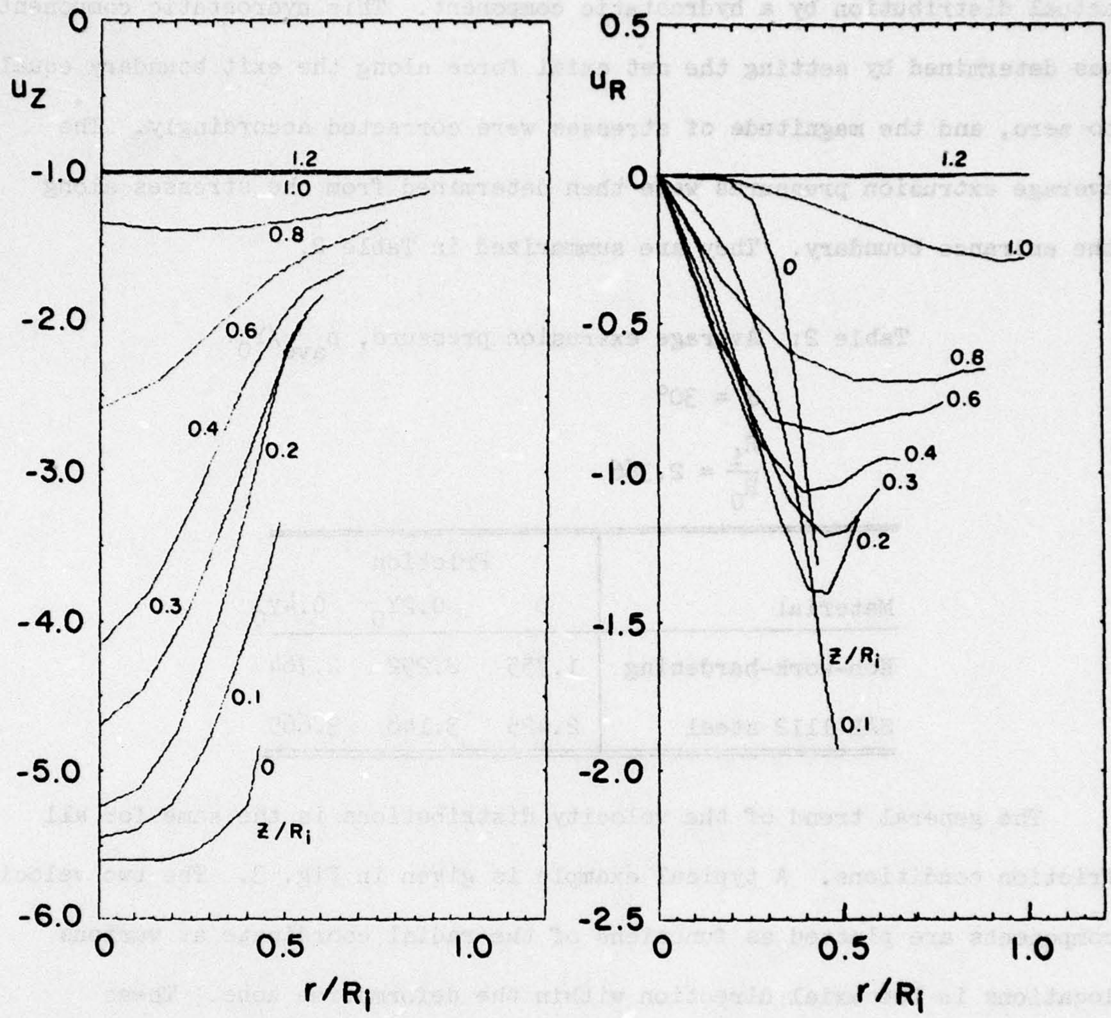

Fig. 3 Computed velocity distributions for SAE 1112 steel under the conditions $\alpha = 30°$, $R_i/R_0 = 2.366$, and $f = 0.2Y_0$.

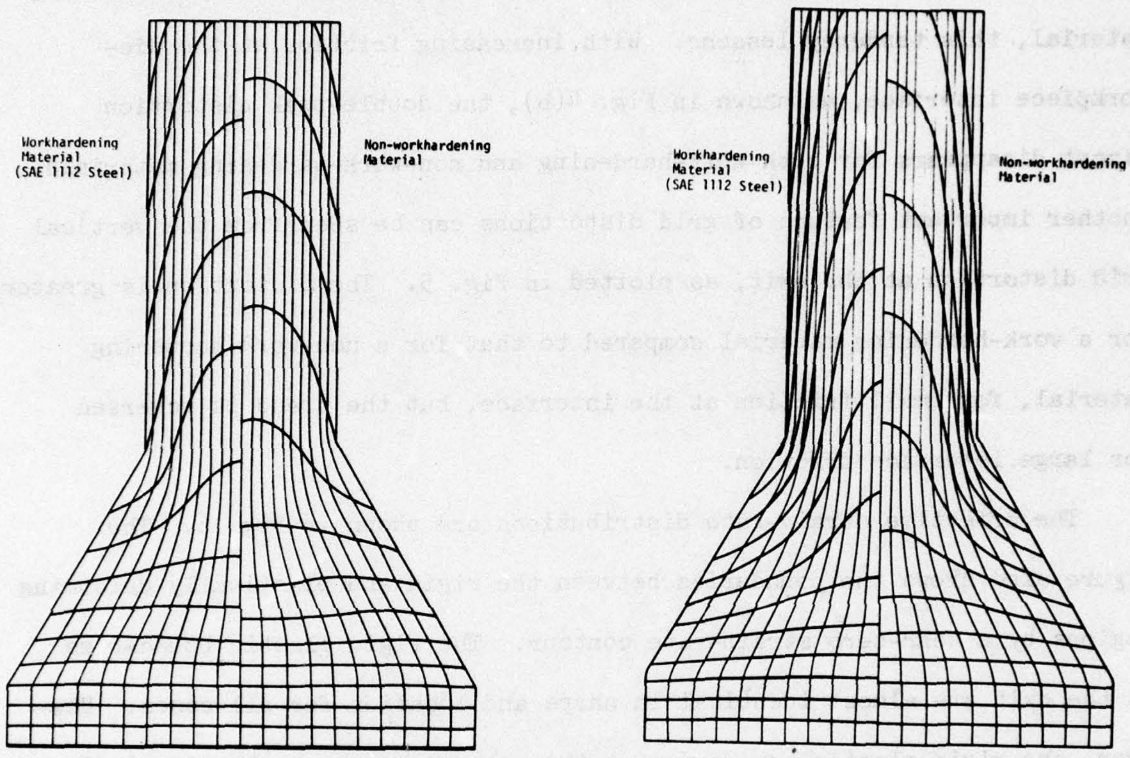

Fig. 4 Grid distortion patterns for non-workhardening and workhardening materials with (a) die frictional stress $f = 0$, and (b) $f = 0.4Y_0$.

it is clearly seen that the grid lines that are originally perpendicular to the axis of the workpiece distort and show the double peak in the extruded part for non-work-hardening material. However, for a work-hardening material, this tendency lessens. With increasing friction at the die-workpiece interface, as shown in Fig. 4(b), the double-peak distortion almost disappears for both work-hardening and non-work-hardening materials. Another important feature of grid distortions can be seen from the vertical grid distortion at the exit, as plotted in Fig. 5. The distortion is greater for a work-hardening material compared to that for a non-work-hardening material, for small friction at the interface, but the trend is reversed for large interface friction.

The effective strain-rate distributions are shown in Fig. 6. The figure also shows the boundaries between the rigid and plastically deforming regions by a near-zero strain-rate contour. The rigid plastic boundaries at the exit are almost identical in shape and location for all cases. However, the rigid-plastic boundaries at the entrance moves backwards, indicating larger deforming zones, with increasing interface friction. This observation applies to both work-hardening and non-work-hardening materials. Also, the results show that the deformation zone size becomes larger for work-hardening. The difference is more pronounced with increasing friction. Neglecting small details, the effective strain-rate distribution is identical for both materials. The strain-rate increases gradually from the entrance toward the exit and near the exit there is a sharp drop. As might be expected, there is some degree of strain-rate concentration near the die corner.

The effective strain-rates are integrated along the flow lines to yield

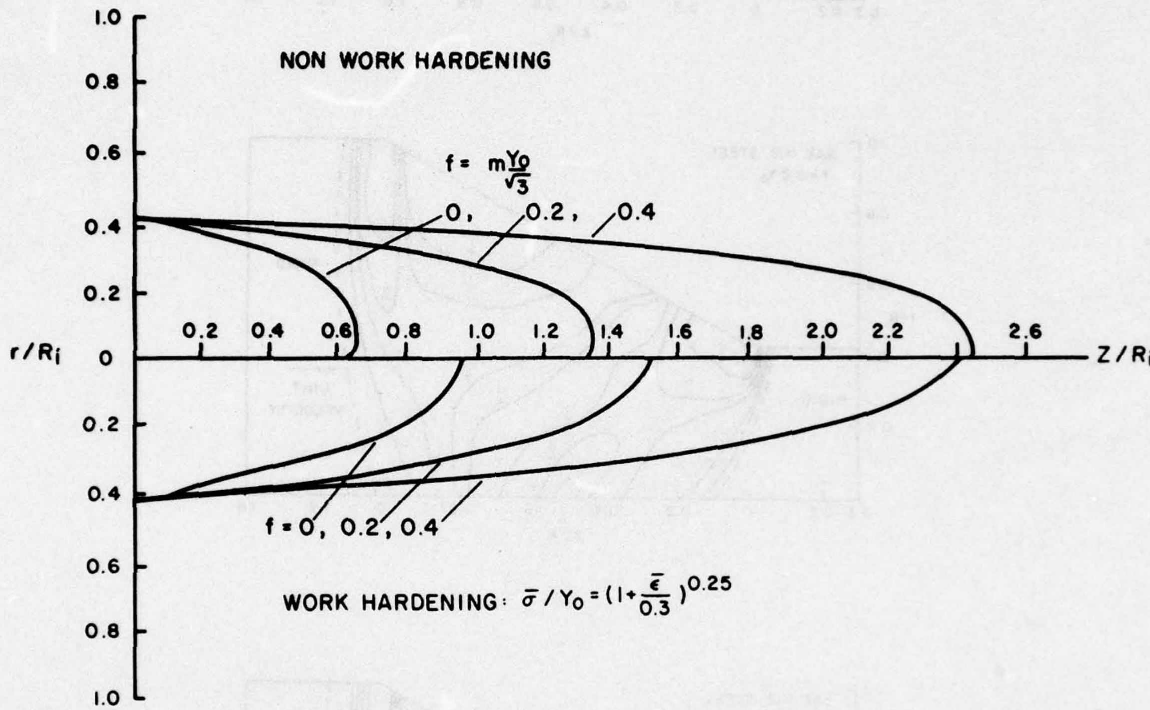

Fig. 5 Total grid distortions for various friction conditions; $\alpha = 30^o$, $R_i/R_0 = 2.366$.

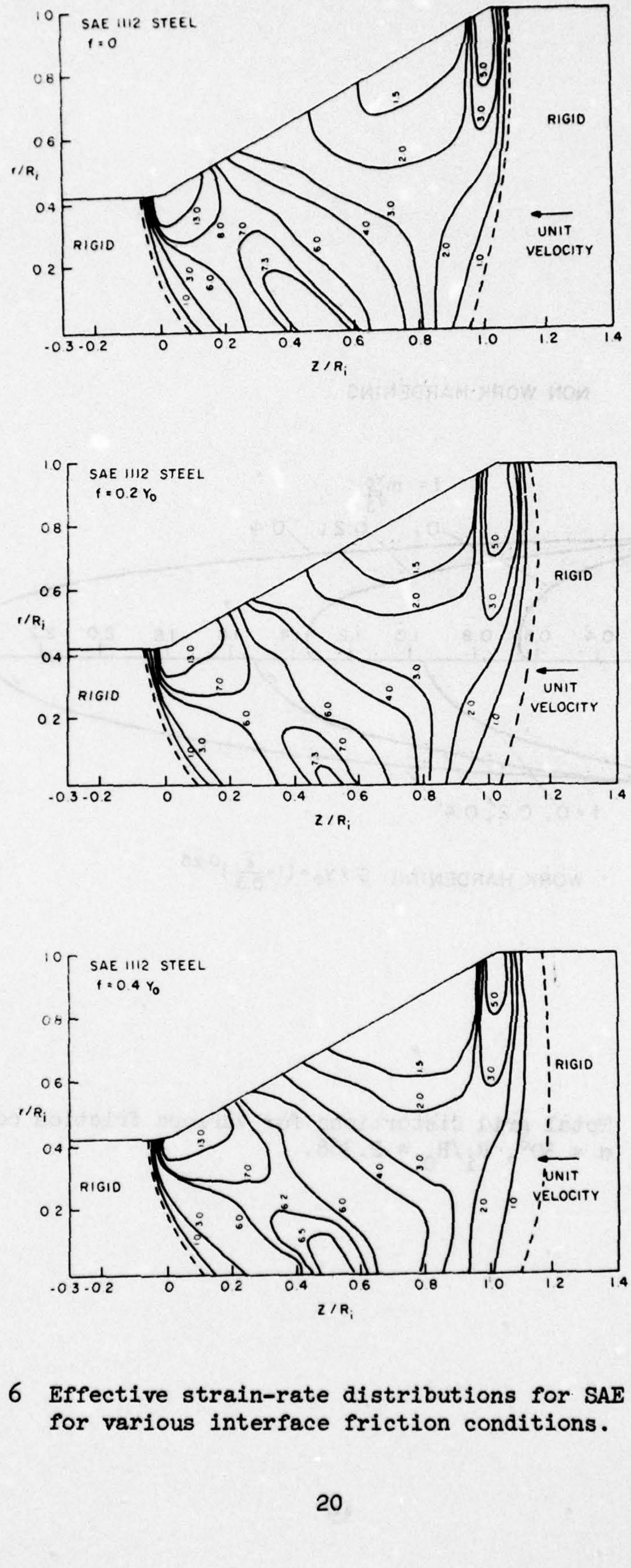

Fig. 6 Effective strain-rate distributions for SAE 1112 steel for various interface friction conditions.

the effective strain distributions. A typical effective strain distribution is given in Fig. 7. As for vertical sections, the strain is the highest near the die and the lowest near the extrusion axis throughout the deformation zone. The effective strain distribution at the exit section is also shown in the figure, which indicates that the strain is the lowest near the extrusion axis and increases toward the periphery. The strain distributions in the final product of the two materials are plotted for several friction values in Fig. 8. For both materials nonuniformity of deformation increases with increasing die-workpiece interface friction. The degree of nonuniformity is greater for small friction and less for large friction in work-hardening materials, while the opposite holds true for non-work-hardening materials. These results reflect exactly the findings in the vertical grid line distortion discussed with reference to Fig. 5.

The distributions of the hydrostatic pressure ($-\sigma_m/\bar{\sigma}$) are shown for the two friction conditions in Fig. 9. The distribution patterns are the same for both friction conditions and for both materials with and without work-hardening. Note that the hydrostatic pressure increases its magnitude throughout the deformation zone with increasing friction at the die-workpiece interface. It can be observed also that along the die-workpiece interface, the hydrostatic pressure is largest at the entrance and shows a minimum at some distance from the exit. This particular feature is seen in the normal pressure distributions along the die interface shown in Fig. 10. The pressure is the highest at the entrance and it decreases toward the exit, then increasing again near the exit. With increasing friction, the pressure increases but the distribution pattern remains the same. The trend of the curves for nonhardening and work-hardening materials is also the same with difference in magnitude of a constant amount.

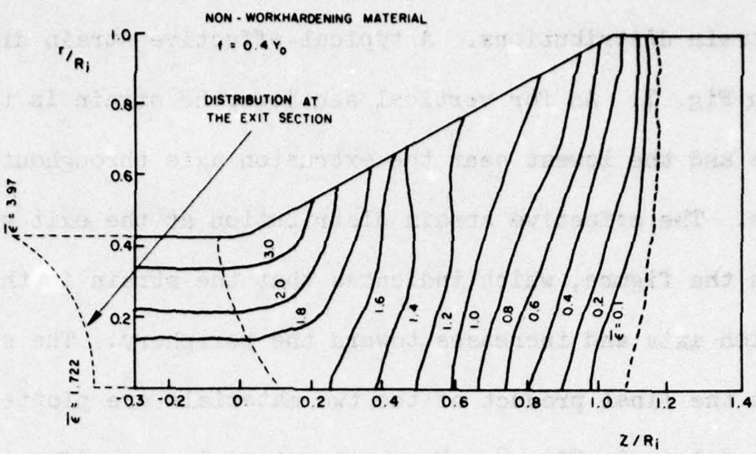

Fig. 7 A typical effective strain distribution.

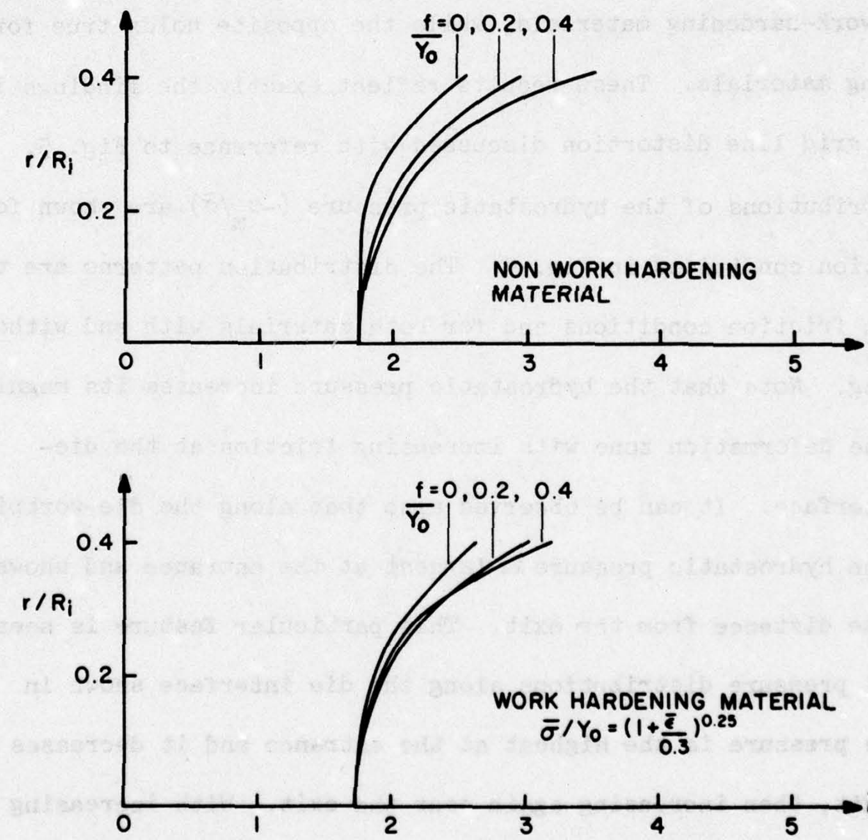

Fig. 8 Effective strain distributions at the exit sections for workhardening and non-workhardening materials under various interface friction conditions.

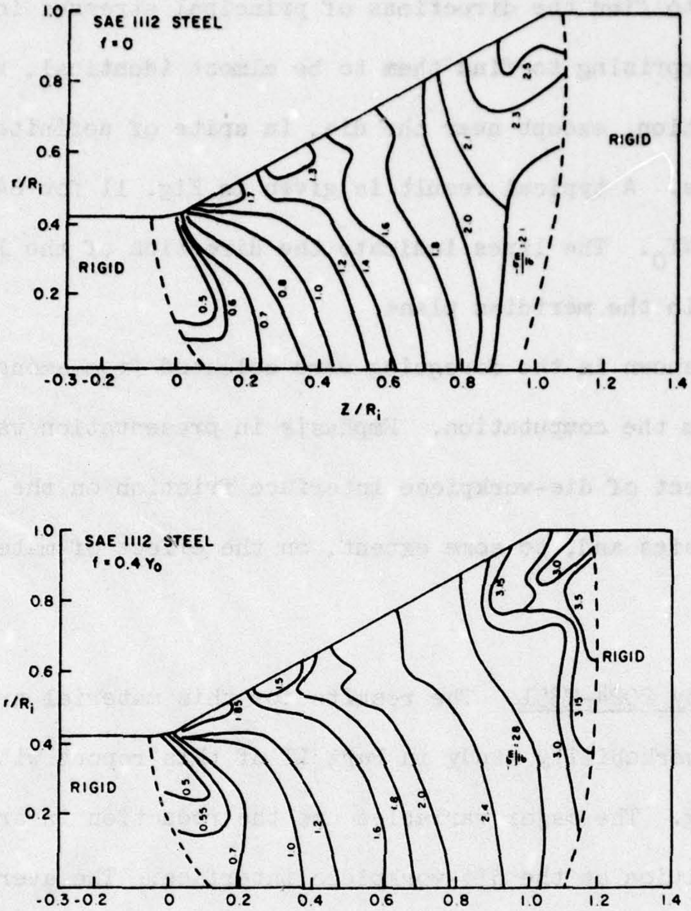

Fig. 9 Distributions of the hydrostatic pressure in SAE 1112 steel extrusion for the two friction conditions.

In other results obtained by the finite-element analysis, it is not only interesting to find the directions of principal stresses in the deformation zone, but surprising to find them to be almost identical, regardless of interface friction, except near the die, in spite of definite deviations of some quantities. A typical result is given in Fig. 11 for SAE 1112 steel with $f = 0.4Y_0$. The lines indicate the direction of the larger principal stress in the meridian plane.

The results shown in the foregoing were selected from among information obtained from the computation. Emphasis in presentation was placed mainly on the effect of die-workpiece interface friction on the detailed deformation mechanics and, to some extent, on the effect of materials properties.

Aluminum alloy 2024-T351 The results for this material are also utilized for the workability study in Part II of this report with regard to center bursting. The major variables are the reduction in area and the friction condition at the die-workpiece interface. The average extrusion pressures for various reductions and for the two friction conditions are summarized in Table 3.

Table 3: Average extrusion pressure, p_{ave}/Y_0.
$\alpha = 45°$

Friction	R_i/R_0 1.25	1.6	1.8	2.0
$f = 0$	2.102	2.913	3.289	3.567
$f = 0.4Y_0$	2.310	3.408	3.826	4.202

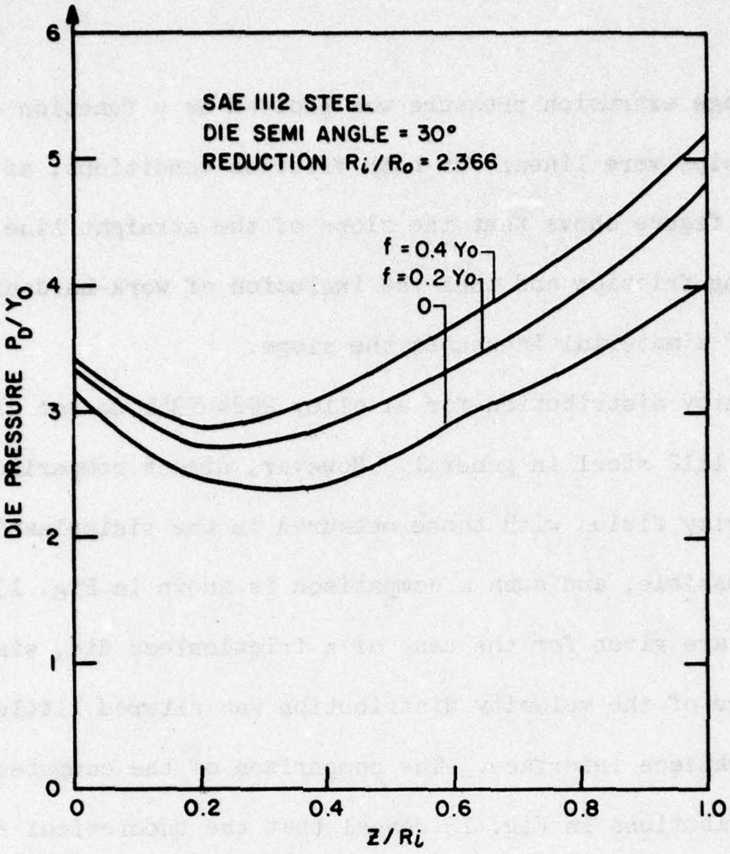

Fig. 10 The die pressure distributions under various friction conditions.

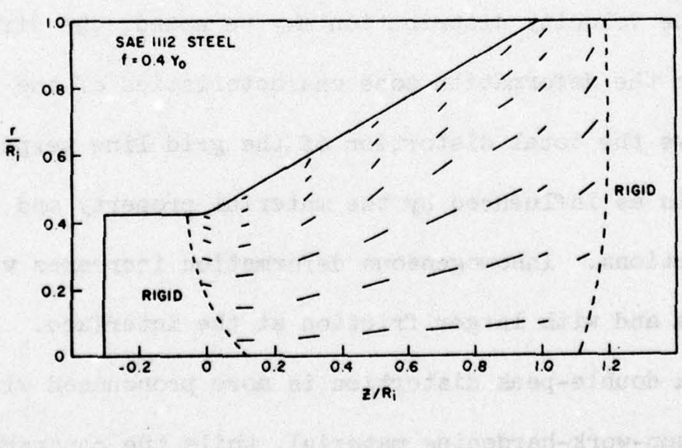

Fig. 11 Principal stress directions in extrusion.

When the average extrusion pressure was plotted as a function of $\ln(\frac{R_i}{R_0})$, the relationships were linear for both friction conditions, as shown in Fig. 12. The figure shows that the slope of the straight line increases with increasing friction and that the inclusion of work-hardening characteristics of a material increases the slope.

The velocity distribution for al alloy 2024-T351 do not differ from those for SAE 1112 steel in general. However, direct comparison of the computed velocity fields with those measured in the visioplasticity study [11] is now possible, and such a comparison is shown in Fig. 13. The computed results are given for the case of a frictionless die, since the general picture of the velocity distribution was altered little by friction at the die-workpiece interface. The comparison of the computed and measured velocity distributions in Fig. 13 reveal that the theoretical results in both velocity components are in agreement with the experimental results in every detail of distribution characteristics. This is one of the convincing evidences of the accuracy of the rigid-plastic finite-element analysis. Although in comparing Fig. 13 with Fig. 3 for SAE 1112 steel, some minor differences in the velocity distribution may be noted, the differences are mainly due to the deformation zone characteristics of the two materials.

Fig. 14 shows the total distortion of the grid line perpendicular to the extrusion axis as influenced by the material property and friction for several reductions. Inhomogeneous deformation increases with increasing reduction in area and with larger friction at the interface. An interesting feature is that a double-peak distortion is more pronounced with increasing reduction for a non-work-hardening material, while the contrary is true for a work-hardening material.

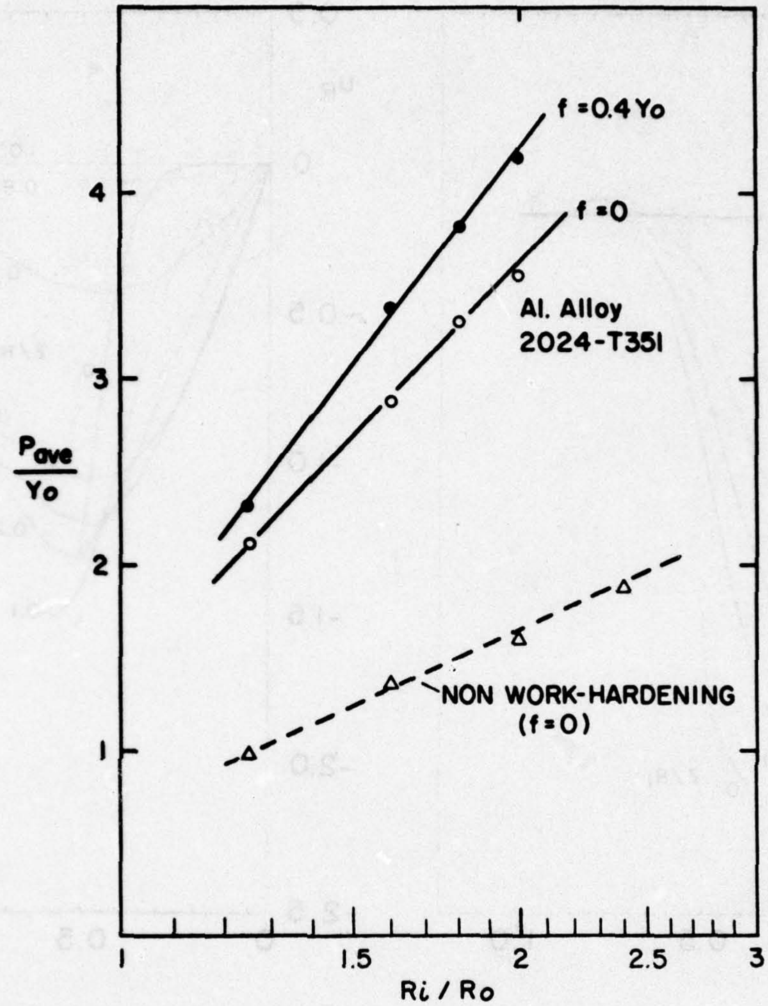

Fig. 12 Average extrusion pressures as functions of area reduction for aluminum alloy 2024-T351.

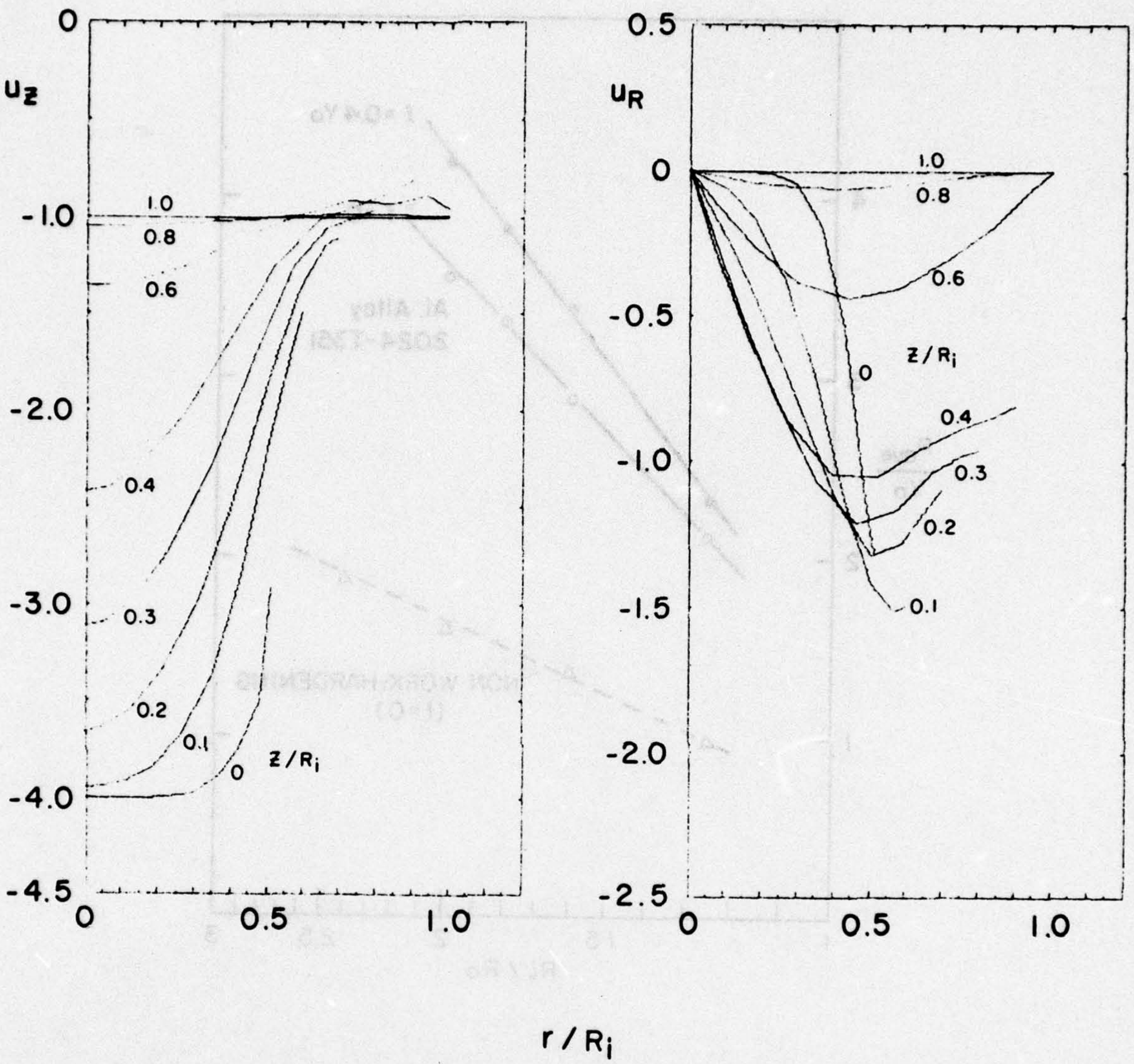

(a)

Fig. 13 Comparison of (a) computed and (b) experimental [11] velocity distributions; $R_i/R_0 = 2$, semi-die angle $\alpha = 45°$ (frictionless in computation).

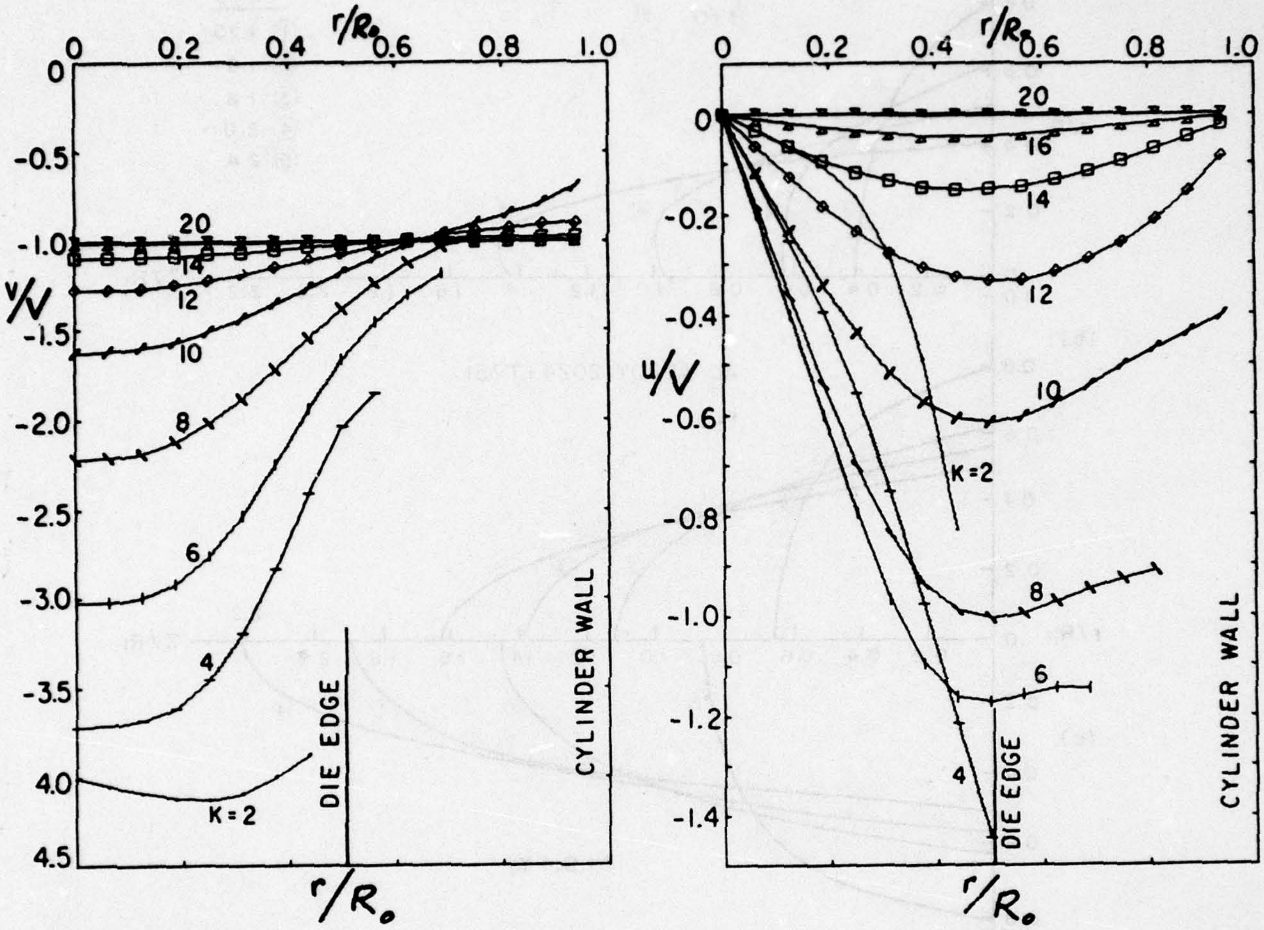
r/Ro
0
0.2
0.4
0.6
0.8
1.0
-0.5
-1.0
-1.5
-2.0
-2.5
-3.0
-3.5
4.0
4.5
v/V
20
14
12
10
8
6
4
K=2
DIE EDGE
CYLINDER WALL
r/Ro
-0.2
-0.4
-0.6
-0.8
-1.0
-1.2
-1.4
u/V
16
K=2

(b)

Figure 13

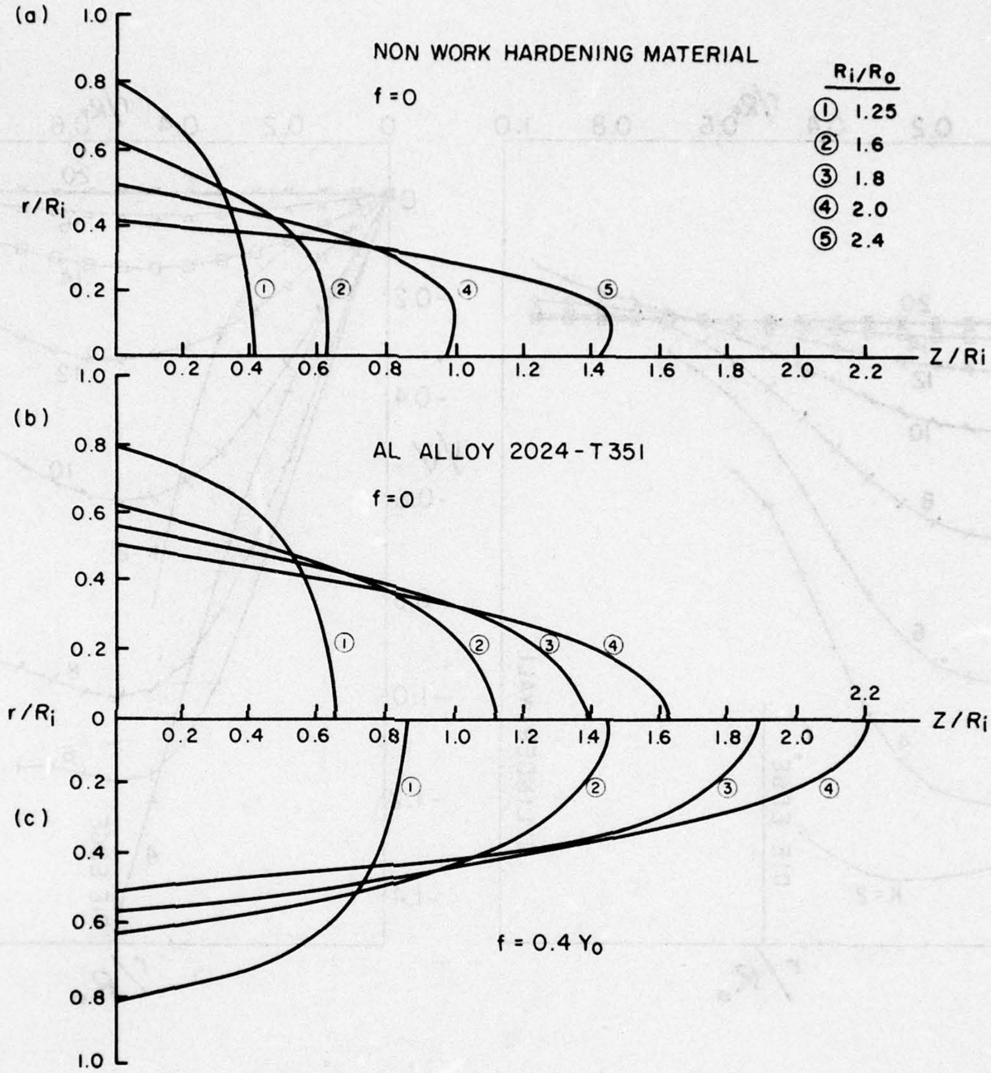

Fig. 14 Total grid distortions for various area reductions.

The effective strain-rate distributions for various area reductions, with two friction conditions, are shown in Fig. 15. With regard to the effect of friction on the deformation zone, the exit boundary remains about the same but the deformation zone expands as friction at the die-workpiece interface increases. This conclusion is the same as that drawn for SAE 1112 steel.

As the reduction in area increases, naturally the deformation zone becomes larger and the magnitude of strain-rate increases. Common features of the strain-rate distributions for all the reductions investigated are: (1) strain-rate concentrations occur near the corners at the entrance and at the exit, and (2) along the axis of symmetry the strain-rate peak appears in the middle of the deformation zone. The effective strain distributions across the extruded bar are plotted in Fig. 16. The strain is largest at the surface and smallest at the center. An interesting result is that the degree of nonuniformity in strain (difference between the largest and smallest strains) is greatest for the smallest area reduction. Also, the effect of friction on the final strain distribution is practically none, except that the magnitude of the surface strain increases slightly with increasing interface friction.

The distribution of the mean stress is similar to the pattern obtained for SAE 1112 steel. As the reduction decreases, the mean stress increases and becomes tensile in the zone near the center, as shown in Fig. 17. Another finding is seen, with respect to the die pressure, in Fig. 18. The die pressure is highest for the smallest reduction. This implies that the pressure distributions for smaller reductions are critical for die design. The distribution pattern is the same as that for SAE 1112 steel showing a minimum at some distance from the die exit.

Finally, the directions of the largest principal stresses are plotted for two reductions in Fig. 19. Again, the effect of die-workpiece interface friction is negligible and the pattern appears to be determined solely by the geometrical constraints.

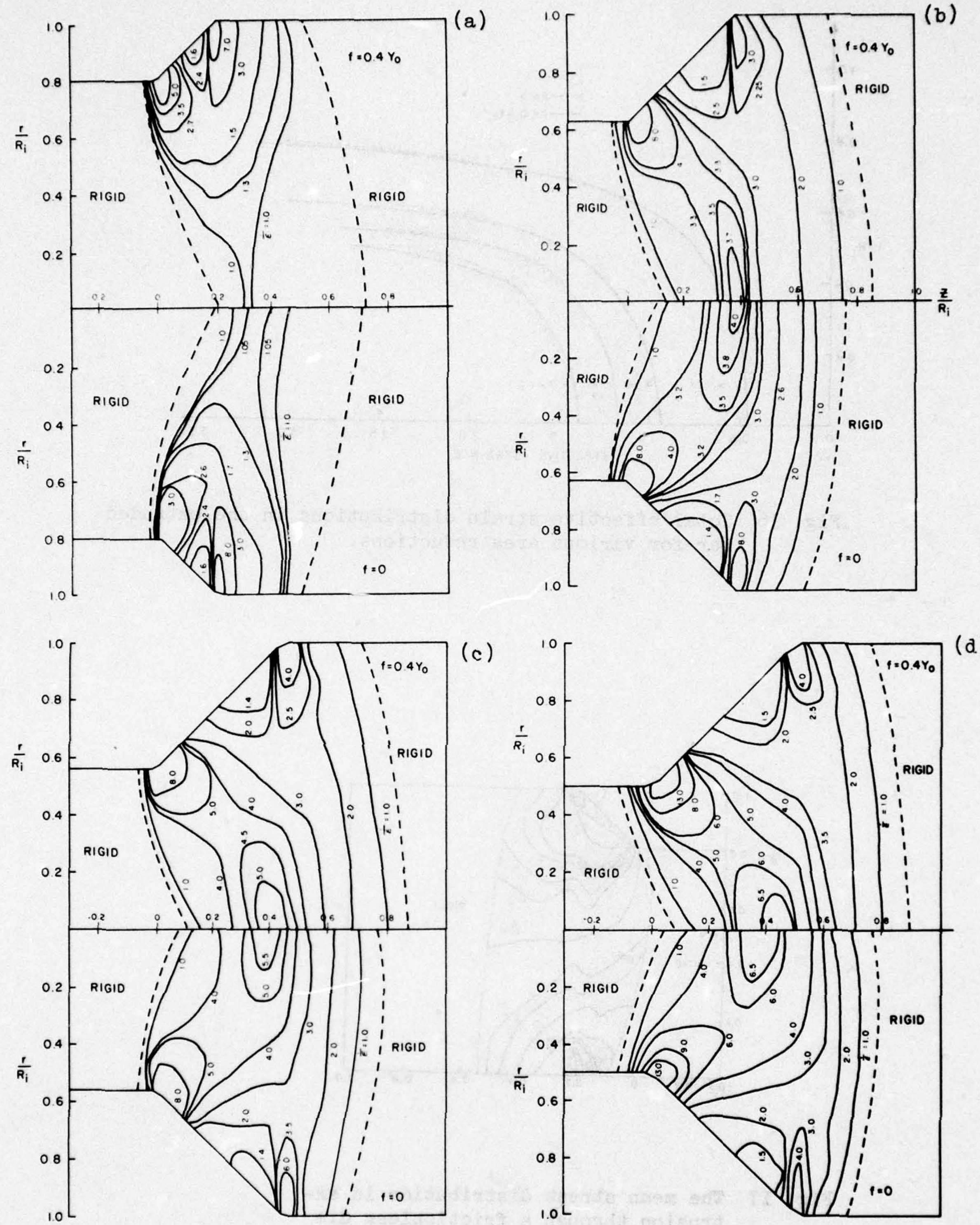

Fig. 15 Strain-rate distributions for two friction conditions at reductions of (a) $R_i/R_0 = 1.25$; (b) $R_i/R_0 = 1.6$; (c) $R_i/R_0 = 1.8$; (d) $R_i/R_0 = 2$.

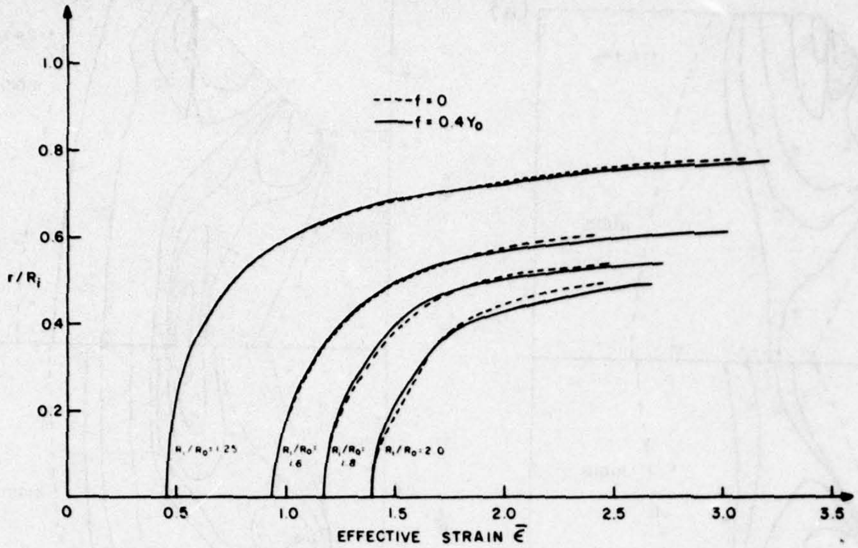

Fig. 16 Total effective strain distributions in the extruded bar for various area reductions.

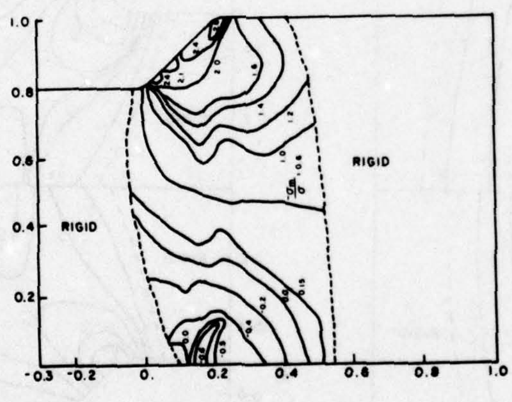

Fig. 17 The mean stress distribution in extrusion through a frictionless die at $R_i/R_0 = 1.25$.

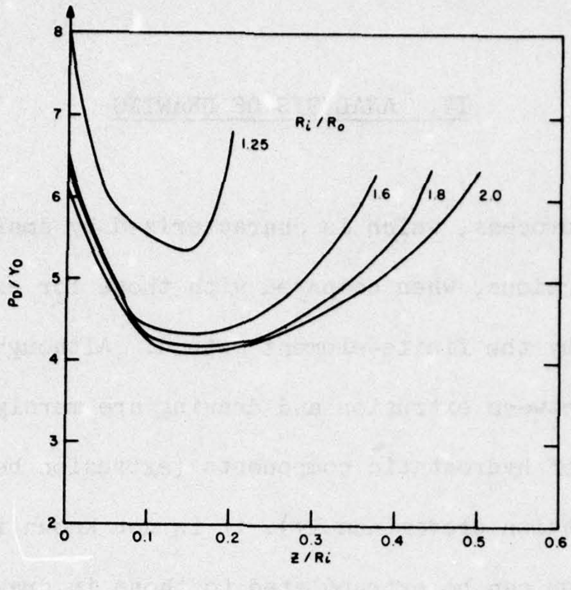

Fig. 18 Die pressure distributions for various area reductions.

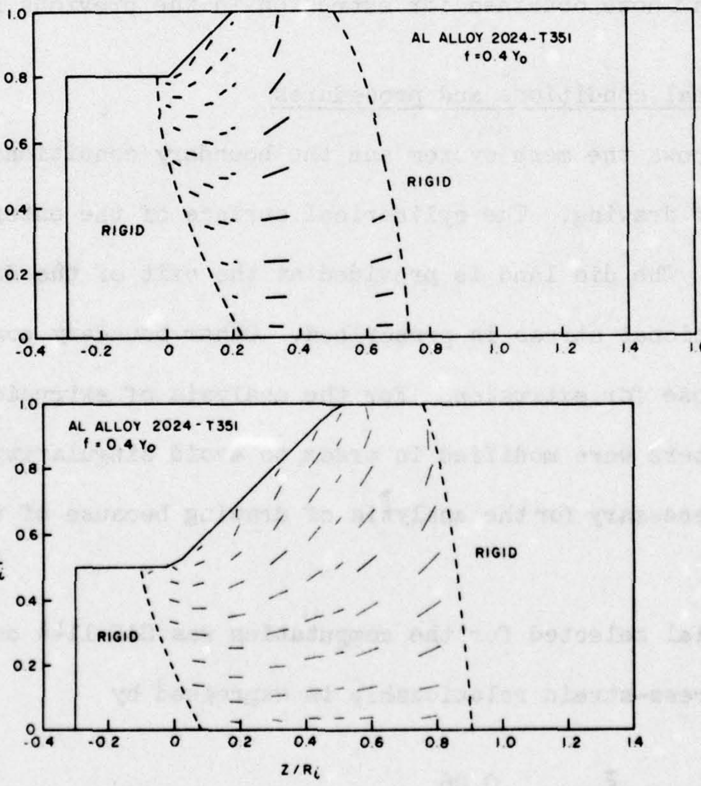

Fig. 19 Directions of the largest principal stresses.

IV. ANALYSIS OF DRAWING

The drawing process, which is characterized by smaller die angles and smaller area reductions, when compared with those for extrusion, has not yet been treated by the finite-element method. Although it appears that the differences between extrusion and drawing are merely geometrical and in the magnitude of hydrostatic components (extrusion being in compression and drawing in tension predominantly), it is not known if the results obtained in extrusion can be extrapolated to those in drawing according to the geometrical conditions and a simple concept of pushing and pulling. Therefore, we discuss the analytical results in drawing, emphasizing a comparison with those obtained for extrusion in the previous section.

A. Computational conditions and procedures

Fig. 20 shows the mesh system and the boundary conditions used for the analysis of drawing. The cylindrical surface of the entering bar is traction-free. The die land is provided at the exit of the die, along which the frictional stress is prescribed. Other boundary conditions are the same as those for extrusion. For the analysis of extrusion the shape of the die corners were modified in order to avoid singularity. However, this was not necessary for the analysis of drawing because of the small die angle.

The material selected for the computation was SAE 1144 cold-drawn steel whose stress-strain relationship is expressed by

$$\frac{\bar{\sigma}}{Y_0} = \left(1 + \frac{\bar{\varepsilon}}{0.262 \times 10^{-4}}\right)^{0.06}$$

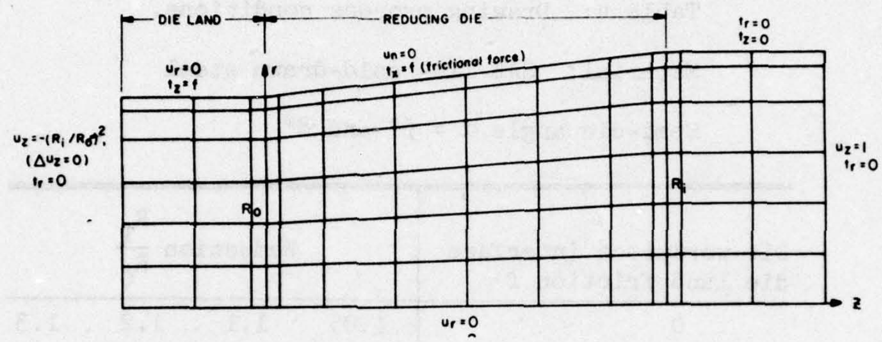

Fig. 20 The mesh system and boundary conditions for drawing.

with Y_0 = 84,800 psi

$= 584.68\ MN/m^2$.

This material was selected mainly for the workability study in drawing given in Part 2 of this report.

The drawing process conditions for which the computation was performed are summarized in Table 4.

Table 4: Drawing process conditions.

Material: SAE 1144 cold-drawn steel

Semi-die angle $\alpha = 6°$ and $8°$

Die-workpiece interface die land friction f	Reduction $\frac{R_i}{R_0}$			
0	1.05	1.1	1.2	1.3
$0.25\ Y_0$	1.05	1.1	1.2	-

For computation purposes the solution of extrusion for $\alpha = 45°$ and $R_i/R_0 = 1.25$ was used as an initial guess for drawing with $\alpha = 6°$ and $R_i/R_0 = 1.2$ by modifying the solution according to geometrical proportions. Thirty-four (34) iterations were required to achieve the converged solution with

$$\sum_m \left\{ \left(\frac{\partial \tilde{\phi}^{(m)}}{\partial \underset{\sim}{u}^{(m)}} \right)^2 + \left(\frac{\partial \tilde{\phi}^{(m)}}{\partial \lambda^{(m)}} \right)^2 \right\} = 10^{-6}, \quad \left(\frac{\| \Delta \underset{\sim}{u} \|}{\| \underset{\sim}{u} \|} \sim 4 \times 10^{-6} \right).$$

This solution was then used as an initial guess for the computation of all the other cases. The convergence was excellent and only 6 to 10 iterations were necessary to obtain the solutions in most cases.

B. Results and discussion

The results for $\alpha = 6^{\circ}$ are presented and discussed here. The results for $\alpha = 8^{\circ}$ are presented and discussed in terms of workability in drawing in Part 2 of this report.

An example of the velocity distribution is shown for $R_i/R_0 = 1.2$ and $f = 0.25Y_0$ in Fig. 21. The distribution pattern looks somewhat different from those for extrusion. This is because of small reduction and small die angle and because the total distortion is small. Fig. 22 shows vertical grid line distortion in drawn bars. Greater friction produces more distortion. The difference in the total distortion due to die friction increases with increasing reductions.

The general pattern of the effective strain-rate distribution is the same as that for extrusion, as seen in Fig. 23. Concentrations of strain rate occur at the die corners. Along the axis of symmetry, strain-rate distribution shows a peak at the midpoint of the deformation zone. The deformation zone expands with larger die-workpiece interface friction as it did for extrusion.

The variation of effective strain distribution in drawn bars is comparatively small due to a small die angle and small reductions (Fig. 24). Fig. 24 shows also that the effect of the die friction on the strain distribution is negligible. By comparing Fig. 24 with the results of extrusion in Fig. 16, it can be seen that the die angle is a most important variable in controlling nonuniformity of the extruded or drawn bar properties.

The hydrostatic pressure distribution is shown in Fig. 25. It shows the combined characteristics of those for small reductions similar to

Fig. 17 and those for relatively extended deformation zone similar to Fig. 9. The magnitude of the hydrostatic component increases with larger die friction in drawing. This is contrary to the results with extrusion shown in Fig. 9. The die pressure distribution is plotted for various reductions and for two die friction conditions in Fig. 26. Higher die pressure is obtained for smaller reduction as it was for extrusion. However, contrary to the case of extrusion, the die pressure is higher with frictionless dies than those with friction. These findings on die pressure are in agreement with experimental results [12], although empirical values are average die pressures.

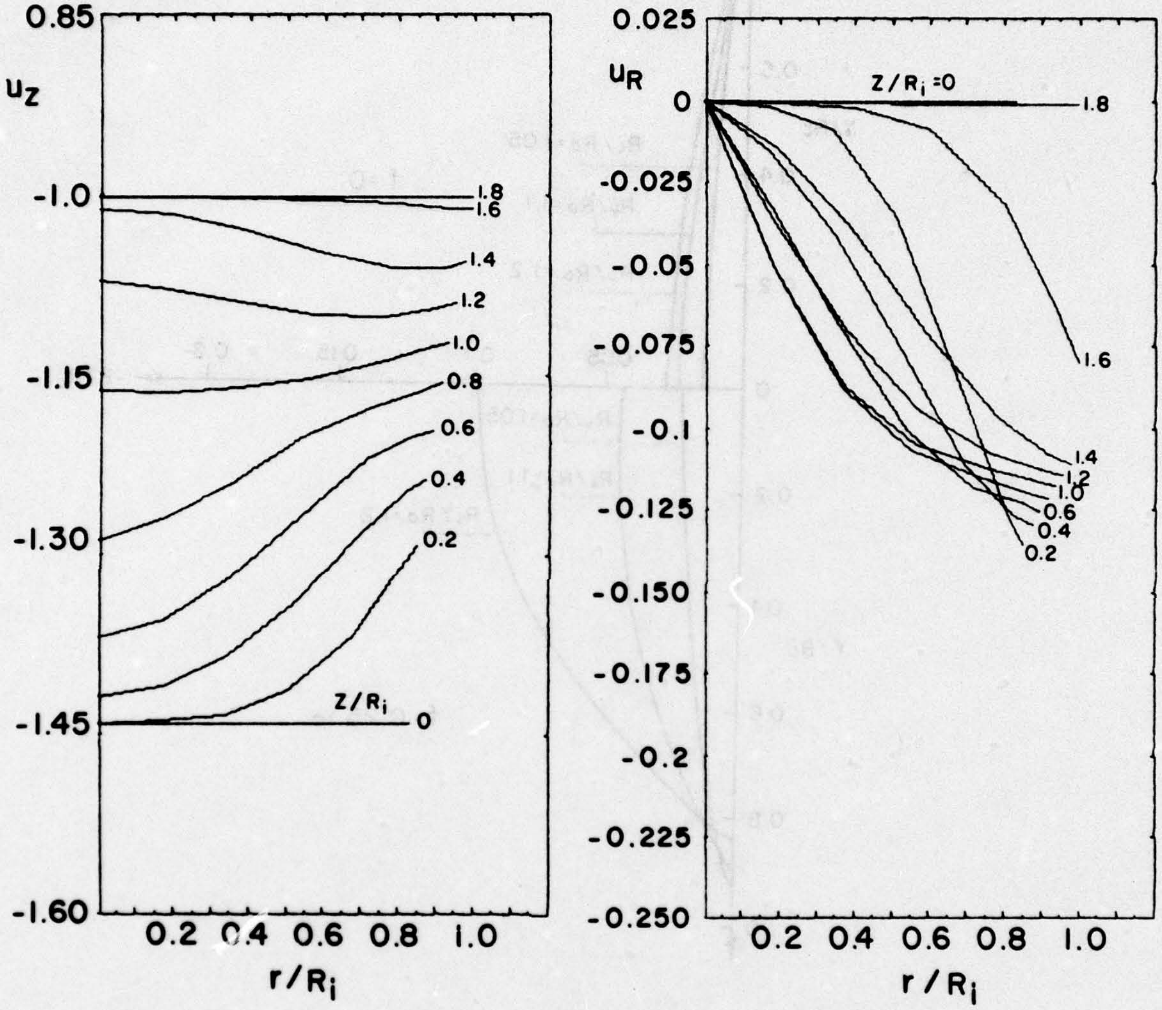

Fig. 21 Velocity distributions in drawing with $\alpha = 6°$, $R_i/R_0 = 1.2$, and $f = 0.25Y_0$.

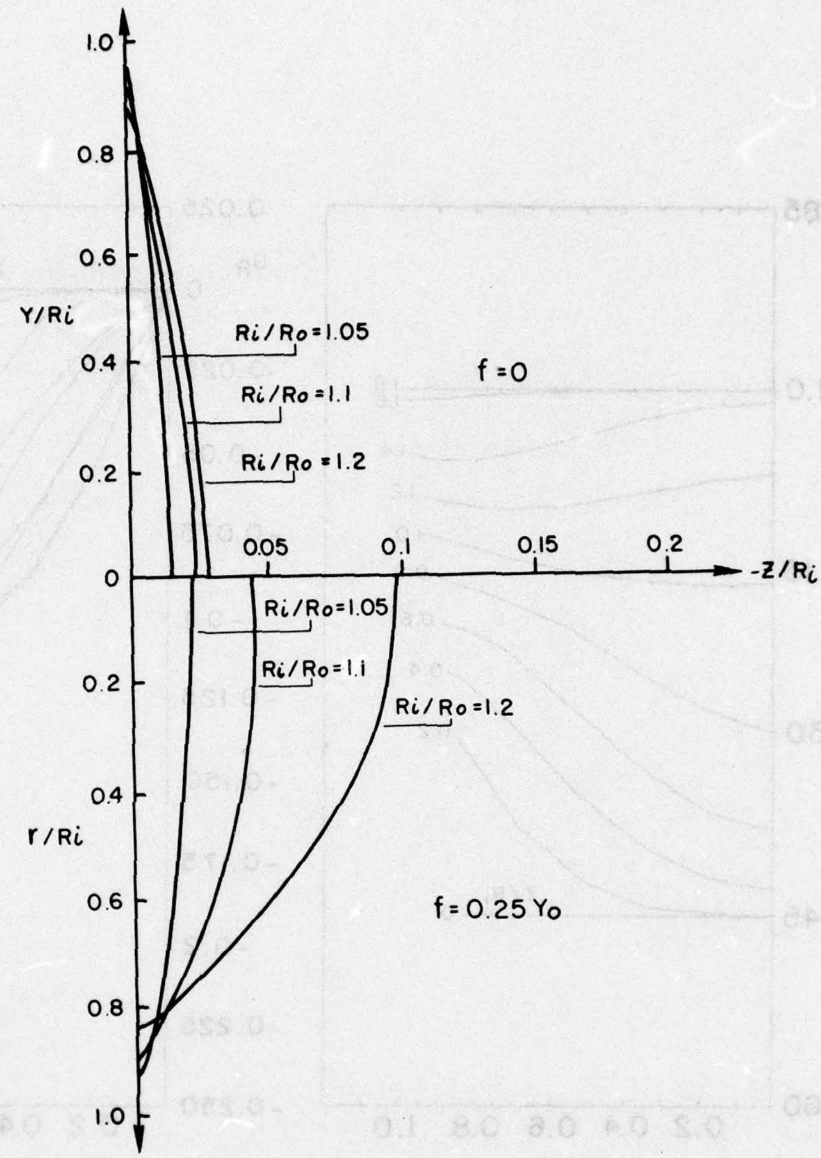

Fig. 22 Total distortion of a line originally perpendicular to the axis of drawing for various area reductions.

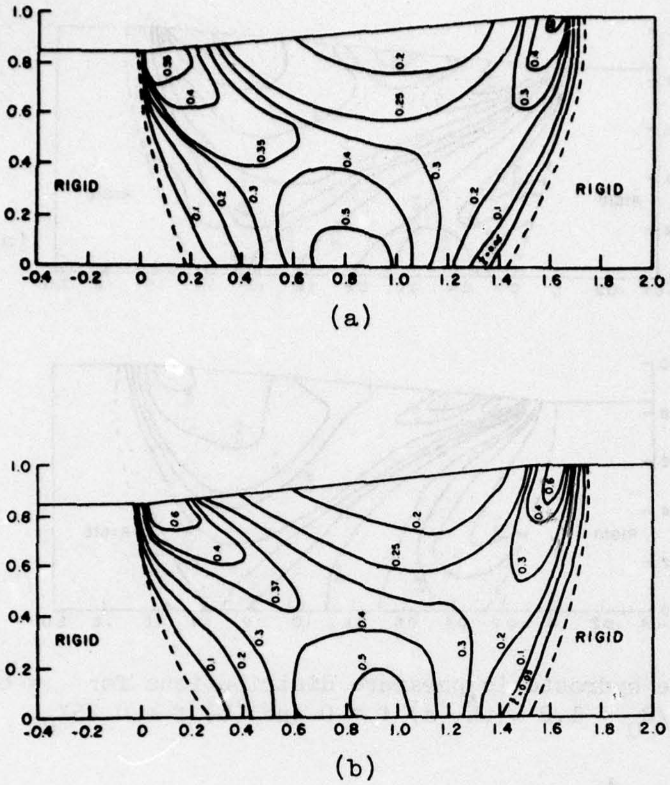

Fig. 23 Strain-rate distributions for $\alpha = 6^\circ$ and $R_i/R_0 = 1.2$ with (a) $f = 0$ and (b) $f = 0.25Y_0$.

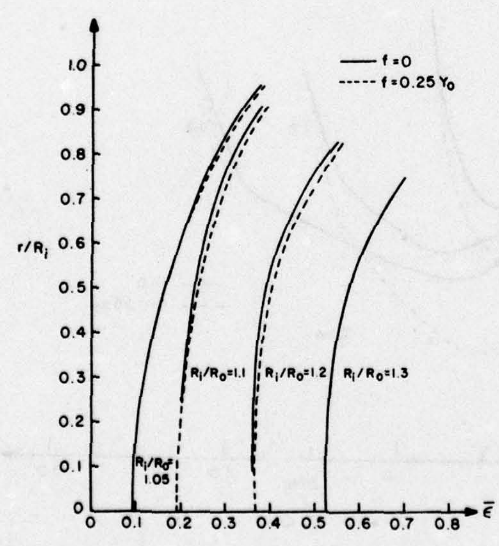

Fig. 24 Effective strain distributions in drawn bars.

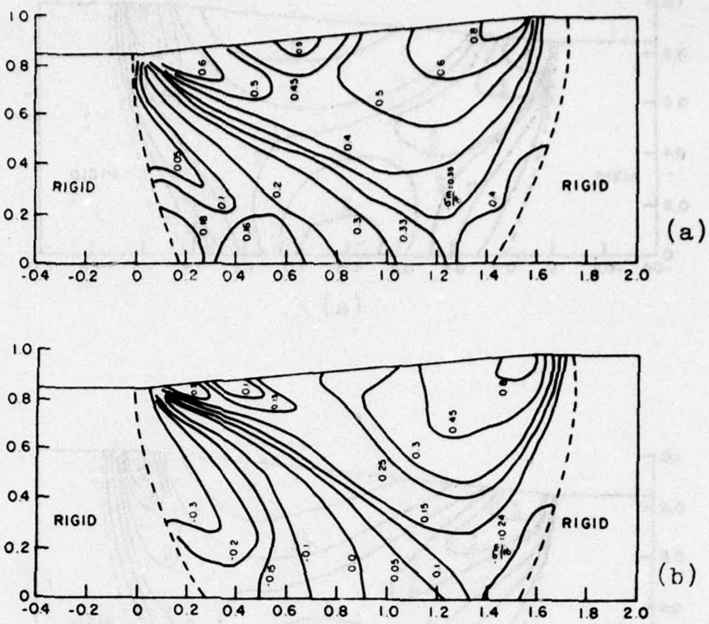

Fig. 25 The hydrostatic pressure distributions for = 6° and $R_i/R_0 = 1.2$ with (a) $f = 0$ and (b) $f = 0.25Y_0$.

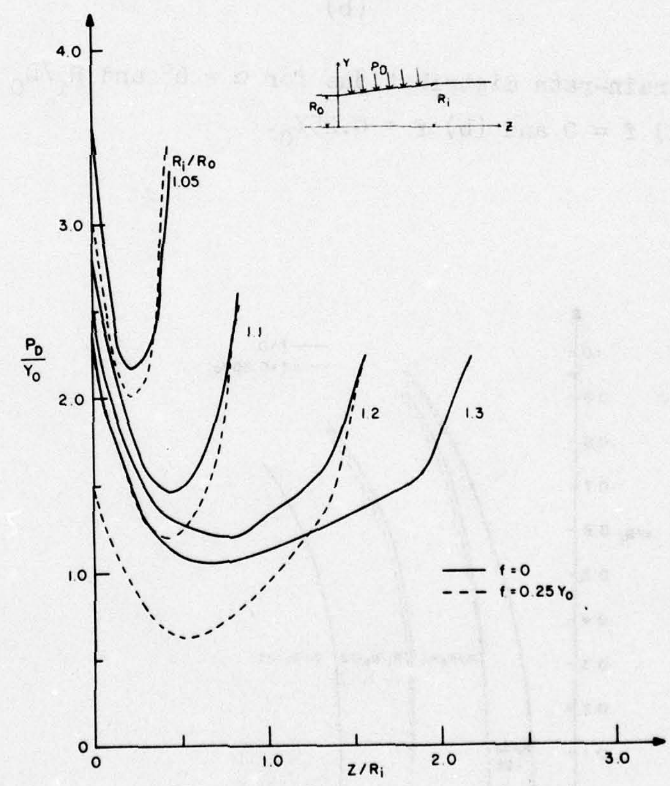

Fig. 26 The die pressure distributions for various reductions and for the two die-friction conditions.

V. SUMMARY AND CONCLUSIONS

In recent years the matrix method has been applied to the analysis of various metalworking processes, including the steady-state extrusion process. The present matrix method program incorporates the treatment of friction at the die-workpiece interface and an improvement of computational efficiency by adopting a new convergence criterion. Using this program, the detailed mechanics of steady-state extrusion and drawing were obtained under various process conditions. The stress-strain properties of SAE 1112 steel and aluminum alloy 2024-T351 were used for extrusion and the stress-strain curve of SAE 1144 cold-drawn steel was used for drawing. The variables included for the computation were the die angle, die-workpiece interface friction, and the area reduction. The computed results were presented in terms of velocity distribution, grid distortion, strain-rate distribution, and stress and strain distributions.

Although materials properties apparently influence metal flow, as seen in grid distortion patterns, their effects on the overall deformation characteristics appear to be insignificant in extrusion and drawing processes. Among other variables, friction at the die-workpiece interface plays an important role in determining the detailed mechanics in these processes. With increasing friction the degree of grid distortion becomes larger and the deformation zone size expands in both processes. But the effect of friction on nonuniformity of product properties is less significant, while the die angle is an important variable in controlling this nonuniformity. The contrast between the extrusion process and the drawing process can be

found in the die pressure distribution and the distribution of hydrostatic stress components. In both processes, the die pressure decreases with increasing reduction in area. However, the die pressure is greater for larger interface friction in extrusion, while the reverse is true in drawing. Similarly, the magnitude of the hydrostatic stress component is less with larger interface friction in extrusion, but increases with increasing friction in drawing.

It is concluded that the matrix method is indeed an efficient numerical method which provides useful information on the detailed deformation characteristics for various process variables. In order to ascertain the accuracy of the solutions presented here, however, an extensive theoretical and experimental investigation is still needed.

Part 2

WORKABILITY IN EXTRUSION AND DRAWING

I. INTRODUCTION

For occurrence of cracks at the free surface, such as in edge-cracking in sheet rolling and surface cracks in upsetting, the fracture criterion can be constructed experimentally. However, for predicting internal fracturing, formulations of fracture criteria under general deformation are required. In this part of the present investigation, the validity of the theory on ductile fracture developed in the previous report [1] was examined by the experimental data found in the literature. Then, combining the formulation of fracture criterion with the deformation mechanics found in Part 1, the workability of materials in extrusion and drawing was determined.

In an attempt to develop a general fracture criterion, a model for void growth was proposed to examine the stress and strain fields around voids. The solutions were obtained by the finite-element method. The results show that deformation is concentrated along the narrow band in the maximum shear stress direction. The fracture criterion assumed that voids of orders of magnitude smaller than the primary voids are distributed throughout and that fracturing occurred when the small voids grow and touch each other along the band connecting the large voids. The McClintock analysis was used for predicting the growth and coalescence of small voids. Based on this concept, the fracture strain formulation by McClintock was modified. Then the modified form, along with the formulation by Cockroft and Latham, was tested by the experiments on surface cracks and by the tension data by Bridgman. Its validity was further examined by applying the criterion to the determination of workability in bar extrusion and drawing.

II. FRACTURE CRITERIA

McClintock and his coworkers [13], [14] developed solutions for void growth under the transverse stress state. Their model consists of a single elliptic cylindrical void extending in one direction and imbedded in a rigid plastic media. The major and minor axes of the void coincide with the principal stress directions. They derived an approximate solution for the rigid work-hardening materials, $\bar{\sigma} = K\bar{\varepsilon}^{n}$, as

$$\log_e\left(\frac{R}{R_0}\right) = \frac{\sqrt{3}\,\bar{\varepsilon}}{2(1-n)} \sinh\left[\frac{\sqrt{3}(1-n)}{2}\,\frac{\sigma_a + \sigma_b}{\bar{\sigma}}\right] + \left(\frac{\varepsilon_a + \varepsilon_b}{2}\right) ; \tag{9}$$

$$m = \left(\frac{\sigma_a - \sigma_b}{\sigma_a + \sigma_b}\right) + \left[m_0 - \left(\frac{\sigma_a - \sigma_b}{\sigma_a + \sigma_b}\right)\right] \exp\left[-\frac{\sqrt{3}\,\bar{\varepsilon}}{(1-n)} \sinh\left\{\frac{\sqrt{3}(1-n)}{2}\left(\frac{\sigma_a + \sigma_b}{\bar{\sigma}}\right)\right\}\right] \tag{10}$$

where R and R_0 are the current and initial mean radii of the hole, respectively; σ_a and σ_b, principal stress components along the major and minor axes, respectively; $\bar{\sigma}$ is the effective stress and $\bar{\varepsilon}$ is the effective strain; m is the eccentricity of the ellipse defined in terms of the semi-major and semi-minor axes a and b, as

$$m = \frac{a - b}{a + b} , \tag{11}$$

and m_0 is the initial eccentricity. They assumed that the cylindrical hole is contained in the cell and that the material is composed of these cells. Fracturing was assumed to occur at the point where a growing void touches the cell boundary whose deformation is assumed to be the same as that of the boundary at infinity. The fracture strain, neglecting the void inter-

action, is then expressed (dropping a transient term) by

$$\bar{\varepsilon}_f = \frac{\log_e\left(\dfrac{\ell_a^0}{2a_0}\right)}{\left\{\dfrac{\sqrt{3}}{2(1-n)} \sinh\left[\dfrac{\sqrt{3}(1-n)}{2} \cdot \left(\dfrac{\sigma_a + \sigma_b}{\bar{\sigma}}\right)\right] + \dfrac{3}{4}\left(\dfrac{\sigma_b - \sigma_a}{\bar{\sigma}}\right)\right\}} \tag{12}$$

where ℓ_a^0 and a_0 are the initial values of hole spacing ℓ_a and a, respectively. The above derivation was given for generalized plane strain as an approximation for three-dimensional deformations. In three-dimensional configurations, there are six modes of fracture, two in each of the three perpendicular planes. Whichever one of these six modes gives the smallest fracture strain is the actual mode.

The model considers only the case where holes form at zero strain by complete separation of the particle-matrix interface. The review of the investigations on ductile fracture revealed that void nucleation is a complex process and that the nucleation pattern depends on particle size, particle composition, and possibly, particle distribution. The general observation is that void nucleation occurs at the large particles first. If a number of voids form and grow, then these voids may act as a stress raiser in the matrix and cause further void nucleation at other particle sites. Also, there are many indications that, during deformation, shear bands between large voids develop and that voids form at small particles in these bands, while the particles outside the bands remain relatively inactive. Thus, the formation of shear bands between large voids and growth and coalescence of small voids in the shear band may be a mechanism of eventual fracture.

Assuming this mechanism for fracture, a model for the growth of large voids has been proposed. Fig. 27 shows an assumed distribution of large voids, extending in arrays to infinity. The plane-strain condition is assumed in the direction perpendicular to the (x_a, x_b) plane. The minimum and maximum principal stresses act along the boundary at infinity in the directions of coordinate axes $(\sigma_a^\infty, \sigma_b^\infty)$. The solutions of this void growth model were obtained by the elastic-plastic finite-element model [1]. A result of the computation is shown in Fig. 28. As Fig. 28 indicates, deformation is concentrated along the narrow band in the maximum shear stress direction, and the concentration of strain along the band is about $2 \sim 3$ times the overall strain for most of the band and about $4 \sim 5$ greater near a large void. This implies that the band is the most favorable place for small voids to nucleate and grow.

The modified form of fracture criterion was obtained by assuming that voids of orders of magnitude smaller than the primary voids are distributed throughout and that fracturing occurred when the small voids grow and touch each other along the band connecting the large voids. When the McClintock analysis is applied locally under the condition prevailing within the shear band, we obtain

$$\bar{\varepsilon}^f = \frac{K}{\dfrac{2}{\sqrt{3}(1-n)} \sinh\left\{\dfrac{\sqrt{3}(1-n)}{2} \dfrac{\sigma_a + \sigma_b}{\bar{\sigma}}\right\} + \dfrac{\sigma_b - \sigma_a}{\bar{\sigma}}} \tag{13}$$

where $K = \frac{4}{3f} \log_e\left(\frac{\ell_a^0}{2a_0}\right)$ and f is a factor indicating the strain concentration along the shear band.

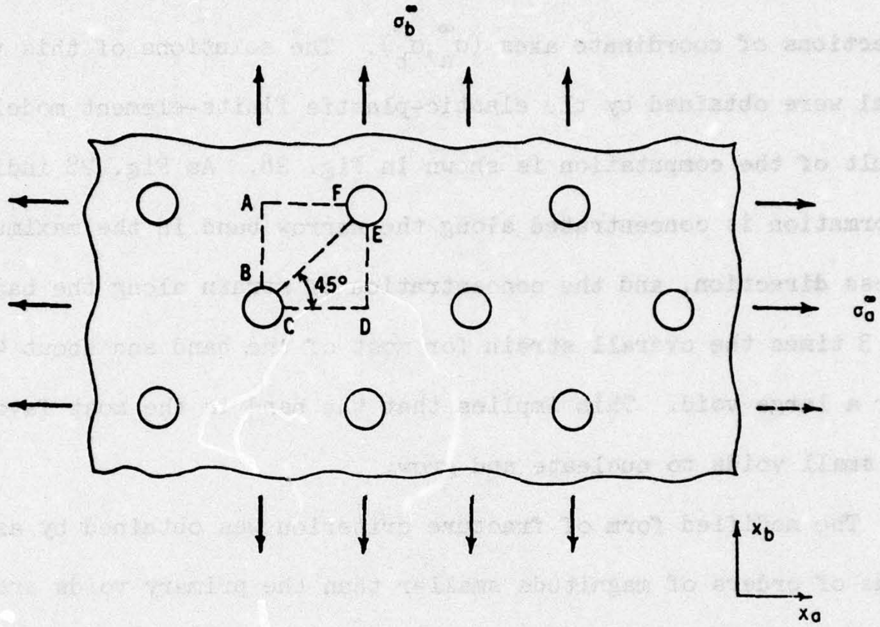

Fig. 27 Model for distribution of large voids.

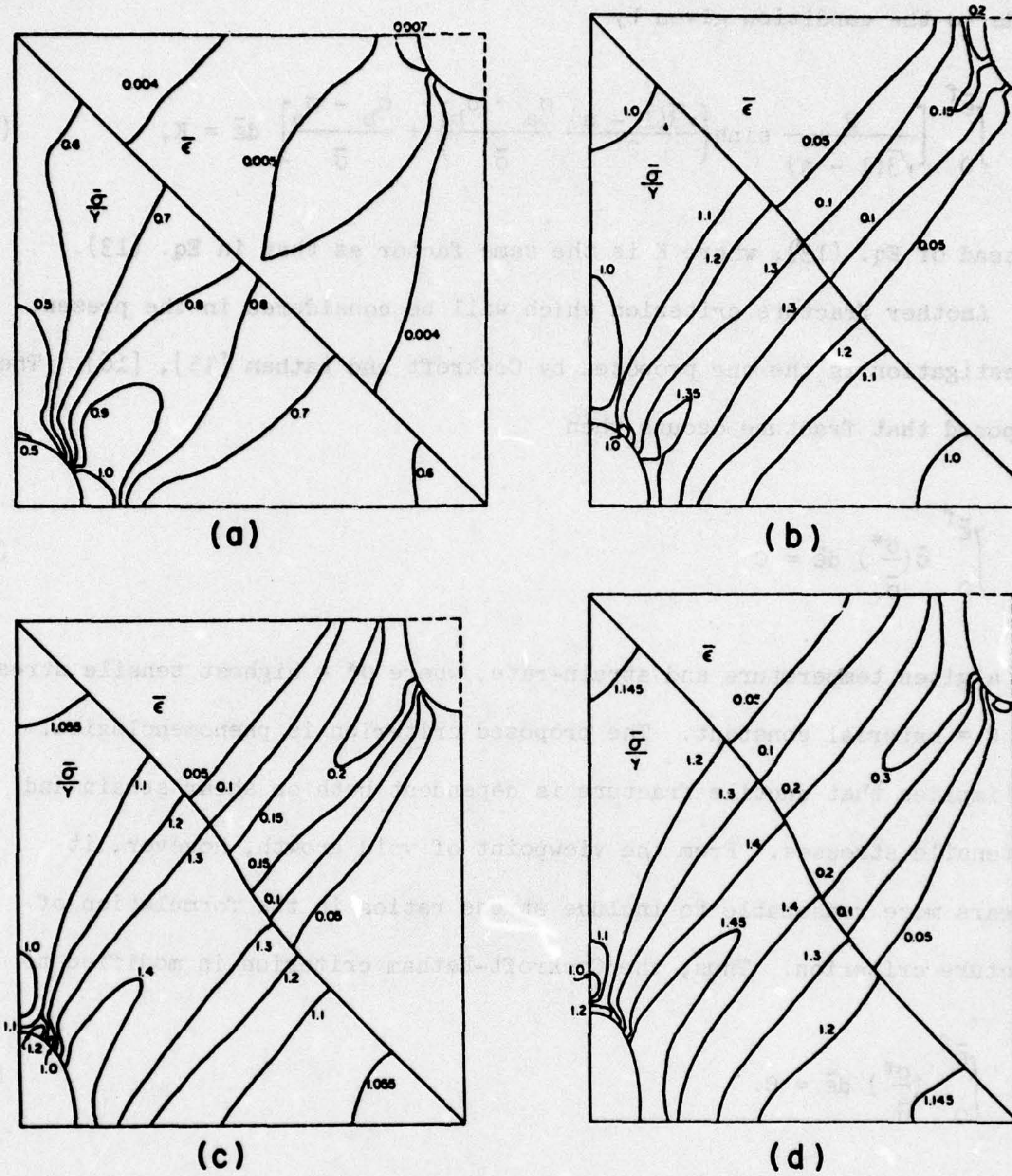

Fig. 28 Effective stress and effective strain distributions in the unit section. (a) $e_2 = 0.00525$; (b) $e_2 = 0.0423$; (c) $e_2 = 0.0699$; (d) $e_2 = 0.1163$.

When the stress ratios vary during deformation, McClintock's model leads to the condition given by

$$\int_0^{\bar{\varepsilon}^f} \left[\frac{2}{\sqrt{3}(1 - n)} \sinh\left\{ \frac{\sqrt{3}(1 - n)}{2} \frac{\sigma_a + \sigma_b}{\bar{\sigma}} \right\} + \frac{\sigma_b - \sigma_a}{\bar{\sigma}} \right] d\bar{\varepsilon} = K, \tag{14}$$

instead of Eq. (13), where K is the same factor as that in Eq. (13).

Another fracture criterion which will be considered in the present investigation is the one proposed by Cockroft and Latham [15], [16]. They proposed that fracture occurs when

$$\int_0^{\bar{\varepsilon}^f} \bar{\sigma}\left(\frac{\sigma^*}{\bar{\sigma}}\right) d\bar{\varepsilon} = C \tag{15}$$

for a given temperature and strain-rate, where σ^* = highest tensile stress and C = material constant. The proposed criterion is phenomenological and implies that ductile fracture is dependent both on shear strain and on tensile stresses. From the viewpoint of void growth, however, it appears more reasonable to include stress ratios in the formulation of fracture criterion. Thus, the Cockroft-Latham criterion is modified to

$$\int_0^{\bar{\varepsilon}^f} \left(\frac{\sigma^*}{\bar{\sigma}}\right) d\bar{\varepsilon} = C. \tag{16}$$

It may be of interest to note that Eq. (14) reduces to Eq. (16) with K = 2C, if the argument of sinh is small so that the hyperbolic sine function is approximated by a linear function. The magnitude of the argument of sinh depends on the stress state as well as on the work-hardening coefficient. When n = 1, Eqs. (14) and (16) are identical. For other values

of the work-hardening coefficient, the difference between the two criteria is small if $\frac{\sigma_a + \sigma_b}{\bar{\sigma}} < 1$, but increases with increasing values of $\frac{\sigma_a + \sigma_b}{\bar{\sigma}}$, as shown in Fig. 29.

We now examine in more detail the two criteria expressed by Eq. (14) and by Eq. (16).

A. Surface fracture

Since the fracture condition applicable to the free-surface cracks can be observed experimentally, several investigators [17]-[20] have used upsetting of cylindrical specimens for the study of ductile fractures. It was concluded from these investigations that the fracture criterion is expressed by

$$\varepsilon_1 = a - \frac{1}{2} \varepsilon_2, \tag{17}$$

where a is a material constant and ε_1 and ε_2 are the circumferential strain and the axial strain at the equatorial free surface, respectively. The two principal stresses in the surface, σ_1 and σ_2 ($\sigma_1 > \sigma_2$), during plastic deformation, are expressed by

$$\sigma_1 = \frac{\bar{\sigma}}{\sqrt{3}} \frac{2 + \alpha}{\sqrt{1 + \alpha + \alpha^2}} + \sigma_e , \quad \sigma_2 = \frac{\bar{\sigma}}{\sqrt{3}} \frac{1 + 2\alpha}{\sqrt{1 + \alpha + \alpha^2}} + \sigma_e , \tag{18}$$

where $\alpha = \frac{d\varepsilon_2}{d\varepsilon_1}$ and σ_e is a hydrostatic stress acting on the surface. The incremental effective strain $d\bar{\varepsilon}$ is given by

$$d\bar{\varepsilon} = \frac{2}{\sqrt{3}} \sqrt{1 + \alpha + \alpha^2}\, d\varepsilon_1 , \tag{19}$$

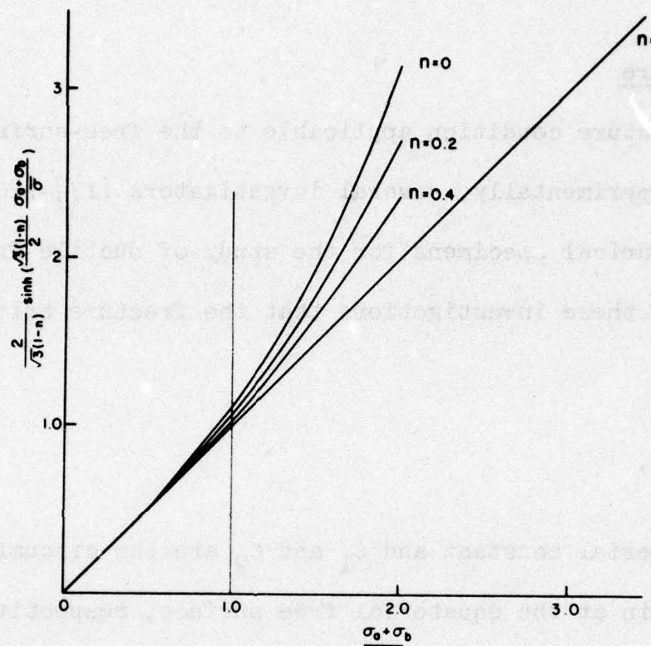

Fig. 29 Plot of hyperbolic sine function for various values of the work-hardening coefficient.

Under these conditions, the fracture criteria given by Eqs. (14) and (16) are both path-dependent, except when Eq. (16) becomes path-independent for $\sigma_e = 0$. Taking linear strain paths under $\sigma_e/\bar{\sigma}$ = const., and noting that σ_a and σ_b are the minimum and maximum stresses, respectively, Eq. (14) gives, for non-work-hardening materials (n = 0), the fracture strain as

$$\varepsilon_1^f = \frac{\sqrt{3}}{2\sqrt{1 + \alpha + \alpha^2}} \left[\frac{K}{\frac{2}{\sqrt{3}} \sinh\left(\frac{\sqrt{3}}{2} \frac{\sigma_1 + \sigma_2}{\bar{\sigma}}\right) + \frac{\sigma_1 - \sigma_2}{\bar{\sigma}}} \right] \tag{20}$$

for $\alpha \leq -\frac{1}{2}$, and

$$\varepsilon_1^f = \frac{\sqrt{3}}{2\sqrt{1 + \alpha + \alpha^2}} \left[\frac{K}{\frac{2}{\sqrt{3}} \sinh\left(\frac{\sqrt{3}}{2} \frac{\sigma_1 + \sigma_e}{\bar{\sigma}}\right) + \frac{\sigma_1 - \sigma_e}{\bar{\sigma}}} \right] \tag{21}$$

for $-\frac{1}{2} \leq \alpha \leq 0$. The criterion given by Eq. (16) becomes

$$\int^{\bar{\varepsilon}^f} \frac{\sigma^*}{\bar{\sigma}} \, d\varepsilon = \int_0^{\bar{\varepsilon}_f} \frac{\sigma_1}{\bar{\sigma}} \, d\bar{\varepsilon}$$

from which

$$\varepsilon_1^f = \frac{\sqrt{3}}{2\sqrt{1 + \alpha + \alpha^2}} \left(\frac{C}{\sigma_1/\bar{\sigma}}\right) = \frac{C}{\frac{2}{3}(2 + \alpha) + \frac{2}{\sqrt{3}}\left(\sqrt{1 + \alpha + \alpha^2}\left(\frac{\sigma_e}{\bar{\sigma}}\right)\right)}. \tag{22}$$

Eqs. (20), (21), and (22), with $\sigma_e/\bar{\sigma} = 0$ are plotted for K = 0.5 and C = 0.25 in Fig. 30.

It can be seen in Fig. 30 that the fracture line given by Eq. (22) has a slope of $-\frac{1}{2}$ for $\sigma_e/\bar{\sigma} = 0$ (free-surface cracks), and Eqs. (20) and

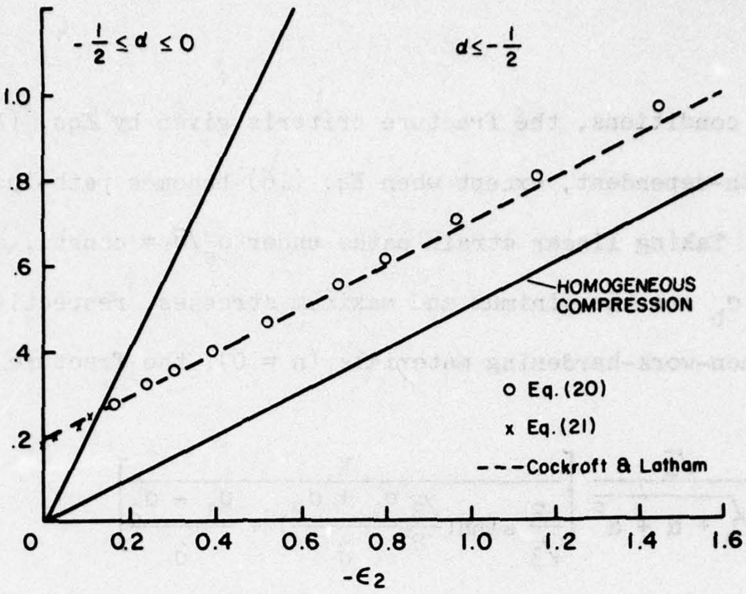

Fig. 30 Fracture conditions predicted from Eqs. (20) and (21) and by Cockroft and Latham [16].

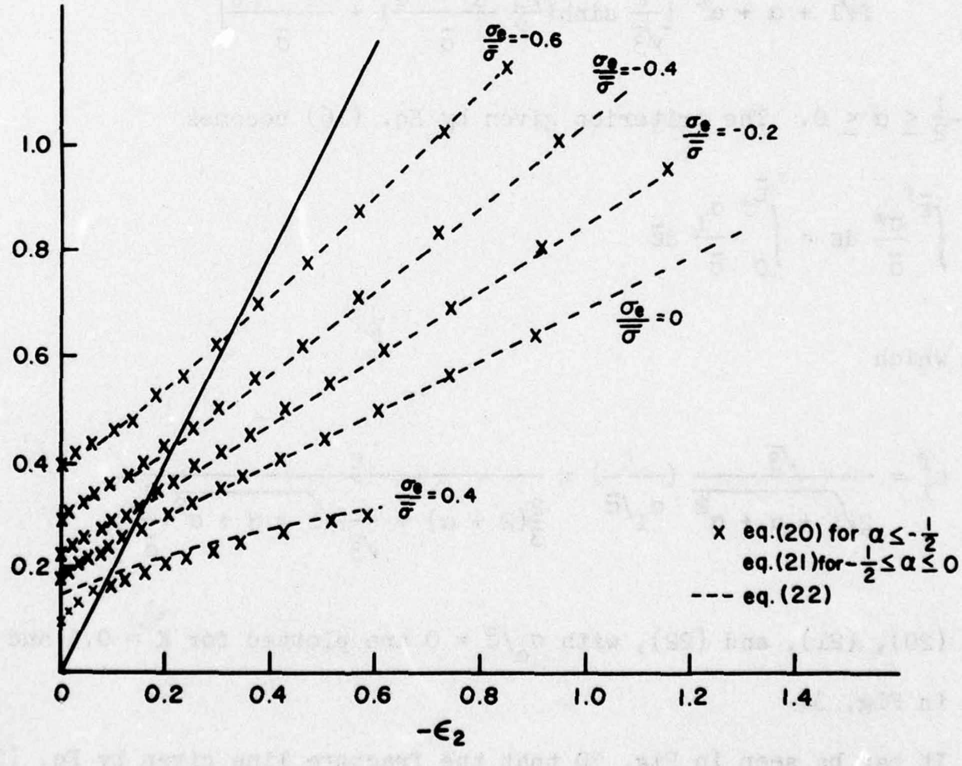

Fig. 31 Comparison of two fracture criteria for various values of $\sigma_e/\bar{\sigma}$.

(21) result in almost the same fracture strains as those according to Eq. (22) if the relationship K = 2C is maintained. Similar plots of Eqs. (20), (21), and (22) for various values of $\sigma_e/\bar{\sigma}$ are given in Fig. 31.

B. Fracture in uniaxial tension

Bridgman [21] investigated plastic flow and fracture with special emphasis on the effects of hydrostatic pressure, using uniaxial tension. The two criteria given by Eqs. (14) and (16) are examined for internal fracturing, using the Bridgman experimental results. In uniaxial tension of a bar, the critical site for fracture is at the axis of symmetry in the neck section where $\varepsilon_1 = \varepsilon_z$ and $\alpha = -\frac{1}{2}$. Therefore, $\sigma_a = \sigma_r = \sigma_e$ and $\sigma_b = \sigma_z = \bar{\sigma} + \sigma_r$. Then, Eq. (14) is expressed by

$$\int_0^{\bar{\varepsilon}^f} (F_1 + 1)\, d\bar{\varepsilon} = K, \qquad (23)$$

where $F_1 = h$ when $h > -1$,

$F_1 = -1$ when $h \leq -1$

and

$$h = \frac{2}{\sqrt{3}(1-n)} \sinh\left\{\frac{\sqrt{3}(1-n)}{2}\left(1 + 2\,\frac{\sigma_r}{\bar{\sigma}}\right)\right\},$$

assuming that the negative damage rate is not permitted.

The criterion given by Eq. (16) becomes

$$\int_0^{\bar{\varepsilon}^f} (F_2 + 1)\, d\bar{\varepsilon} = C, \qquad (24)$$

where

$$F_2 = \frac{\sigma_r}{\bar{\sigma}} \quad \text{for } \frac{\sigma_r}{\bar{\sigma}} > -1$$

and

$$F_2 = -1 \quad \text{for } \frac{\sigma_r}{\bar{\sigma}} \leq -1.$$

Eqs. (23) and (24) are compared with experiments in Figs. 32 and 33, respectively. The experimental results by Bridgman used for comparison are summarized in Table 5.

In deducing experimental points in the figures from the data in Table 5, several assumptions and approximations are introduced: (1) the effective stress $\bar{\sigma}$ was assumed to be independent of the hydrostatic pressure, (2) the stress σ_r at the neck was estimated according to the Bridgman analysis, and (3) the effect of work-hardening coefficients was neglected.

The comparison shown in Figs. 32 and 33 reveals that the fracture criteria are both reasonably good for predicting the fracture strains.

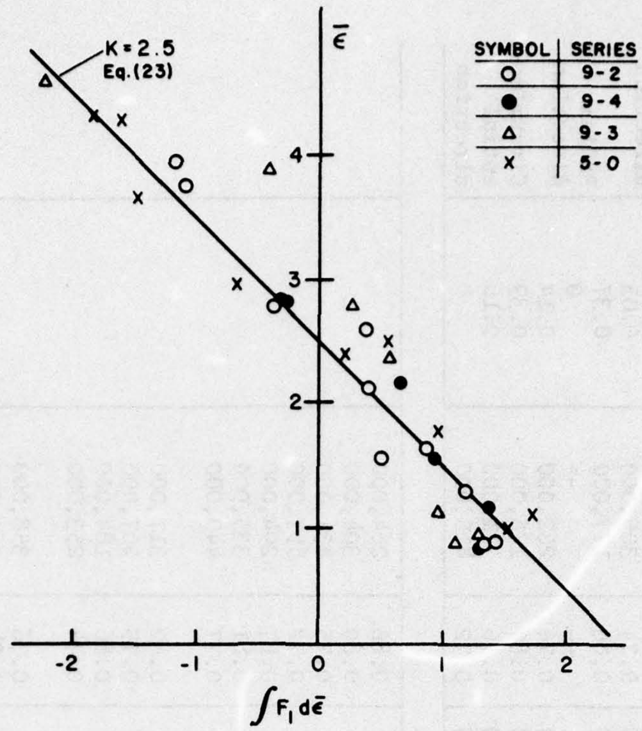

Fig. 32 Comparison between the fracture criterion given by Eq. (23) and Bridgman's fracture data.

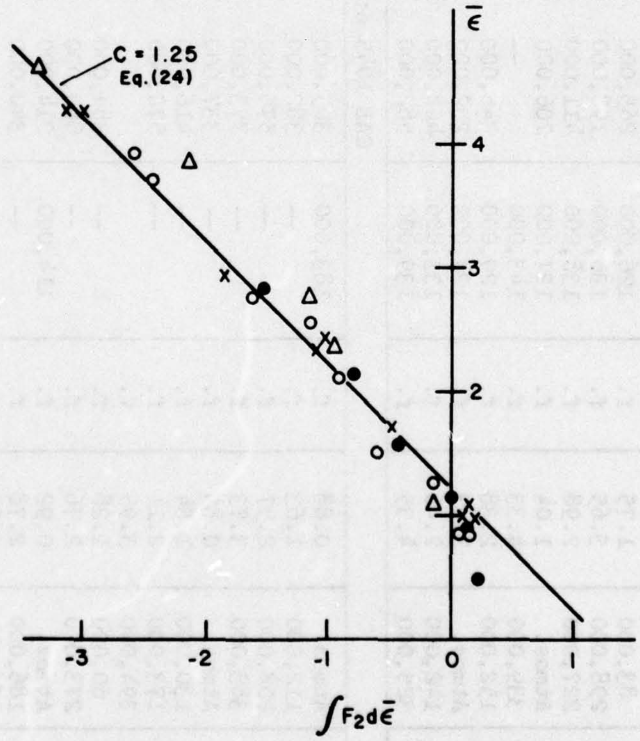

Fig. 33 Comparison between the fracture criterion given by Eq. (24) and Bridgman's fracture data.

Table 5 Bridgman experimental data.

Specimen	Pressure psi	Strain $\log_e A_i/A$	Fract. or not	Ave. stress at max.load psi	Ave.final stress,psi	a/R	Corr. factor	Final flow stress F,psi	Ratio of areas in fracture	Remarks
					Navy Gun Steel, as received					
5-0-1	Atmos.	1.12	f.	125,000	214,000	(0.74)	0.86	184,000	0.38	Longi-tudinal direction
5-0-2	83,000	1.75	f.	126,000	265,000	(1.19)	0.80	213,000	0.25	
5-0-3	298,000	3.65	f.	136,000	198,000	(1.96)	0.73	143,000	0	
5-0-5	227,000	2.98	f.	138,000	411,000	(1.78)	0.74	305,000	0.03	
5-0-6	Atmos.	1.04	f.	127,000	206,000	(0.70)	0.86	177,000	0.37	
5-0-8	339,000	4.33	f.	143,000	--	--	--	--	0	Radial direction
5-0-9	152,000	2.38	f.	129,000	345,000	(1.53)	0.76	262,000	0.14	
5-0-10	Atmos.	1.03	f.	124,000	202,000	(0.69)	0.87	175,000	0.39	Circumfer-ential direction
5-0-11	142,000	2.46	f.	133,000	408,000	(1.56)	0.76	311,000	0.16	
5-0-13	325,000	4.35	f.	139,000	582,000	(2.10)	0.72	415,000	0	
					SAE 1045 steel†					
9-2-1	Atmos.	0.88	f.	183,000	305,000	--	0.86	264,000		
9-2-6	112,000	1.63	f.	--	382,000	--	0.80	304,000		
9-2-7	208,000	2.57	f.	--	575,000	--	0.75	431,000		
9-2-8	383,000	3.73	f.	--	773,000	--	0.72	557,000		
9-2-18	Atmos.	0.85	f.	--	337,000	--	0.87	294,000		
9-2-20	130,000	1.54	f.	--	416,000	--	0.81	335,000		
9-2-22	173,000	2.11	f.	--	570,000	--	0.77	440,000		
9-2-23	394,000	3.95	f.							
9-2-24	60,000	1.28	f.	--	384,000	--	0.82	317,000		
9-2-26	273,000	2.76	f.	--	680,000	--	0.75	507,000		
9-3-1	Atmos.	0.92	f.	114,000	214,000	--	0.86	184,000		
9-3-5	186,000	2.78	f.	--	340,000	--	0.74	253,000		
9-3-6	269,000	3.87	f.							
9-3-7	145,000	2.37	f.	--	474,000	--	0.76	358,000		
9-3-9	34,000	1.10	f.	--	250,000	--	0.84	210,000		
9-3-10	387,000	4.61	f.							
9-3-11	Atmos.	0.81	f.	--	206,000	--	0.87	180,000		
9-4-1	Atmos.	0.89	f.	105,000	189,000	--	0.86	163,000		
9-4-7	18,000	1.13	f.	--	149,000	--	0.84	125,000		
9-4-9	116,000	2.14	f.	--	313,000	--	0.77	240,000		
9-4-12	Atmos.	0.90	f.	--	189,000	--	0.86	163,000		
9-4-13	74,000	1.56	f.	--	225,000	--	0.80	180,000		
9-4-14	182,000	2.83	f.	--	396,000	--	0.74	295,000		
9-4-15	389,000	4.80	f.							

Table 5 (continued)

†SAE 1045 steel

9-2 series: Quenched into water from 1575°F; drawn to 800°F

9-3 series: Quenched into salt at 800°F from 1575°F

9-4 series: Quenched into salt at 1100°F from 1575°F

III. WORKABILITY IN EXTRUSION

For workability in extrusion with reference to center bursting, experimental observations are limited and information about the stresses developed in metal being deformed by extrusion is insufficient. Thus, Latham and Cockroft [15] speculated the conditions in axisymmetric extrusion by assuming that the slip-line theory can be applied even though this is appropriate only to plane-strain conditions. Also, it was assumed that lubrication during cold extrusion is sufficiently good for the calculations to be based on zero friction. Based on the tensile plastic work density, they determined a damage factor for a range of extrusion conditions for several metals. Avitzur [22], [23] investigated theoretically center bursting in extrusion, using the upper-bound approach. Because the fracture condition was not incorporated in the approach, some objections may be raised regarding the validity of the results. However, the study led to defining the range of successful extrusions in terms of die angle, friction conditions, and the reduction.

Hoffmanner [24] also performed slip-line analysis for extrusion and compared with visioplasticity results for axisymmetric extrusion. He found that the calculated maximum center line principal stresses were in good agreement with visioplasticity results when the plane strain and axisymmetric results were compared on the basis of equal cross-sections. Combining the slip-line analysis for deformation and the fracture criterion proposed by Cockroft and Latham [16], Hoffmanner examined workability in extrusion. In Fig. 34, the three parabolic curves represent the process-

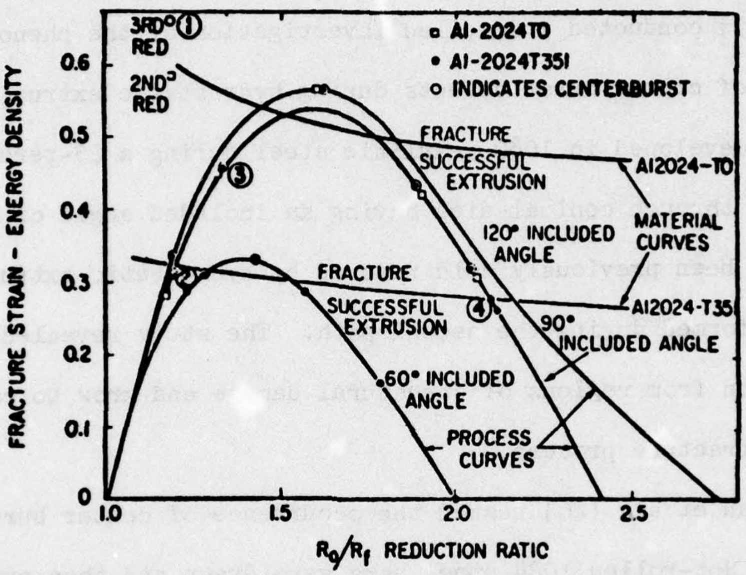

Fig. 34 Workability criteria for center burst based on a maximum tensile stress-strain energy criterion [23].

required strain energy as a function of the reduction ratio for three die angles. Whenever the process-required energy exceeds the energy available for successful deformation of the material, center burst should be observed. The extrusion observations are superimposed on these curves and demonstrate the near-perfect agreement between practice and prediction.

A. Experimental data

Pepe [25] conducted a detailed investigation of the phenomenological development of center burst defects during hydrostatic extrusion. Central bursts were developed in 1080 pearlitic steel during a 25-percent reduction in area pass through conical dies having an included angle of 45°. The material had been previously cold reduced by hydrostatic extrusion. Central bursts were formed during the second path. The study revealed that central bursts develop from regions of structural damage and grow to completion by a two-stage fracture process.

Zimmerman et al. [26] tested the occurrence of center bursting using 1024 steel. Hot-rolled 1024 steel bars were drawn and then extruded in three steps. The final extrusion step was utilized to examine, through a variety of die semi-angles, whether central bursting was produced or not. They found that among 4000 (1000 shafts from each of the four heats) shafts, center bursting was detected in about 45 shafts from one of the heats.

The above observations of center bursting in extrusion, as some other experimental studies show, were all made in material which has been pre-deformed. Although the present theoretical method is applicable to the determination of stress and strain distributions in extrusion for the material which has distributed strength and is capable of following the

previous deformation history, the experimental observation of center bursting during a single pass of deformation has been sought because the process condition in the computation can then be specified more faithfully according to the experimental procedure. In the present investigation, experiments reported by Hoffmanner [24] were used for examining the validity of the workability theory.

Hoffmanner observed center bursting in a single-step extrusion for aluminum alloy 2024-T351 at room temperature. The experimental conditions and the results were as follows:

1. Material: The specimens were obtained from a 3-inch diameter of aluminum alloy 2024 in as-received T351 condition.

2. Tensile test: Testing was performed at room temperature on an Instron testing machine at a nominal strain rate of 0.1 in/in/min. Measurements of extension were performed continuously until fracture with an extensometer exhibiting a strain sensitivity of at least 0.0005 in/in. Measurements of the minimum cross-sectional radius (a) and neck radius of curvature (R) were performed in two directions at 90° to each other either continuously by photographing the specimen or discontinuously by removing the specimen from the test fixtures and performing these measurements on an optical comparator.

3. Compression test: Compression testing was investigated by using simple upsetting of cylinders. For strain measurements, an orthogonal array of Vickers diamond pyramid impressions was accurately placed at 0.050-inch separations about the exact center of the specimens along subsequent directions of principal normal stress. These directions corresponded to the direction of loading and

the direction normal to it through the center of the specimen. Eight impressions were placed in each of the two directions.

4. Extrusion: Extrusion was performed at a ram speed of 12 in/min with dies of (60°), 90°, and (120°) included angles with anhydrous lanolin as a lubricant. Both the billets and the container were lubricated prior to extrusion and load-time curves were recorded on an oscillograph during deformation. The billets were machined with one end contoured to match the die and approximately 0.005 inch under the container diameter. A surface finish in the 20 to 30 microinch rms range was specified. Initial billet diameters of 1.780, 1.412, and 0.812 were used. The two larger diameters were used in extrusion through 90° dies to study single- and multiple-pass extrusion and the 0.812 diameter billets were used in single-pass reductions through all three die angles.

Results

1. Tension test results

Table 6

Specimen number	Gauge section diameter (inch)	Initial a/R ratio	Final a/R ratio	Fracture strain	Remarks
TNLH1	0.250	0	0.294	0.382	Longitudinal specimen
TNLH2	0.250	0	0.342	0.354	Longitudinal specimen
TNTH1	0.250	0	0	0.146	Transverse specimen
TNTH2	0.250	0	0	0.156	Transverse specimen

2. Compression test results

Table 7

Specimen no.	- Initial	Final	Initial height/diameter ratio	Fracture strain	Remarks
UHN-1(upset)	0.50	1.61	1.145	0.265	
UHN-2(upset)	0.50	-	2.24	-	Teflon lub., sheared over
UHN-3(upset)	0.50	1.58	1.145	0.281	

3. Extrusion results

Table 8

Specimen no.	R_o/R_f	Included die angle	Remarks
HN-101A	1.245	90°	Unlubricated, billet stuck
HN-101B	1.326	90°	Centerburst
HN-101C	1.249	90°	Centerburst
HN-451	1.157	90°	Centerburst
HN-452	2.328	90°	
HN-990	1.988	90°	Centerburst
HN-999	1.089	90°	
HN-90B	2.132	90°	

B. Computation, results, and discussion

Using the matrix method, the extrusion process was analyzed for the material, al alloy 2024-T351, and the detailed mechanics were presented in Part 1 of this report. The process conditions were: semi-cone angle $\alpha = 45°$, area reduction $R_i/R_0 = 1.25, 1.6, 1.8,$ and 2.0 for the two friction conditions, $f = 0$ and $0.4Y_0$. The critical site for occurrence of center bursting is along the axis of extrusion. The stress and strain states along the axis of extrusion resulted from the computation described in Part 1. Because the strain system along the axis of extrusion is identical

to that in uniaxial tension, the quantities necessary for workability are

$$\int_0^{\bar{\varepsilon}} (F_1 + 1)\, d\bar{\varepsilon} \quad \text{from Eq. (23) for one criterion}$$

and

$$\int_0^{\bar{\varepsilon}} (F_2 + 1)\, d\bar{\varepsilon} \quad \text{from Eq. (24) for another.}$$

These quantities are plotted as functions of area reduction in Figs. 35 and 36. From the figures, some conclusions immediately follow. The two quantities are almost identical, with a factor of 2. The magnitudes decreased greatly when work-hardening of materials was included. The magnitudes decreased further with friction at the die-workpiece interface. Note that the curve for non-work-hardening materials in Fig. 36 is in good agreement with the Hoffmanner result given in Fig. 34 for 90° included angle. This is somewhat surprising because the curve by Hoffmanner was obtained by approximations based on the slip-line analysis.

The critical values of these quantities (K in Eq. (23) and C in Eq. (24)) above which fracturing is predicted can be obtained from the fracture data in tension or compression tests. Hoffmanner estimated $C \simeq 0.3$ ($K = 2C$) from the tension test results. On the other hand, another estimate of $C \simeq 0.08$ was obtained from the compression test results. If we apply the critical value of $C = 0.3$ to the results in Fig. 36, fracturing should not occur in all the reductions. If we assume $C = 0.08$ to be a critical value, then center bursting would be observed over the range $1.08 < R_i/R_0 < 1.86$ with frictionless die and $1.16 < R_i/R_0 < 1.60$ with friction $f = 0.4Y_0$.

Although the prediction of workability with a critical value, $C = 0.08$, appears to be in good agreement with the experimental results in Table 8,

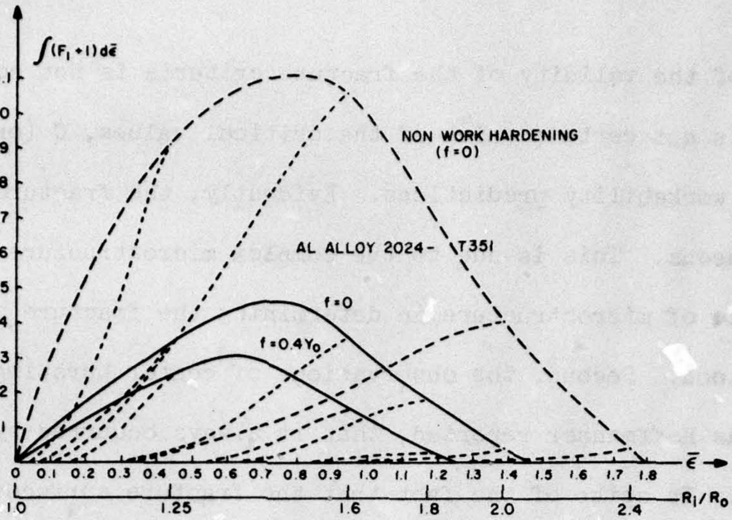

Fig. 35 Variations of $\int_0^{\bar{\varepsilon}} (F_1 + 1)\, d\bar{\varepsilon}$ as a function of area reduction in extrusion. Materials: non-work-hardening and al alloy 2024-T351.

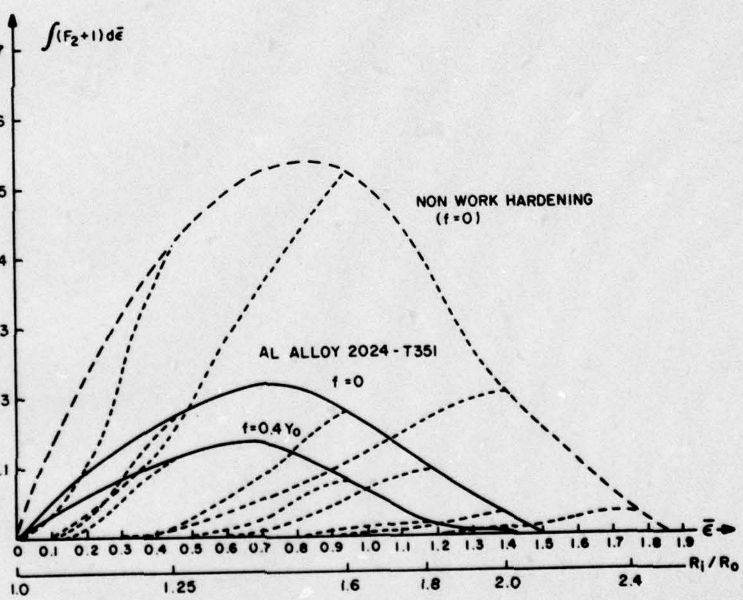

Fig. 36 Variations of $\int_0^{\bar{\varepsilon}} (F_2 + 1)\, d\bar{\varepsilon}$ as a function of area reduction in extrusion. Materials: non-work-hardening and al alloy 2024-T351.

the proof of the validity of the fracture criteria is not conclusive. First, it is not certain which of the critical values, C (or K), is proper to use for workability predictions. Evidently, the fracture behavior is not homogeneous. This is due to the complex microstructure of the material and the role of microstructure in determining the fracture strains is not yet understood. Second, the observations of center bursting in Table 8 revealed, as Hoffmanner reported, that it always occurred by complete separation. In spite of the fact that the fracture surfaces always possessed the centrally located conical cavity typical of the center burst, whether fracturing initiated at the center is in doubt.

IV. WORKABILITY IN DRAWING

To determine workability in drawing, the same approach as that for extrusion was applied. The process mechanics were analyzed by the matrix method and the stress and strain distributions along the axis of drawing were computed for various reductions of area. The tension and compression tests were performed to obtain the stress and strain property of the material and to determine the critical value for fracturing. Combining these data, the workability in drawing was predicted. The drawing experiments were conducted at room temperature to examine the predictions. The material was SAE 1144 cold-drawn steel. The stress-strain property of the material is given in Part 1.

A. Process mechanics

The process conditions were: semi-die angle $\alpha = 8°$; area reduction $R_i/R_0 = 1.05, 1.10, 1.2, 1.3$; and friction $f = 0, 0.25Y_0$. The stress and strain distributions were obtained and the significant quantities for fracturing were determined for each area reduction.

Because the two fracture criteria discussed in the previous sections resulted in almost identical predictions of fracture conditions, only the quantities (normalized energy density) defined by $\int_0^{\bar{\varepsilon}} (F_2 + 1)\, d\bar{\varepsilon}$ was shown as a function of the area reduction in Fig. 37. In calculating the energy density, the stress components were determined by correcting the hydrostatic part of the stress components from the total force balance. It is seen in Fig. 37 that the energy densities for the critical path along the axis of drawing increased monotonically with increasing area reduction.

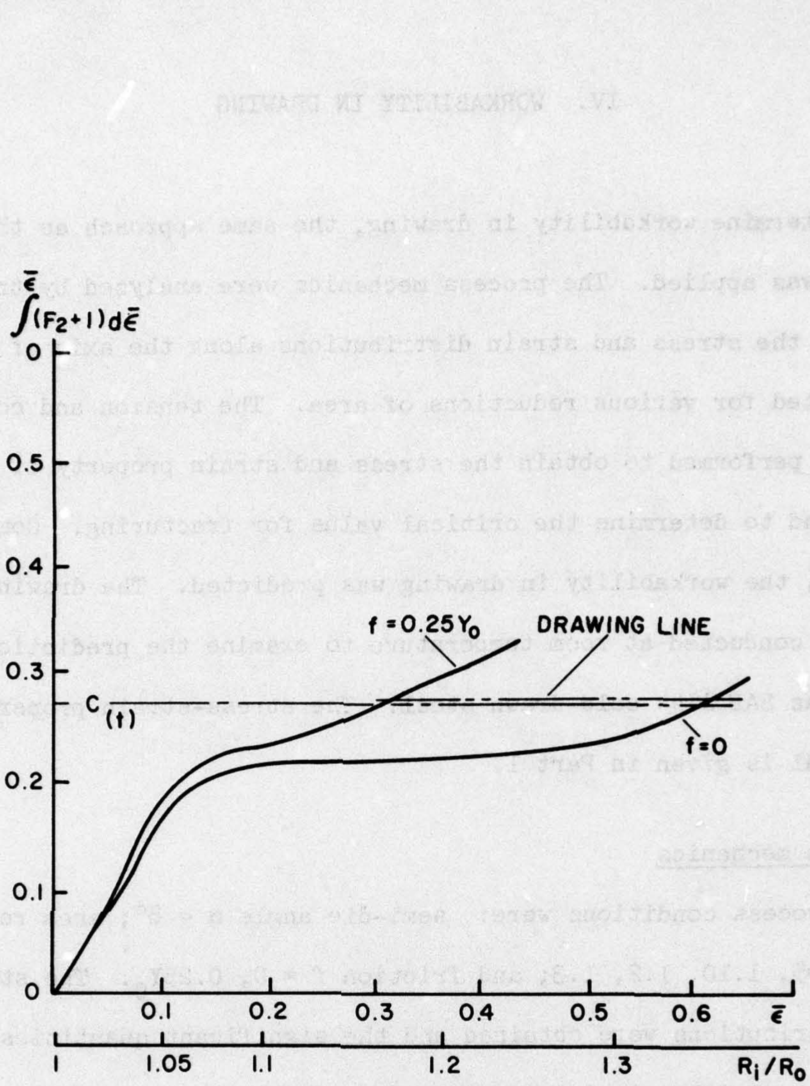

Fig. 37 Variations of $\int_0^{\bar{\varepsilon}} (F_2 + 1)\, d\bar{\varepsilon}$ as a function of area reduction in drawing. Material: SAE 1144 cold-drawn steel.

They were larger for larger die-workpiece interface friction. This is contrary to the extrusion results shown in Figs. 35 and 36. To determine workability, this energy density level must be compared with the critical value C for fracturing, estimated from the fracture data in tension and compression tests.

B. Tension and compression tests

Tension specimens were machined longitudinally from a 0.5-in. diameter bar. Testing was performed on an Instron machine with a plate speed of 0.02 in/min. The load-displacement curve was recorded and the instantaneous neck radii, as well as neck diameter, was measured until fracture. The critical energy density was estimated from the tension test as $C_{(t)} = 0.271$. The Bridgman analysis was used for an approximate stress analysis during neck formation.

Compression specimens were machined from the same bar of 0.5-in. diameter. The height and the diameter of the specimens were 0.50 in. and 0.49 in., respectively. The grid lines were printed on the cylindrical surface of the specimens, and the strains at fracture were determined from the grid distortion of the deformed specimens. The critical value C was estimated from the fracture strains according to Eq. (22) and was given by $C_{(c)} = 0.093$. It is to be noted that the fracture behavior is different in tension and in compression.

C. Workability

The energy density in drawing shown in Fig. 37 is compared with the critical value for fracturing in order to predict workability of SAE 1144

steel in drawing. It is seen again that the prediction is drastically different depending upon which critical value of tension and compression is applied. With the critical value of 0.09 which was estimated from the compression tests, center bursting would occur in all drawing with the area reduction larger than $R_i/R_0 = 1.03$, with very little effect of die-workpiece interface. On the other hand, if $C_{(t)}$ is taken as the critical value, the prediction is that for frictionless dies no center burst would occur up to $R_i/R_0 = 1.36$, and that this limiting value decreases with increasing die friction; for example, for friction $f = 0.25Y_0$, center burst would not be observed for R_i/R_o less than 1.16.

In order to examine the workability predictions, bar drawing experiments were performed. The bar specimen configuration is shown in Fig. 38. A threaded grip was used for drawing. This scheme, however, sets the drawing limit according to the maximum drawing force which can be sustained by the threaded part of the specimen. Commercially available carbide drawing dies with 8° semi-included die angle were used. The steady-state drawing force was measured, and the occurrence of center bursting was checked with drawn bars. The experimental conditions and results are summarized in Table 9.

Table 9 Experimental conditions and results.

Specimen no.	(Outlet diam.) $2R_0$	(Inlet diam.) $2R_i$	(Reduc. ratio) R_i/R_0	Lubrication	Ave. drawing pressure $(L/\pi R_0^2 Y_0)$	Center bursting
4	0.388"	0.485"	1.25	White lead in oil	0.907	No
8	0.388"	0.465"	1.198	"	0.713	No
5	0.4195"	0.485"	1.156	"	0.691	No
16	0.4195"	0.465"	1.108	"	0.361	No
1	0.451"	0.485"	1.075	"	0.435	No
9	0.451"	0.465"	1.031	"	0.428	No
21	0.451"	0.5"	1.109	Dry	0.664	No
7	0.465"	0.465"	1.198	Dry	0.997	No

In Fig. 38 the experimental and theoretical average drawing stresses were plotted as functions of the reduction ratio R_i/R_0. Theoretical curves were for frictionless dies ($f = 0$) and for the frictional stress $f = 0.25Y_0$. The experimental values with and without lubrication fell between these two theoretical curves. The drawing limit due to the present experimental scheme is also shown in Fig. 38. Under the lubricated condition, drawing over the reduction range of $R_i/R_0 = 1.031 \sim 1.25$ produced no center bursting. This suggests that the use of the critical value $C_{(c)}$, estimated from the compression fracture data for workability prediction, was not appropriate. With regard to the critical value of $C_{(t)} = 0.271$, it was found that the drawing limit set by the present experimental scheme was very close to the critical value $C_{(t)}$, as shown in Fig. 37. In fact, drawing was not possible for three cases of drawing under the dry condition. As a result, it was not possible to determine the applicability of $C_{(t)}$ as a fracture criterion to the occurrence of center bursting in bar drawing.

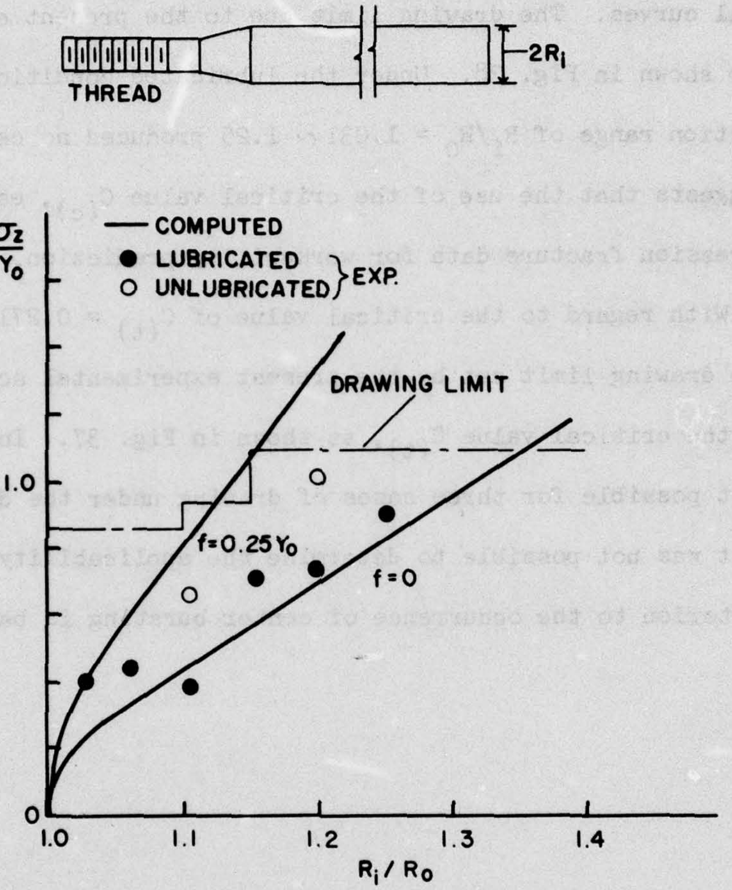

Fig. 38 Computed and experimental average drawing stress as functions of area reduction.

V. SUMMARY AND DISCUSSION

For workability in metalworking processes, formulation of a ductile fracture criterion must be simple (or in the form of easy applicability) and yet reflect physical mechanisms of fracture so that the predicted fracture behavior is close to the one of real materials within reasonable accuracy. With a two-size voids model a modified interpretation to the McClintock formulation of fracture strains was given. It was shown then that this formulation and the one by Cockroft and Latham resulted in almost identical fracture strains for occurrence of free-surface cracks and for fracturing in uniaxial tension. It was demonstrated further that these formulations predicted reasonably well the experimentally observed fracture strains. In examining the validity of the prediction by experiments, the stress-strain histories at a critical site were determined by using the continuous experimental observations on distortion in the case of surface cracks and by the Bridgman analysis combined with experimental measurements of load and neck geometry in the case of uniaxial tension. In applying the criteria to occurrence of center bursting in axisymmetric extrusion and drawing, the determination of stress and strain paths at a critical site was provided theoretically by the matrix method of analysis. The critical value of the material's capability against fracturing was obtained by tension and compression experiments. Workability in extrusion was examined for aluminum alloy 2024-T351 using the data found in the literature and the experiments of workability in drawing was attempted for SAE 1144 cold-drawn steel to test the predictions. The results of

validation were inconclusive. This is attributed to the fact that the fracture behavior has directionality as evidenced from the tension and compression fracture data. Furthermore, most of the previous investigations on center bursting in extrusion and drawing have reported observations of center bursting in pre-deformed materials. Although al alloy 2024-T351 was reported to have produced center bursting in a single extrusion path at room temperature, it occurred always by complete separation. With regard to bar drawing of SAE 1144 steel, the drawing limit set by the present experimental scheme was very close to the limiting energy density level, thereby making it extremely difficult to perform drawing near the critical boundary of the sound and defect zones.

In spite of inconclusive results of workability, the present investigation revealed several significant findings. In extrusion, the energy density level critical for center bursting was less for work-hardening materials when compared with that for a non-work-hardening material. This energy density level is reduced with increasing friction at the die-workpiece interface. It increases first with increasing area reduction and then decreases indicating a maximum as a function of area reduction. In drawing, the energy density level monotonically increases with the area reduction, and increases, as opposed to that in extrusion, with increasing interface friction.

Although conclusive validity of the present workability theory in extrusion and drawing awaits more extensive and systematic experimental investigations, as well as theoretical calculations, the method of computation is available and the approach has been cleared toward complete understanding of ductile fracture in metalworking processes.

REFERENCES

1. S. N. Shah, S. I. Oh, and Shiro Kobayashi, "Theories on Flow and Fracture in Metalworking Processes," USAF Technical Report AFML-TR-76-1, May 1976.

2. C. H. Lee and S. Kobayashi, "New Solutions to Rigid-plastic Deformation Problems Using a Matrix Method," Trans. ASME, J. of Engrg for Ind., vol. 95, 1973, pp. 865-873.

3. K. Washizu, Variational Methods in Elasticity and Plasticity, Pergamon Press, 1950.

4. O. C. Zeinkiewicz and Y. K. Cheung, The Finite-Element Method in Structural and Continuum Mechanics, McGraw-Hill, London, 1967.

5. G. Strang and G. J. Fix, An Analysis of the Finite-Element Method, Prentice-Hall, Englewood Cliffs, N.J., 1973.

6. S. N. Shah and Shiro Kobayashi, "A Theory on Metal Flow in Axisymmetric Piercing and Extrusion," to be published in J. Prod. Engrg, vol. 1, 1977.

7. T. Murota, T. Jimma, and K. Kato, "Analysis of Axisymmetric Extrusion," Bulletin of the JSME, vol. 13, 1970, pp. 1366-1374.

8. K. Iwata, K. Osakada, and S. Fujino, "Analysis of Hydrostatic Extrusion by the Finite-Element Method," Trans. ASME, J. of Engrg. for Ind., vol. 94, 1972, pp. 697-703.

9. C. H. Lee, H. Iwasaki, and S. Kobayashi, "Calculation of Residual Stresses in Plastic Deformation Processes," Trans. ASME, J. of Engrg. for Ind., vol. 95, 1973, pp. 283-291.

10. E. H. Lee, R. L. Mallett, and W. H. Yang, "Stress and Deformation Analysis of the Metal Extrusion Process," SUDAM No. 76-2, Stanford University, June 1976.

11. A. H. Shabaik and E. G. Thomsen, "Investigation of the Application of the Visioplasticity Methods of Analysis to Metal Deformation Processes," Final Report-Part II, Department of the Navy, 1968.

12. J. G. Wistreich, "Investigation of the Mechanics of Wire Drawing," Proc. Inst. Mech. Engrs., vol. 169, 1955, pp. 654-665.

13. F. A. McClintock, "A Criterion for Ductile Fracture by the Growth of Holes," J. Appl. Mech., 1968, p. 363.

14. F. A. McClintock, S. M. Kaplan, and C. A. Berg, "Ductile Fracture by Hole Growth in Shear Band," Int. J. of Fracture Mechanics, vol. 2, 1966, p. 614.

15. D. J. Latham and M. G. Cockroft, "The Effect of Stress System on the Workability of Metals," National Engineering Laboratory, Report No. 216, February 1966.

16. M. G. Cockroft and D. J. Latham, "A Simple Criterion of Fracture for Ductile Metals," National Engineering Laboratory, Report No. 240, July 1966.

17. H. Kudo and K. Aoi, "Effect of Compression Test Condition upon Fracturing of a Medium Carbon Steel--Study on Cold Forgeability Test, Part II," J. Japan Soc. for Tech. of Plasticity, vol. 8, 1967, pp. 17-27.

18. S. Kobayashi, "Deformation Characteristics and Ductile Fracture of 1040 Steel in Simple Upsetting of Solid Cylinders and Rings," Trans. ASME, J. Engrg. Ind., vol. 92, 1970, pp. 391-399.

19. Shiro Kobayashi, C. H. Lee, and S. I. Oh, "Workability Theory of Materials in Deformation Processes," USAF Technical Report AFML-TR-73-192, May 1973.

20. P. W. Lee and H. A. Kuhn, "Fracture in Metal-working Processes," Technical Report to American Iron and Steel Institute, April 1972.

21. P. W. Bridgman, Studies in Large Plastic Flow and Fracture, Harvard University Press, Cambridge, Mass., 1964, pp. 51-57.

22. B. Avitzur, "Analysis of Central Bursting Defects in Extrusion and Wire Drawing," ASME Trans. J. Engrg. Ind., vol. 90, 1968, pp. 79-91.

23. Z. Zimmerman and B. Avitzur, "Analysis of the Effect of Strain Hardening on Central Bursting Defects in Drawing and Extrusion," ASME Trans. J. Engrg. Ind., vol. 92, 1970, pp. 135-145.

24. A. L. Hoffmanner, "Workability Testing Techniques," Technical Report AFML-TR-69-174, June 1969.

25. J. J. Pepe, "Central Burst Formation During Hydrostatic Extrusion," Metals Engineering Quarterly, February 1976, pp. 46-58.

26. Z. Zimerman, H. Darlington, and E. H. Kottcamp, Jr., "Selection of Operating Parameters to Prevent Central Bursting Defects During Cold Extrusion," Metal Forming Interrelation Between Theory and Practice, edited by A. L. Hoffmanner, 1970, pp. 47-62.

APPENDIX

COMPUTER PROGRAM OF THE MATRIX METHOD

FOR THE ANALYSIS OF AXISYMMETRIC EXTRUSION AND DRAWING

I. Program Interpretation and Input Data Cards

The program was written according to the numbering system of nodal points and elements and the mesh system as shown in the figure.

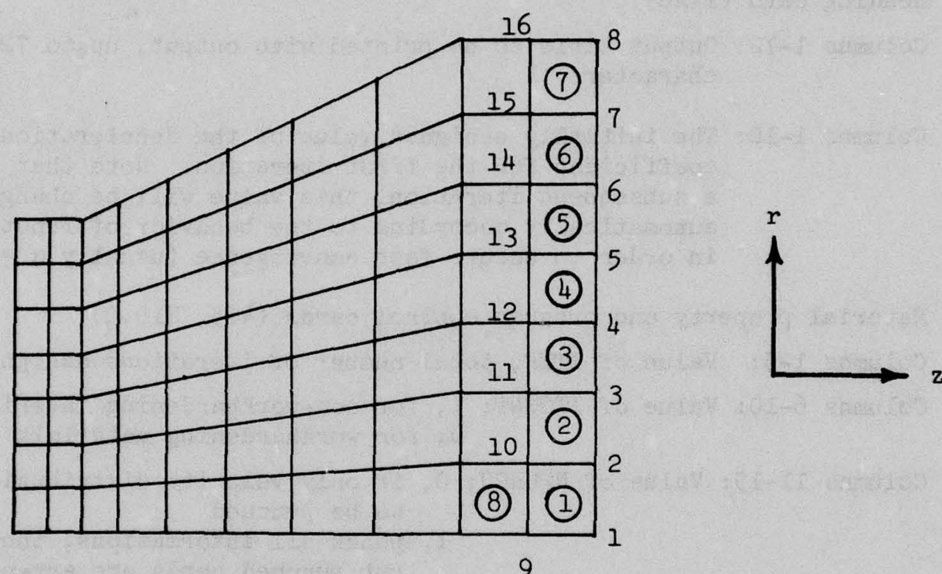

The four surrounding nodal points (I, J, K, L) of an element are arranged in a clockwise direction with the lowest index assigned to I (e.g., for the first element in the figure (I, J, K, L) = (1, 9, 10, 2)).

The output values of stress and die force are all normalized by the initial yield stress and are positive in the sense of positive r or z direction.

In addition to preparing the input data cards, the following variables in program PURT need to be specified according to the mesh system and geometry considered:

THETA: Semi-included angle of conical die

NIPTS: Number of lines in mesh system parallel to the axis of symmetry

NJPTS: Number of lines in mesh system perpendicular to the axis of symmetry

NTIMES: Number of flow lines to be constructed

NMAX: Total number of increments for strain integration

RENTER: Radius of the billet at entrance (it is convenient to choose RENTER = 1.0)

YEXIT: z-coordinate of the billet at the die exit (YEXIT = 0.0)

A. Sequence of input data card preparation for the main program

1. Heading card (12A6)

   Columns 1-72: Output title to be printed with output, up to 72 characters

2. Columns 1-10: The initially assigned value of the deceleration coefficient for the first iteration. Note that in a subsequent iteration, this value will be changed automatically according to the behavior of functions in order to ensure fast convergence (usually $\alpha = 0.5$)

3. Material property and program control cards (4I5, F10.0)

   Columns 1-5: Value of ITER, total number of iterations assigned

   Columns 6-10: Value of ITCONT; 1, for non-workhardening materials
   0, for workhardening materials

   Columns 11-15: Value of NPUNCH; 0, if only velocity distributions to be punched
   1, punch all informations; the output punched cards are arranged as follows:
   a. Nodal point velocity distributions (u_r, u_z) (8F10.6)
   b. Total effective strain $(\bar{\varepsilon})$ distribution (8F10.6)
   c. Strain rate $(\dot{\varepsilon}_r, \dot{\varepsilon}_z, \dot{\varepsilon}_\theta, \dot{\varepsilon}_{rz}, \dot{\bar{\varepsilon}})$ distributions (8F10.6)
   d. Stress $(\sigma_r, \sigma_z, \sigma_\theta, \sigma_{rz}, \bar{\sigma}, \sigma_m)$ distributions (8F10.6)
   e. Boundary nodal point forces and velocities (F_r, F_z, u_r, u_z) (8F10.6)

   Columns 15-20: Value of NPRINT; 1, if nodal point and element data are to be printed
   0, otherwise

   Columns 21-30: Value of FLIMIT, assigned value of accuracy desired $(\|\Delta u\|/\|u\|)$, program will stop if this value is achieved (recommend value is 0.00008)

4. Geometry and traction boundary control card (4I5)

Columns 1-5: Value of NUMNP, total number of nodal points

Columns 6-10: Value of NUMEL, total number of elements

Columns 11-15: Value of NUMPC, number of traction boundary condition cards to be read (see Sequence 6, below)

Columns 16-20: Value of NBF, total number of nodal points along the die surface at which force calculation is required (see Sequence 6, below)

5. Nodal point data cards (I5, F5.0, 2F10.0)

The numbering system of nodal points for the boundary conditions

Columns 1-5: Nodal point number

Columns 6-10: Code for this nodal point
0.0 if R- and z-forces are specified
1.0 if R-velocity and z-force are specified
2.0 if R-force and z-velocity are specified
3.0 if R- and z-velocity are specified
5.0 for special boundary condition (nodal points on die surface)

Columns 11-20: R-coordinate of the nodal point

Columns 21-30: z-coordinate of the nodal point

6. Force calculation nodal points cards (16I5)

These cards provide the nodal point numbers at which the force calculations are desired. Each card provides 16 nodal points punched in every five columns. The total number of these nodal points should be the same as NBF specified in Sequence 4.

7. Traction boundary condition cards (2I5, 4F10.0)

These cards provide prescribed traction stresses along boundaries. If the prescribed stresses are all zero or no traction stresses are prescribed (e.g., for the case of extrusion (or drawing) with frictionless dies), these cards can be omitted and put NUMPC = 0 of Columns 11-15 of Sequence 4.

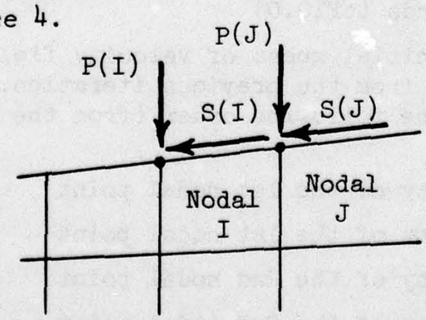

For the case with constant frictional stress (in terms of initial yield stress), these cards are needed. The total number of cards

AD-A048 842 CALIFORNIA UNIV BERKELEY DEPT OF MECHANICAL ENGINEERING F/G 13/8
DUCTILE FRACTURE IN AXISYMMETRIC EXTRUSION AND DRAWING. PART 1.--ETC(U)
JUN 77 C C CHEN, S I OH, S KOBAYASHI F33615-75-C-5151

UNCLASSIFIED AFML-TR-77-96 NL

2 OF 2
AD
A048 842

END
DATE
FILMED
2-78
DDC

should be the same as the value of NUMPC. The shear stress and the normal stress are positive in the direction shown in the figure, which is opposite to the output positive stress and die force directions.

Columns 1-5: Nodal point number for point I

Columns 6-10: Nodal point number for point J

Columns 11-20: Prescribed normal stress in terms of initial yield stress at point I

Columns 21-30: Prescribed normal stress in terms of initial yield stress at point J (if normal stresses are not prescribed, put 0.0 into these two values)

Columns 31-40: Prescribed shear stress in terms of yield stress at point I

Columns 41-50: Prescribed shear stress in terms of yield stress at point J (e.g., for the case of constant friction stress with $f = 0.4Y_0$, put "-0.4" into these two values)

8. Flow line data cards (8F10.0)

Specify the R-coordinates of every flow line to be constructed before entering the die. The total number of these points should be the same as NTIMES specified in the program PURT. Each card is to be punched 8 entering points each in 10 columns.

9. Element data cards (5I5)

For each element these cards provide the four surrounding nodal point numbers (I,J,K,L) in a clockwise direction

Columns 1-5: Element number

Columns 6-10: Nodal point number of point I

Columns 11-15: Nodal point number of point J

Columns 16-20: Nodal point number of point K

Columns 21-25: Nodal point number of point L

10. Input velocity field cards (8F10.0)

These cards can be an initial guess of velocity field or a new velocity field obtained from the previous iteration. These input cards are arranged in the following order (from the nodal point to the last nodal point)

Columns 1-10: R-velocity of the 1st nodal point

Columns 11-20: z-velocity of the 1st nodal point

Columns 21-30: R-velocity of the 2nd nodal point

Columns 31-40: z-velocity of the 2nd nodal point

Each card provides four nodal point velocities

B. Sequence of input data cards for program EXDRSUM

The output stress distributions from the matrix iteration method are different from a uniform hydrostatic stress from the actual solution over all elements in extrusion or drawing.

This program calculates the average extrusion (or drawing) stress by either the energy balance method or the method of zero total axial force at the entrance boundary (for drawing) or at the exit boundary (for extrusion). After the converged solution is obtained from the main program, the output punched cards are then used in this program to calculate the correct stresses according to the following sequence of input data cards:

1. Problem control card (I5)

   Columns 1-5: Value of IEXDR; 1, for the extrusion problem
   0, for the drawing problem

2. Geometry control card (4I5, F10.0)

   Columns 1-5: Value of NUMNP, same as in the main program

   Columns 6-10: Value of NUMEL, same as in the main problem

   Columns 11-15: Value of NIPTS, same as in the main problem

   Columns 16-20: Value of NBF, same as in the main problem

   Columns 21-30: Value of THETA, semi-included cone die angle

3. Initial yield stress card (F10.0)

   Columns 1-10: Value of YIELD, initial yield stress of the material considered

4. Nodal point data cards (I5, F5.0, 2F10.0)

   Same as Sequence 5 of the main program

5. Element data cards (5I5

   Same as Sequence 9 of the main program

6. Input strain-rate distribution cards

   From output of the main program (Sequence 3-c)

7. Input stress distribution cards

   From output of the main program (Sequence 3-d)

8. Input boundary nodal point force and velocity cards

   From output of the main program (Sequence 3-e)

II. Computer program listing

```
      PROGRAM EXDSM1(INPUT,OUTPUT,PUNCH)
C
C ***********************************************************************
C SINCE FOR EXTRUSION OR DRAWING, THE OUTPUT STRESS DISTRIBUTION FROM
C MATRIX ITERATION METHOD ARE IN DIFFERENCE OF A UNIFORM HYDROSTATIC
C PRESSURE FROM THE ACTURE SOLUTION OVER ALL ELEMENTS.   THIS PROGRAM
C CALCULATES THE AVERAGE EXTRUSION OR DRAWING PRESSURE AND THE CORREC-
C TION FACTOR OF THE MEAN STRESS.   THE OUTPUT STRESS AND DIE PRESSURE
C DISTRIBUTIONS OF THIS PROGRAM ARE THE ACTUAL SOLUTIONS.
C ***NOTE THAT ALL QUONTITIES INVOLVING VOLUMN OR SURFACE INTEGRAL ARE
C     MEASURED PER RADIAN(I.E. QUANTITIES DIVIDED BY (2*PAI))****
C ***NOTE ALSO ALL OUTPUT OF STRESSES AND DIE PRESSURE ARE IN TERMS
C     OF INITIAL YIELD STRESS  ***************
C ***********************************************************************
C
      DIMENSION R(242),Z(242),UR(20),UZ(20),F(20),EFSTRN(210),IEL(210,4)
     1 ,FZ(20),FR(20),STS(4,210),EFSTPS(210),ICAL(20),STSCR(4,210),
     2 UDIE(20),NF(20),CODE(210)
C
C ***********************************************************************
C   READ  PROGRAM AND GEOMITRY CONTROL CARDS
C IEXDR=1...AXI-SYMMETRIC EXTRUSION PROBLEM
C       0...AXI-SYMMETRIC DRAWING PROBLEM
C NUMNP=TOTAL NODAL POINTS
C NUMEL=TOTAL ELEMENTS
C NIPTS=TOTAL LINES IN MESH SYSTEM PARALLEL TO AXIS
C NBF=TOTAL INPUT CARDS OF SURFACE NODAL POINT FORCE FROM OUTPUT OF MAIN
C     PROGRAM.
C THETA=SEMI-INCLUDED CONIC DIE ANGLE
C YIELD=INITIAL YIELD STRESS
C ***********************************************************************
C
      READ 2300,IEXDR
      READ 2311,NUMNP,NUMEL,NIPTS,NBF,THETA
      READ 3312, YIELD
      PAI=4.*ATAN(1.)
      ANG=PAI*THETA/180.
      BCOS=COS(ANG)
      BSIN=SIN(ANG)
C
C ***********************************************************************
C READ NODAL POINT DATA AND ELEMENT DATA CARDS
C ***********************************************************************
C
      DO 100 I=1,NUMNP
      N=I
  100 READ 1000,N,CODE(N),R(N),Z(N)
      REXIT=R(NUMNP)
      RENTER=R(NIPTS)
      VEXIT=-(RENTER/REXIT)*(RENTER/REXIT)
      N=0
  130 READ 1001,M,(IEL(M,I),I=1,4)
  140 N=N+1
      IF(M-N) 170,170,150
  150 DO 160 J=1,4
  160 IEL(N,J)=IEL(N-1,J)+1
  170 IF(M-N) 180,180,140
  180 IF(NUMEL-N) 190,190,130
  190 CONTINUE
C
C ***********************************************************************
C READ INPUT DATA CARDS
C ALL INPUT DATAS BELOW ARE FROM THE OUTPUTS OF THE MAIN PROGRAM
C EFSTRN=EFFECTIVE STRAIN RATE
C STS(1,N)=R-STRESS OF N-TH ELEMENT
C STS(2,N)=Z-STRESS OF N-TH ELEMENT
C STS(3,N)=TH-STRESS OF N-TH ELEMENT
C STS(4,N)=RZ-STRESS OF N-TH ELEMENT
C EFSTRS=EFFECTIVE STRESS
C AX, AY ,AZ,AM STAND FOR INPUT DATAS WHICH ARE NOT USED IN DOING THIS
C              PROGRAM.
C UR,UZ,FR,FZ ARE THE VELOCITY AND FORCES AT NODAL POINT IN R AND Z-DIR.
C ***********************************************************************
C
      READ 1003,((AX,AY,AZ,AM,EFSTRN(N)),N=1,NUMEL)
      READ 1003,(((STS(I,N),I=1,4),EFSTPS(N),AX),N=1,NUMEL)
      DO 220 I=1,NBF
  220 READ 1002,NF(I),UR(I),UZ(I),FR(I),FZ(I)
      IF(IEXDR.EQ.1) PRINT 3303
      IF(IEXDR.EQ.0) PRINT 3304
      PRINT 2201
```

```
      PRINT 2202,(K,CODE(K),R(K),Z(K),K=1,NUMNP)
      PRINT 2204
      DO 250 I=1,NBF
      FR(I)=FR(I)/YIELD
      FZ(I)=FZ(I)/YIELD
      J=NF(I)
  250 PRINT 2203,NF(I),CODE(J),UR(I),UZ(I),FR(I),FZ(I)
C
C ***********************************************************************
C FRTOTL=TOTAL DIE FORCE IN Z-DIRECTION BEFORE CORRECTION
C ***********************************************************************
C
      FRTCTL=0.
      DO 300 I=1,NBF
      J=NF(I)
      IF(CODE(J).EQ.5.0.OR.CODE(J).EQ.15.0) GO TO 301
      GO TO 300
  301 FRTCTL=FRTOTL+FZ(I)
  300 CONTINUE
C
C ***********************************************************************
C METHOD=1...IF ENERGY BALANCE MEHOD IS USED
C        2...IF ZERO TOTAL Z-FORCE AT RIGID BOUNDARY METHOD IS USED
C ***********************************************************************
C
      DO 900 METHOD=1,2
      IF(METHOD.EQ.1) GO TO 901
      IF(METHOD.EQ.2) GO TO 902
C
C ***********************************************************************
C ***ENERGY BALANCE METHOD************
C CALCULATE DISSIPATION ENERGY RATE OVER DIE SURFACE DUE TO FRICTION
C ***********************************************************************
C
  901 CONTINUE
      FRICTN=0.
      DO 103 I=1,NBF
      J=NF(I)
      IF(CODE(J).EQ.5.0.OR.CODE(J).EQ.15.0) GO TO 102
      GO TO 103
  102 FRICTN=FRICTN+(FR(I)*RSIN+FZ(I)*RCOS)*(UR(I)*RSIN+UZ(I)*RCOS)
  103 CONTINUE
C
C ***********************************************************************
C CALCULATE TOTAL STRAIN ENERGY RATE OVER TEH DEFORMED PORTION
C ***********************************************************************
C
      DSENGY=0.
      DO 210 N=1,NUMEL
      EFSS=EFSTRN(N)
      IF(EFSTRN(N).LE.0.01) EFSS=0.0
      I1=IEL(N,1)
      I2=IEL(N,2)
      I3=IEL(N,3)
      I4=IEL(N,4)
      VOL1=(Z(I2)-Z(I1))*(R(I1)*R(I1)+R(I2)*R(I2)+R(I1)*R(I2))
      VOL2=(Z(I4)-Z(I3))*(R(I4)*R(I4)+R(I3)*R(I3)+R(I4)*R(I3))
      VOL3=(Z(I3)-Z(I2))*(R(I3)*R(I3)+R(I2)*R(I2)+R(I3)*R(I2))
      VOL4=(Z(I1)-Z(I4))*(R(I4)*R(I4)+R(I1)*R(I1)+R(I1)*R(I4))
      VOLUMN=(VOL1+VOL2+VOL3+VOL4)/6.
      DSENGY=DSENGY+EFSTRS(N)*EFSS*VOLUMN
  210 CONTINUE
C
C ***********************************************************************
C CALCULATE AVERAGE EXTRUSION PRESSURE OR AVERAGE DRAWING PRESSURE (EXT-
C   PSS) AND CORRECTION HYDROSTATIC PRESSURE(ALANDA) BY ENERGY BLANCE-
C   METHOD.
C ***********************************************************************
C
      PRINT 3300
      IF(IEXDR.EQ.1) GO TO 502
  501 EXTPSS=(DSENGY-FRICTN)*2./(-VEXIT*REXIT*REXIT)
      ALANDA=(2.*FRTOTL-EXTPSS*REXIT*REXIT)/(RENTER*RENTER-REXIT*REXIT)
      GO TO 503
  502 EXTPSS=(DSENGY-FRICTN)*2./(RENTER*RENTER)
      ALANDA=(2.*FRTOTL-EXTPSS)/(RENTER*RENTER-REXIT*REXIT)
      GO TO 503
C
  902 CONTINUE
C
C ***********************************************************************
C ******METHOD OF ZERO TOTAL Z-FORCE OVER THE RIGID BOUNDARY**********
C ***********************************************************************
```

```
EXDRSUM      C
EXDRSUM            NI=NIPTS-1
EXDRSUM            IF(IEXDR.EQ.1) GO TO 705
EXDRSUM      C
EXDRSUM      C ************************************************************************
EXDRSUM      C CHECK ELEMENTS NEXT TO RIGID BOUNDARY AT ENTRANCE FOR DRAWING
EXDRSUM      C ************************************************************************
EXDRSUM      C
EXDRSUM            DO 708 I=1,NI
EXDRSUM            J=I
EXDRSUM        706 IF(EPSTRN(J).LE.0.01) GO TO 707
EXDRSUM            ICAL(I)=J
EXDRSUM            GO TO 708
EXDRSUM        707 J=J+NI
EXDRSUM            GO TO 706
EXDRSUM        708 CONTINUE
EXDRSUM            GO TO 800
EXDRSUM      C
EXDRSUM      C ************************************************************************
EXDRSUM      C CHECK ELEMENTS NEXT TO RIGID BOUNDARY AT EXIT FOR EXTRUSION
EXDRSUM      C ************************************************************************
EXDRSUM      C
EXDRSUM        705 DO 718 I=1,NI
EXDRSUM            J=NUMEL-NI+I
EXDRSUM        716 IF(EPSTRN(J).LE.0.01) GO TO 717
EXDRSUM            ICAL(I)=J
EXDRSUM            GO TO 718
EXDRSUM        717 J=J-NI
EXDRSUM            GO TO 716
EXDRSUM        718 CONTINUE
EXDRSUM        800 CONTINUE
EXDRSUM      C
EXDRSUM      C ************************************************************************
EXDRSUM      C CALCULATE TOTAL Z-FORCE(BEFORE CORRECTION) FOR ELEMENTS NEXT TO
EXDRSUM      C    RIGID BOUNDARY
EXDRSUM      C ************************************************************************
EXDRSUM      C
EXDRSUM            TFORCE=0.
EXDRSUM            I=1
EXDRSUM            INDEX=1
EXDRSUM        801 KK=ICAL(I)
EXDRSUM            I1=IEL(KK,1)
EXDRSUM            I2=IEL(KK,2)
EXDRSUM            I3=IEL(KK,3)
EXDRSUM            I4=IEL(KK,4)
EXDRSUM            Z1=0.
EXDRSUM            Z2=(Z(I1)-Z(I2))/2.
EXDRSUM            R2=(R(I3)+R(I4))/2.
EXDRSUM            IF(INDEX.EQ.1) GO TO 808
EXDRSUM            AREA1=(R2*R2-R1*R1)/2.
EXDRSUM            AREA2=R1*Z2
EXDRSUM            GO TO 809
EXDRSUM        808 R1=(R(I1)+R(I2))/2.
EXDRSUM            AREA1=(R2*R2-R1*R1)/2.
EXDRSUM            AREA2=0.
EXDRSUM        809 TFORCE=TFORCE+AREA1*STS(2,KK)+AREA2*STS(4,KK)
EXDRSUM            IF(I.EQ.NI) GO TO 810
EXDRSUM            R1=R2
EXDRSUM            KABOVE=KK+1
EXDRSUM            IF(KABOVE-ICAL(I+1)) 753,750,753
EXDRSUM        750 I=I+1
EXDRSUM            INDEX=1
EXDRSUM            GO TO 801
EXDRSUM        753 IF(KABOVE.LT.ICAL(I+1)) KNEXT=KABOVE+NI
EXDRSUM            IF(KABOVE.GT.ICAL(I+1)) KNEXT=KABOVE-NI
EXDRSUM            I1=IEL(KNEXT,1)
EXDRSUM            I2=IEL(KNEXT,2)
EXDRSUM            I3=IEL(KNEXT,3)
EXDRSUM            I4=IEL(KNEXT,4)
EXDRSUM            R2=(R(1)+R(2)+R(3)+R(4))/4.
EXDRSUM            AREA1=(R2*R2-R1*R1)/2.
EXDRSUM            AREA3=R1*Z1
EXDRSUM            AREA2=R2*Z2
EXDRSUM            TFORCE=TFORCE+STS(2,KABOVE)*(AREA1+AREA3)+STS(4,KABOVE)*AREA2
EXDRSUM            R1=R2
EXDRSUM            Z2=(Z(I1)-Z(I2))/2.
EXDRSUM            Z1=Z2
EXDRSUM            IF(KNEXT .EQ. ICAL(I+1)) GO TO 803
EXDRSUM            KABOVE=KNEXT
EXDRSUM            GO TO 753
EXDRSUM        803 I=I+1
EXDRSUM            INDEX=2
EXDRSUM            GO TO 801
EXDRSUM      C
EXDRSUM      C ************************************************************************
EXDRSUM      C CALCULATE CORRECTION HYDROSTATIC PRESSURE BY REQUIRING TOTAL Z-FORCE
EXDRSUM      C EQUAL TO ZERO AFTER CORRECTION (ALANDA).  CALCULATE AVERAGE EXTRUSION
EXDRSUM      C PRESSURE OR AVERAGE DRAWING PRESSURE (EXTPSS) BY FORCE BALANCING.
EXDRSUM      C ************************************************************************
```

```
C
  810 PRINT 3301
      PRINT 2307,(ICAL(I),I=1,NI)
      IF(IEXDR.EQ.1) GO TO 811
      ALANDA=-(TFORCE/(RENTER*RENTER))*2.
      EXTPS1=-ALANDA*(RENTER*RENTER-REXIT*REXIT)+2.*FRTOTL
      EXTPSS=EXTPS1/(REXIT*REXIT)
      GO TO 503
  811 ALANDA=-(TFORCE/(REXIT*REXIT))*2.
      EXTPSS=-ALANDA*(RENTER*RENTER-REXIT*REXIT)+2.*FRTOTL
  503 CONTINUE
      PRINT 2301,EXTPSS
      PRINT 2302,ALANDA
C
C **********************************************************************
C CALCULATE THE ACTURE DIE PRESSURE
C **********************************************************************
C
      PRINT 3310
      DO 400 I=1,NBF
      J=NF(I)
      IF(CODE(J).EQ.5.0.OR.CODE(J).EQ.15.0) GO TO 409
      GO TO 400
  409 J2=J+NIPTS
      J1=J-NIPTS
      IF(J1.LT.NIPTS) J1=J
      IF(J2.GT.NUMNP) J2=J
      R1=(R(J)+R(J2))/2.
      R2=(R(J1)+R(J))/2.
      H=(Z(J1)-Z(J2))/2.
      AREA=(R1+R2)*SQRT((R2-R1)*(R2-R1)+H*H)/2.
      P=((FR(I)*BCOS-FZ(I)*BSIN)/AREA)+ALANDA
      PRINT 2303,J,CODE(J),R(J),Z(J),AREA,P
  400 CONTINUE
C
C **********************************************************************
C CALCULATE THE ACTURAL STRESS DISTRIBUTION
C **********************************************************************
C
      IF(METHOD.EQ.1) PRINT 3300
      IF(METHOD.EQ.2) PRINT 3301
      PRINT 2304
      DO 405 N=1,NUMEL
      STSCR(4,N)=STS(4,N)
      DO 406 I=1,3
  406 STSCR(I,N)=STS(I,N)+ALANDA
      AVES=(STSCR(1,N)+STSCR(2,N)+STSCR(3,N))/3.
  405 PRINT 2305,N,(STSCR(I,N),I=1,4),AVES,EFSTRS(N),EFSTRN(N)
  900 CONTINUE
C
 1000 FORMAT(I5,F5.0,5F10.0)
 1001 FORMAT(16I5)
 1002 FORMAT(I9,4F17.0)
 1003 FORMAT(8F10.0)
 2201 FORMAT(/,5X,*NODAL*,5X,*CODE*,5X,*R-COORD...*5X,*Z-COORD...*)
 2202 FORMAT(5X,I5,5X,F5.2,5X,F10.6,5X,F10.6)
 2203 FORMAT(2X,I5,5(2X,F10.6))
 2204 FORMAT(///,5X,*INPUT DATA*/,2X,*NODAL* ,6X,*CODE*,8X,*R-VELOCITY*
     1,2X,*Z-VELOCITY*,2X,*R-FORCE...*,2X,*Z-FORCE*)
 2300 FORMAT(I5)
 2301 FORMAT(//,5X,*AVERAGE EXTRUSION( OR DRAWING) PRESSURE=*,F12.6)
 2302 FORMAT(//,5X,*THE CORRECTION HYDROSTATIC PRESSURE=*,F12.6)
 2303 FORMAT(2X,*NODAL POINT=*,I4,2X,*CODE=*F5.2,2X,*R-COORD.=*F10.6,
     1 2X,*Z-COORD.=*F10.6,2X,*AREA=*,F10.6,2X,*DIE PRESSURE=*,F15.8)
 2304 FORMAT(/,10X,*ACTURAL STRESS DISTRIBUTION*//
     1,5X,*ELE.NO.*,5X,*R-STRESS*,5X,*Z-STRESS*,5X,*TH-STRESS*,
     2 5X,*RZ-STRESS*,*..MEAN STRESS..EF-STRESS*,3X,*EFF-STRAIN RATE*)
 2305 FORMAT(7X,I6,7F13.6)
 2307 FORMAT(//,5X,*ELEMENTS NEXT TO RIGID BOUNDARY=*,/,6X,16I5)
 2311 FORMAT(4I5,F10.0)
 3300 FORMAT(1H1,5X,*ENERGY BALANCE METHOD*)
 3301 FORMAT(1H1,5X,*TOTAL ZERO Z-FORCE AT  RIGID BOUNDARY METHOD*)
 3303 FORMAT(1H1,*....EXTRUSION PROBLEM....*)
 3304 FORMAT(1H1,*....DRAWING PROBLEM....*)
 3310 FORMAT(///,5X,*THE ACTUAL DIE PRESSURE DISTRIBUTION*)
 3312 FORMAT(F10.0)
      STOP
      END
```

```
      PROGRAM PURT(TAPE1,INPUT,OUTPUT,TAPE5=INPUT,TAPE6=OUTPUT,PUNCH)
C
C ***********************************************************************
C PROGRAM FOR STEADY STATE EXTRUSION OR DRAWING BY MATRIX METHOD.
C NOTE THAT THE FOLLOWUNG PROGRAM IS WRITING ACCORDING TO THE RIGHT
C ORDERING OF NODAL POINTS AND ELEMENT NUMBERS (SEE EXPLANATION)
C ***********************************************************************
C
      COMMON/GENCON/NUMNP,NUMEL,HED(12),VOL,NEQ,NS,ITERNO,ISTOP,
     1YIELD,MBAND,TEST,MDIAG,NBF,NUMPC,ITER,NBF2,NSCALE,NPUNCH,NPRINT,
     2 NCHECK,ACFINI
      COMMON /WALL/ THETA,FT,TANTH
      COMMON /STRPATH/ STEP,YSTART,YDIE,YEXIT,YMIN,RENTER,REXIT,VEXIT
      COMMON /DIMEN/ M1,M2,M3,M4,M5,M6,M7,M8,M9,M10,M11,M12,M13,M14
C
C ***********************************************************************
C  PROGRAM PURT IS FOR CONTROLLING THE DIMENSION OF THE COMPLETE PROGRAM
C  ITS PURPOSE IS TO PREVENT ASSIGNING A LARGER THAN NECESSARY DIMENSION
C  FOR ANY ARRAY THROUGH THE USE OF FOLLOWING STATEMENT...
C ***********************************************************************
C
      COMMON A(24650)
C
C ***********************************************************************
C  NFIELD IS THE DIMENSION OF ARRAY A. ITS VALUE CAN BE DETERMINED
C  PRECISELY BY RUNNING THE PROGRAM ONCE.
C ***********************************************************************
C
      NFIELD=24650
      PAI=4.*ATAN(1.0)
C
C ***********************************************************************
C  THETA              SEMI-INCLUDED CONIC DIE ANGLE.
C  YSTART             Z-COORDINATE OF STARTING POINT TO CALCULATE TOTAL
C                     EFFECTIVE STRAIN AND IS SETTING SLIGHTLY LESS THAN
C                     THE CENTER OF FIRST ELEMENT.
C  STEP               THE INCREMENT SIZE FOR STRAIN-RATE INTEGRATION
C  YDIE               Z-COORDINATE AT ENTRANCE TO THE DIE
C  YEXIT              Z-COORDINATE AT EXIT FROM DIE
C  YMIN               MINIMUM Z-COORDINATE OF THE CONTROL VOLUME
C  RENTER             RADIUS OF BILLET BEFORE EXTRUSION
C  REXIT              RADIUS OF BILLET AFTER EXTRUSION
C  VEXIT              EXIT VELOCITY OF THE PRODUCT
C  NTIMES             NUMBER OF FLOW LINES TO BE CONSTRUCTED
C  NIPTS              NUMBER OF LINES IN MESH SYSTEM PARALLEL TO AXIS
C  NJPTS              NUMBER OF LINES IN MESH SYSTEM PERPENDICULAR TO AXIS
C  NMAX               TOTAL NUMBER OF INCREMENTS FOR INTEGRATION
C ***********************************************************************
C
      THETA=6.
      THETA=THETA*PAI/180.
      TANTH=TAN(THETA)
      YEXIT=0.
      RENTER=1.0
      NTIMES=11
      NIPTS=7
      NJPTS=15
      NMAX=350
C
C ***********************************************************************
C       READ THE INPUT DATA CONTROL CARDS
C HED=OUTPUT TITLE UP TO 72 CHARACTERS.
C ACFINI=INITIAL DECCELARATION COEFFICINTS, FOR FIRST ITERATION ONLY.
C ITER=TOTAL NUMBER OF ITERATIONS ASSIGNED.
C ITCONT=1, FOR NONWORKHARDENING MATERIALS
C        0, FOR WORK-HARDENING MATERIALS.
C NPUNCH=0, IF NOTHING OTHER THAN VELOCITIES TO BE PUNCHED.
C        1, OTHERWISE.
C NPRINT=1, IF THE NODAL POINT DATAS TO BE PRINTED.
C        0, OTHERWISE.
C FLIMIT=VALUE OF (ERROR NORM)/(SOLUTION NORM) REQUIRED FOR FINAL RESULT
C NUMNP=NUMBER OF NODAL POINTS(TOTAL).
C NUMEL=NUMBER OF ELEMENTS(TOTAL)
C NUMPC=NUMBER OF TRACTION BOUNDARY CONDITIONS CARDS TO BE READ.
C NBF=NUMBER OF NODAL POINTS AT WHICH FORCE CALCULATIONS ARE REQUIRED.
C ***********************************************************************
C
      READ(5,1000) HED
      READ(5,1004)ACFINI
      READ(5,1003) ITER,ITCONT,NPUNCH,NPRINT,FLIMIT
      READ(5,1005) NUMNP,NUMEL,NUMPC,NBF
```

```
      NIPTS=NIPTS+1
      NBF2=NBF*2
      NB=NBF
      NB2=NBF2
      NEL=NUMEL
      NPC=NUMPC
      NEQ=3*NUMNP
      NO=NEQ
      NI=NIPTS
      NJ=NJPTS
C
C ************************************************************************
C DETERMINE THE LOCATION OF THE STARTING POINTS OF DIFFERENT ARRAYS ON
C ARRAY A
C ************************************************************************
C
      N1=1
      N2=N1+NUMNP
      N3=N2+NUMNP
      N4=N3+NUMNP
      N5=N4+NUMNP
      N6=N5+NUMNP
      N7=N6+4*NUMEL
      N8=N7+NUMEL
      N9=N8+6*NUMEL
      N10=N9+5*NUMEL
      N11=N10+5*NUMEL
      N12=N11+NBF
      N13=N12+NBF2
      N14=N13+2*NUMPC
      N15=N14+4*NUMPC
      N16=N15+NBF
      N17=N16+NBF
      N18=N17+NBF
      N19=N18+NTIMES
C
C ************************************************************************
C READ THE INPUT DATA
C ************************************************************************
C
      CALL PRELIM (A(N1),A(N2),A(N3),A(N4),A(N5),A(N6),A(N11),A(N13),
     1  A(N14),A(N18),NEL,NPC,NTIMES,NIPTS,YSTART,YMIN,REXIT)
      YDIE=(RENTER-REXIT)/TANTH
      VEXIT=-(RENTER/REXIT)**2
      STEP=(YSTART-YMIN)/(NMAX*1.15)
      WRITE(6,1007) ACFINI,ITCONT,FLIMIT
      WRITE(6,1008) STEP,YSTART,YDIE,VEXIT,YMIN,RENTER,REXIT,VEXIT,
     1 NTIMES,NIPTS,NJPTS,NMAX
C
      N20=N19+NEQ
C
C
C ************************************************************************
C SINCE AFTER THE SOLUTION OF STIFFNESS EQUATIONS, THE STIFFNESS MATRIX
C IS NOT NEEDED FOR THAT ITERATION, THE SPACE PROVIDED FOR STIFFNESS
C MATRIX WILL BE USED FOR CONSTRUCTION OF FLOW LINES AND FOR STRAIN-
C RATE INTEGRATION. THE NUMBERS M1 TO M14 ARE FOR DETERMINING THE
C LOCATION OF PROPER ARRAY
C ************************************************************************
C
      M1=1
      M2=M1+NI*NJ
      M3=M2+NI*NJ
      M4=M3+NJ
      M5=M4+NI
      M6=M5+NI*NJ
      M7=M6+NI*NJ
      M8=M7+NTIMES*NMAX
      M9=M8+NTIMES*NMAX
      M10=M9+NUMEL
      M11=M10+NUMEL
      M12=M11+NI*NJ
      M13=M12+NJ
      M14=M13+NTIMES*NMAX
C
C ************************************************************************
C HOWEVER,IF THE SPACE OF STIFFNESS MATRIX IS NOT ENOUGH FOR STRAIN RATE
C INTEGRATION, CREATES MORE SPACE AS REQUIRED.
C ************************************************************************
C
      NNN=MBAND*NEQ
      N21=N20+NNN
      IF(M14.GE.NNN) N21=N20+M14
      N22=N21+NBF2*(2*MBAND-1)
      N23=N22+NEQ
      N24=N23+NEQ
```

```
C
C ***********************************************************************
C N24 IS TOTAL SPACE REQUIRED, IF NFIELD , THE INITIAL ASSIGNED SPACE,
C IS NOT ENOUGH, STOP THE PROGRAM.
C ***********************************************************************
C
      IF(N24.LE.NFIELD) GO TO 100
      WRITE(6,1001) N24
      STOP
  100 CONTINUE
      WRITE(6,1002) N24
C
C ***********************************************************************
C THE FOLLOWING SUBROUTINE PLAST DOING THE MAIN PART OF MATRIX ITERATION
C METHOD OF PRESENT PROBLEM.
C ***********************************************************************
C
      CALL PLAST(A(N1),A(N2),A(N3),A(N4),A(N5),A(N6),A(N7),A(N8),A(N9),
     1A(N10),A(N11),A(N12),A(N13),A(N14),A(N15),A(N16),A(N17),A(N18),
     2A(N19),A(N20),A(N21),A(N22),A(N23),NO,NEL,NPC,NB2,
     3FLIMIT,ITCONT,NTIMES,NIPTS,NJPTS,NMAX)
C
 1000 FORMAT(12A6)
 1001 FORMAT(///* THE DIMENSION OF THE ARRAY (A) IS TOO SMALL*/
     1* THE SIZE OF THE ARRAY (A) MUST BE *, I7)
 1002 FORMAT(//* THE NECCESSARY SIZE OF THE ARRAY (A) IS*, I7)
 1003 FORMAT(4I5,F10.0)
 1004 FORMAT(8F10.0)
 1005 FORMAT(4I5)
 1007 FORMAT(//* ACOEF = *,F8.5,10X,* ITCONT = *,I2,
     1  10X,* FLIMIT=*,F10.6,//)
 1008 FORMAT(//* STEP SIZE = *,F8.4,10X,* YSTART = *,F8.4,10X,* YDIE = *
     1  F8.4,10X,* YEXIT = *,F8.4,//* YMIN = *,F8.4,10X,* RENTER = *,
     2  F8.4,10X,* REXIT = *,F8.4,10X,* VEXIT = *,F8.4,//* NTIMES = *,
     3  I4,10X,* NIPTS = *,I3,10X,* NJPTS = *,I3,10X,* NMAX = *,I4,/)
 1009 FORMAT(/ * STORAGE SPACE AVAILABLE FOR THE STRAIN CALCULATIONS IS
     1NOT ENOUGH*/)
C
      STOP
      END


      SUBROUTINE PRELIM (R,Z,UR,UZ,CODE,IEL,NF,IJBC,PSBC,RR,NEL,NPC,
     1  NTIMES,NIPTS,YSTART,YMIN,REXIT)
      COMMON/GENCON/NUMNP,NUMEL,HED(12),VOL,NEQ,NS,ITERNO,ISTOP,
     1YIELD,MBAND,TEST,MDIAG,NBF,NUMPC,ITER,NBF2,NSCALE,NPUNCH,NPRINT,
     2  NCHECK,ACFINI
      DIMENSION R(1),Z(1),CODE(1),UR(1),UZ(1),IEL( NEL ,1),NF(1),
     1  IJBC(NPC,1),PSBC(NPC,1),RR(1)
C
C ***********************************************************************
C THIS SUBROUTINE READS AND PRINTS ALL CONTROL INFORMATIONS AND
C NODAL POINT DATAS AND BOUNCARY CONDITIONS.
C ***********************************************************************
C
      WRITE(6,1000)
      WRITE (6,2000) HED,NUMNP,NUMEL
C
C ***********************************************************************
C CALCULATE INITINAL YIELD STRESS.
C ***********************************************************************
C
      CALL HARD(0.,YIELD)
      WRITE(6,2010) YIELD
      WRITE(6,2011)ITER
C
C ***********************************************************************
C     READ AND PRINT OF NODAL POINT DATA
C ***********************************************************************
C
      L=0
      IF(NPRINT.EQ.0) GO TO 60
      WRITE (6,1114)
      WRITE (6,2004)
   60 READ  (5,1002) N,CODE(N),R(N),Z(N)
   90 IF(NUMNP-N) 100,110,60
  100 WRITE (6,2009) N
      CALL EXIT
  110 CONTINUE
      YSTART=(Z(1)+Z(NIPTS+2))/2.-0.001
      YMIN=Z(NUMNP)
      REXIT=R(NUMNP)
      IF(NPRINT.EQ.0) GO TO 120
      WRITE (6,2002) (K,CODE(K),R(K),Z(K),K=1,NUMNP)
```

```
C
C ***********************************************************************
C     READ AND PRINT SPECIAL CONDITIONS ALONG BOUNDARY
C     NRF = TOTAL NUMBER OF NODAL POINTS AT WHICH FORCES ARE DESIRED
C     NF(I) = SEQUENTIAL NUMBER OF NODAL POINTS AT WHICH FORCES ARE DESIRED
C     RR(I)=R-COORDINATE OF FLOW LINES TO BE CONSTRUCTED AT ENTRANCE.
C ***********************************************************************
C
  120 READ(5,1003)      (NF(I),I=1, NRF)
      IF(NUMPC .LE. 0) GO TO 440
      WRITE(6,1007)
C
C ***********************************************************************
C SEE EXPLANATION OF INPUT DATA CARDS PREPARATION
C ***********************************************************************
C
      DO 441 I=1, NUMPC
      READ(5,1005) IJBC(I,1),IJBC(I,2),(PSBC(I,J),J=1,4)
  441 WRITE(5,1008)IJBC(I,1),IJBC(I,2),(PSBC(I,J),J=1,4)
  440 CONTINUE
      WRITE(6,1006) (NF(I),I=1,NRF)
      READ (5,1001) (RR(I),I=1,NTIMES)
      WRITE(6,1013) (RR(I),I=1,NTIMES)
C
C ***********************************************************************
C        READ AND PRINT OF ELEMENT PROPERTIES
C ***********************************************************************
C
      N=0
  130 READ (5,1003) M,(IEL(M,I),I=1,4)
  140 N=N+1
      IF (M-N) 170,170,150
  150 DO 160 J=1,4
  160 IEL(N,J)=IEL(N-1,J)+1
  170 IF (M-N) 180,180,140
  180 IF (NUMEL-N) 190,190,130
  190 CONTINUE
C
      IF(NPRINT.EQ.0) GO TO 210
      WRITE (6,2001)
      DO 205 N=1,NUMEL
  205 WRITE (6,2003) N,(IEL(N,I),I=1,4)
C
C ***********************************************************************
C     DETERMINE BAND WIDTH
C ***********************************************************************
C
  210 J=0
      DO 240 N=1,NUMEL
      DO 240 I=1,4
      DO 230 L=1,4
      KK=IABS(IEL(N,I)-IEL(N,L))
      IF(KK-J) 230,230,220
  220 J=KK
  230 CONTINUE
  240 CONTINUE
      MBAND=3*J+3
      MDIAG=1
  250 WRITE (6,1122) NEQ,MBAND,MDIAG
C
C ***********************************************************************
C FOR EACH ELEMENT, ASSIGN THE MEAN PRESSURE VALUE TO THE NODAL POINT
C OF THE HIGHEST NUMBER AMONG THE FOUR CORNER NODAL POINTS.
C ***********************************************************************
C
      NSTOP=0
      DO 370 J=1,NUMEL
      MID=MAX0(IEL(J,1),IEL(J,2),IEL(J,3),IEL(J,4))
      CODE(MID)=CODE(MID)+10.
      IF(CODE(MID).LT.20.) GO TO 370
      WRITE(6,1012) MID
      NSTOP=1
  370 CONTINUE
      IF(NSTOP.EQ.1) STOP
C
 1000 FORMAT(1H1)
 1001 FORMAT(8F10.0)
 1002 FORMAT (I5,F5.0,5F10.0)
 1003 FORMAT(16I5)
 1005 FORMAT(2I5,4F10.0)
 1006 FORMAT(// * THE NODAL POINTS AT WHICH FORCE CALCULATIONS ARE DESIR
     1ED* // 20I5)
 1007 FORMAT(1H1,15X, 39H LINEARLY DISTRIBUTED BOUNDARY STRESSES/
     1 /    * NODE-I..NODE-J...PRESSURE-I...PRESSURE-J*
     2  *           SHEAR I           SHEAR J*)
 1008 FORMAT(1H ,2I5,4E15.5)
```

```
 1012 FORMAT(/* NODAL POINT ERROR FOR POINT NO. *,I5,*.......IT CONTAINS
     1 MORE THAN ONE ELEMENT INFORMATION*/)
 1013 FORMAT(/* THE STARTING R-COORDINATES FOR STRAIN CALCULATIONS,*//
     1  11F9.4,/)
 1114 FORMAT(1H1, *   NODAL POINT INFORMATION*,//)
 1122 FORMAT(/// * NNUMBER OF EQUATIONS   =*, I4/
     1           * FANDWIDTH              =*, I4/
     2           * DIAGONAL ELEMENTS      =*, I4 )
 2000 FORMAT(1H  12A6/
     1 30H0 NUMBER OF NODAL PCINTS------ I3 /
     2 30H0 NUMBER OF ELEMENTS---------- I3 /)
 2001 FORMAT (1H1,40H ELEMENT NO.      I      J      K      L      )
 2002 FORMAT (I12,F12.2,2F12.3)
 2003 FORMAT (1I13,8I6,1I12)
 2004 FORMAT (/ ,* NODAL POINT        TYPE  R-ORDINATE   Z-ORDINATE*)
 2009 FORMAT (26H0NODAL POINT CARD ERROR N= I5)
 2010 FORMAT(// * INITIAL YIELD STRESS = *, F15.2//)
 2011 FORMAT(///*  MAXIMUM NUMBER OF ITERATIONS ALLOWED=*, I3)
      RETURN
      END

      SUBROUTINE PLAST(R,Z,UR,UZ,CODE,IEL,YY,STS,TEPS,EPS,NF,FPUR,
     1IJBC,PSBC,FR,FZ,SDIE,RR,B,A,FST,ALANDA,GVECTR,NQ,NEL,NPC,
     1NB2,FLIMIT,ITCONT,NTIMES,NIPTS,NJPTS,NMAX)
C
C *******************************************************************
C  PLAST IS THE CONTROLLING SUBROUTINE OF THE MATRIX METHOD
C *******************************************************************
C
      COMMON/GENCON/NUMNP,NUMEL,HED(12),VOL,NEQ,NS,ITERNO,ISTOP,
     1YIELD,MBAND,TEST,MDIAG,NBF,NUMPC,ITER,NBF2,NSCALE,NPUNCH,NPRINT,
     2  NCHECK,ACFINI
      COMMON /WALL/ THETA,FT,TANTH
      COMMON /DIMEN/ M1,M2,M3,M4,M5,M6,M7,M8,M9,M10,M11,M12,M13,M14
      DIMENSION R(1),Z(1),UR(1),UZ(1),CODE(1),IEL( NEL ,1),YY(1)
     1,STS(6,1),TEPS(5,1),EPS(5,1),NF(1),FPUR(1),IJBC(NPC,1),RR(1),
     2PSBC( NPC ,1),FR(1),FZ(1),SDIE(1),B(1),A( NQ,1),FST(NB2 ,1)
      DIMENSION ALANDA(1),GVECTR(1)
C
C*******************************************************************
C INITIALIZED ALL VARIABLES
C GVECTR(N) IS USED FOR STORING THE AMOUNT OF VELOCITY AND MEAN STRESS
C           TO BE MODIFIED FROM THE RESULT OF ITERATION,THESE VALUES
C           ARE REDUCED BY DECCELARATION COEFFICIENT IN ORDER TO ENSURE
C           THE CONVERGENCE OF THE SOLUTION.
C TEPS(5,N)=TOTAL EFFECTIVE STRAIN
C A, B, STAND FOR MATRICES IN EQUATION AX=B, AFTER SOLVINF THIS EQUATION
C       THE X VECTOR IS THEN STORED IN B
C YY(N)= EFFECTIVE STRESS
C TEPS(I,N)= TO STORE THE PREVIOUS VALUE OF YY(N) FOR CHECKING
C            CONVERGENCE FOR WORK-HARDENING MATERIAL
C TEPS(2,N)=DIFFERENCE OF EFFCTIVE STRESS BETWEEN THE PREVIOUS AND NEW
C            SOLUTIONS.(FOR WORK-HARDENING MATERIALS)
C ITST= INDEX FOR CONVERGENCE OF SOLUTIONS(ITST=2 INDICATES THE ITRATION
C         DOES NOT CONVERGENT)
C FSQRI,FF= TOTAL SQUARE NORM OF EQUATIONS IN MINIMIZATION
C FSQRS,FFFF= SQUARE NORM OF EQUATIONS CORRESSPONDING TO
C             INCOMPRESSIBILITY CONDITIONS(VOLUMN CONSISTANCE)
C DIFF=FF-FSQRI, DIFFERENCE OF TOTAL SQUARE NORMS OF PREVIOUS AND
C          PRESENT ITERATIONS
C*******************************************************************
C
      DO 998 I=1,M14
  998 A(I)=0.0
      DO 999 N=1,NEQ
      ALANDA(N)=0.
  999 GVECTR(N)=0.
      DO 442 N=1, NUMEL
      YY(N)=1.0
      DO 442 I=1, 5
  442 TEPS(I,N)=0.
      FSQRI=0.
      FSQRS=0.
      FFFF=0.
      ITST=1
      FF=0.
      DIFF=0.
C
C*******************************************************************
C  READ THE INPUT VELOCITY FIELD
C*******************************************************************
C
      READ(5,1017) (UR(I), UZ(I), I=1, NUMNP)
```

```
C
C***********************************************************************
C DOUBLE CHECK THE INPUT DATA
C***********************************************************************
C
      DO 9888 I=1,NUMNP
      IF(CODE(I).EQ.1..OR.CODE(I).EQ.11..OR.CODE(I).EQ.3..OR.CODE(I)
     1   .EQ.13.) UR(I)=0.0
      IF(CODE(I).EQ.5..OR.CODE(I).EQ.15.) UR(I)=UZ(I)*TANTH
 9888 CONTINUE
      WRITE(6,1020)
      WRITE(6,1017) (UR(I), UZ(I), I=1, NUMNP)
C
C***********************************************************************
C ITER=TOTAL NUMBER OF ITERATIONS ASSIGNED.
C ITERNO =  AN INDEX FOR QUAD1(SEE SUBROUTINE STIFF AND COMMENT BELOW)
C***********************************************************************
C
      ITERNO=1
      DO 2000 KIT=1,ITER
      INOCON=KIT
C
C***********************************************************************
C CHECK IF IT IS FIRST ITERATION
C IF FIRST ITERATION, ITERNO=1,PERFORM QUAD1.   OTHERWISE JUST READ
C RESULTS OF QUAD1 FROM TAPE 1.
C***********************************************************************
C
  579 IF(KIT-1) 599,599,598
C
C***********************************************************************
C NWKHRD IS AN INDEX  TO SUBROUTINE STIFF
C NWKHRD=1 JUST CALCULATE STRAIN RATE IN SUBROUTINE STIFF
C NWKHRD=0 DOING WHOLE THING IN SUBROUTINE STIFF
C***********************************************************************
C
  599 NWKHRD=0
      IF(ITCONT.NE.1) NWKHRD=1
      CALL STIFF (R,Z,UR,UZ,CODE,IEL,YY,STS,EPS,NF,FPUR,FST,
     1IJBC,PSBC,A,B,NEL,NO,NPC,NB2,ALANDA,NWKHRD)
      ITERNO=2
      IF(ITCONT.EQ.1) GO TO 593
C
C***********************************************************************
C UNNECESSARY TO CALCULATE TOTAL EFFECTIVE STRAIN FOR NON-HARDENING
C MATERIALS EXCEPT AT FINAL OUTPUT
C***********************************************************************
C
      CALL STRAINS(R,Z,UR,UZ,IEL,EPS,TEPS,A(M1),A(M2),A(M3),A(M4),A(M5),
     1  A(M6),A(M7),A(M8),A(M9),A(M10),A(M11),A(M12),RR,A(M13),NIPTS,
     2  NJPTS,NTIMES,NEL,NUMNP,NMAX)
C
C***********************************************************************
C CALCULATE NORMALIZED EFFECTIVE STRESS (FOR WORK-HARDENING)
C***********************************************************************
C
      DO 220 N=1, NUMEL
      CALL HARD(TEPS(5,N),YY(N))
      YY(N)=YY(N)/YIELD
  220 TEPS(1,N)=YY(N)
      NWKHRD=0
      CALL STIFF (R,Z,UR,UZ,CODE,IEL,YY,STS,EPS,NF,FPUR,FST,
     1IJBC,PSBC,A,B,NEL,NO,NPC,NB2,ALANDA,NWKHRD)
  593 CALL MODIFY (CODE,A,B,NUMNP,NEQ,MBAND)
  598 CONTINUE
C
C***********************************************************************
C SOLUTION FOR BANDED SYMMETRIC MATRIX
C***********************************************************************
C
      CALL TRIA(NEQ,MBAND,A)
      CALL BACKS(NEQ,MBAND,A,B)
C
C***********************************************************************
C SET CORRESSPONDING VALUE FOR INCLINED SPECIAL BOUNDARY CONDITIONS
C***********************************************************************
C
      DO 769 N=1, NUMNP
      IZ=3*N-1
      IR=IZ-1
  769 IF(CODE(N).EQ.5..OR.CODE(N).EQ.15.) B(IR)=B(IZ)*TAN(THETA)
C
C***********************************************************************
C IF FIRST ITERATION, SET INITIAL STEP LENGTH ACCORDING TO
C DECCELARATION COEFF. ASSIGNED. OTHERWISE FIND THE BEST DECCELARATION
C COEFF. FROM INFORMATION OF PREVIOUS ITERATION.
C***********************************************************************
C
```

```
  507 C4=0.0
      DO 509 I=1,NUMNP
      IZ=3*I-1
      IR=IZ-1
  509 C4=C4+B(IZ)*B(IZ)+B(IR)*B(IR)
      CORNOM=SQRT(C4)
      IF(KIT.EQ.1) GO TO 551
   67 ACOEF=1.0
  510 IF((ACOEF*CORNOM).LT.STEPLH) GO TO 550
  522 ACOEF=0.9*ACOEF
      GO TO 510
  551 ACOEF=ACFINI
      STEPLH=ACOEF*CORNOM
      STEPOR=STEPLH
  550 FF=FSOR1
      FFFF=FSOR5
C
C**********************************************************************
C  CALCULATE FORCES AT NODAL POINTS
C**********************************************************************
C
      CALL CFORCE(NF,FR,FZ,FST,FPUR,B,MBAND,NBF,NBF2)
      WRITE(6,1007)
      WRITE(6,1016) KIT
C
C**********************************************************************
C STS(6,N)=MEAN STRESS AT PRESENT SOLUTION.
C ALANDA(IR)=MEAN STRESS FROM PREVICUS SOLUTION. IF FIRST ITERATION,
C           THESE VALUES ARE THE SAME AS STS(6,N)
C**********************************************************************
C
      DO 133 N=1, NUMEL
      I=MAX0(IEL(N,1),IEL(N,2),IEL(N,3),IEL(N,4))
      IR=3*I
  112 STS(6,N)=B(IR)
      IF(KIT.EQ.1) ALANDA(IR)=B(IR)
      GVECTR(IR)=B(IR)-ALANDA(IR)
  133 B(IR)=0.
C
C**********************************************************************
C  CALCULATION OF SOLUTION NORM FOR VELOCITIES
C SNORM= NORM OF SOLUTION VECTOR OF VELOCITIES
C ENORM= NORM OF ERROR VECTOR OF VELOCITIES
C**********************************************************************
C
      SNORM = 0.
      DO 134 I=1, NUMNP
      IZ=3*I-1
      IR=IZ-1
      IN=IZ+1
      GVECTR(IR)=B(IR)
      GVECTR(IZ)=B(IZ)
      SNORM = SNORM + UR(I)*UR(I) + UZ(I)*UZ(I)
C
C**********************************************************************
C MODIFIY THE VELOCITY FIELDS AND MEAN STRESSES
C**********************************************************************
C
      ALANDA(IN)=ALANCA(IN)+GVECTR(IN)*ACOEF
      UR(I)=UR(I)+B(IR)*ACOEF
      UZ(I)=UZ(I)+B(IZ)*ACOEF
  134 CONTINUE
      ENORM=CORNOM
      SNORM = SQRT(SNORM)
      ESNORM=ENORM/SNORM
C
C *********************************************************************
C PRINT SOLUTION NORM OF VELOCITIES, VELOCITY DISTRIBUTIONS AND NODAL-
C POINT FORCES
C *********************************************************************
C
      IF(NBF .LE. 0) GO TO 125
      DO 123 I=1, NBF
      FR(I)=FR(I)*YIELD
      FZ(I)=FZ(I)*YIELD
  123 CONTINUE
  125 CONTINUE
      WRITE(6,1015) SNORM,ENORM,ESNORM
      WRITE(6,1006) KIT,ACOEF
      DO 439 I=1, NUMNP
      IZ=3*I-1
      IR=IZ-1
      WRITE(6,1002) I,B(IR),B(IZ),UR(I),UZ(I),R(I),Z(I)
  439 CONTINUE
      WRITE(6,1010)
      DO 140 I=1, NBF
      SHEAR=FZ(I)*COS(THETA) + FR(I)*SIN(THETA)
  140 WRITE(6,1012) NF(I),FR(I),FZ(I) ,SHEAR
```

```
C
C ********************************************************************************
C CONSTRUCT THE FLOW LINES AND CARRY OUT THE INTEGRATION OF THE STRAIN
C RATES TO DETERMINE THE TOTAL STRAIN DISTRIBUTION FOR WORK-HARDENING
C MATERIAL. THIS STEP IS PERFORMED ONLY AT FINAL ITERATION FOR NON-
C WORKHARDENING MATERIAL
C ********************************************************************************
C
  563 IF(ESNORM.LE.FLIMIT.OR.KIT.EQ.ITER) GO TO 56
      IF(ITCONT.EQ.1) GO TO 55
   56 IF(ITCONT.EQ.1) GO TO 58
      NWKHRD=1
      CALL STIFF (R,Z,UR,UZ,CODE,IEL,YY,STS,EPS,NF,FPUR,FST,
     1IJBC,PSBC,A,B,NEL,NO,NPC,NB2,ALANDA,NWKHRD)
   58 CALL STRAINS(R,Z,UR,UZ,IEL,EPS,TEPS,A(M1),A(M2),A(M3),A(M4),A(M5),
     1 A(M6),A(M7),A(M8),A(M9),A(M10),A(M11),A(M12),RR,A(M13),NIPTS,
     2 NJPTS,NTIMES,NEL,NUMNP,NMAX)
      IF(ITCONT.EQ.1) GO TO 55
      DO 230 N=1,NUMEL
      CALL HARD(TEPS(5,N),YY(N))
      YY(N)=YY(N)/YIELD
C
C ********************************************************************************
C TEPS(1,N)= PREVIOUS EFFECTIVE STRESS
C TEPS(2,N)=DIFFERENCE OF EFFCTIVE STRESS BETWEEN THE PREVIOUS AND NEW
C              SOLUTIONS.(FOR WORK-HARDENING MATERIALS)
C ********************************************************************************
C
      TEPS(2,N)=YY(N)-TEPS(1,N)
  230 TEPS(1,N)=YY(N)
C
C ********************************************************************************
C  PRINT THE STRESS AND STRAIN-RATE DISTRIBUTIONS AND THE EFFECTIVE
C  STRAIN DISTRIBUTION.
C ********************************************************************************
C
   55 CONTINUE
      WRITE(6,1007)
      WRITE(6,1005) KIT
      DO 222 N=1, NUMEL
      CONST=2.*YY(N)/(3.*EPS(5,N))
      STS(1,N)=EPS(1,N)*CONST
      STS(2,N)=EPS(2,N)*CONST
      STS(3,N)=EPS(3,N)*CONST
      STS(4,N)=EPS(4,N)*CONST/2.
      DO 132 J=1, 3
  132 STS(J,N)=STS(J,N)+STS(6,N)
      STS(5,N)=EFSTRS(STS(1,N),STS(2,N),STS(3,N),STS(4,N))
      WRITE(6,1004) N, ( EPS(I,N),I=1,5),TEPS(5,N),(STS(I,N),I=1,6)
  222 CONTINUE
C
C ********************************************************************************
C CHECK THE CONVERGENCE OF NEW SOLUTION, IF IT IS NOT, THEN REDUCE
C ACCEL. COEFF. AND CORRESPONDING STEP LENGTH AND CHECK IT AGAIN
C FOR FIRST ITERATION, THIS STEP IS OMITTED AND JUST COMPUTE THE TOTAL
C SQUARE NORM OF EQUATIONS AND INCOMPRESSIBILITY CONDITIONS
C ********************************************************************************
C
  564 NWKHRD=0
      CALL STIFF (R,Z,UR,UZ,CODE,IEL,YY,STS,EPS,NF,FPUR,FST,
     1IJBC,PSBC,A,B,NEL,NO,NPC,NB2,ALANDA,NWKHRD)
      CALL MODIFY (CODE,A,B,NUMNP,NEQ,MBAND)
C
C ********************************************************************************
C COMPUTE TOTAL SQUARE NORM OF EQUATIONS(FSQR1) AND SQUARE NORM OF
C INCOMPRESSIBILITY CONDITIONS(FSQR5)
C ********************************************************************************
C
      FSQR5=0.0
      FSQR1=0.0
      DO 501 N=1,NUMNP
      II=3*N
      FSQR1=FSQR1+B(II)*B(II)
      FSQR5=FSQR5+B(II)*B(II)
      DO 891 JJ=2,3
      II=II-1
      BLANII=B(II)
      JA=JJ
      JK=II+JA-1
  888 IF(JA.GT.MBAND) GO TO 889
      BLANII=BLANII-A(II,JA)*ALANDA(JK)
      JA=JA+3
      JK=JK+3
      GO TO 888
  889 IF(N.GT.1) GO TO 792
      GO TO 891
```

```
  792 DO 893 J=3,II,3
      KK=II+1-J
      IF(KK.GT.MBAND) GO TO 891
  893 BLANII=BLANII-A(J,KK)*ALANDA(J)
  891 FSQR1=FSQR1+BLANII*BLANII
  801 CONTINUE
      IF(KIT.EQ.1) GO TO 788
C
C *********************************************************************
C COMPARE SQUARE NORM OF FUNCTIONS WITH PREVIOUS ONE.
C *********************************************************************
C
      DIFF=FF-FSQR1
      IF(FSQR1-FF) 571,571,572
C
C *********************************************************************
C CASE FOR SQUARE NORM OF NEW SOLUTION LARGER THAN PREVIOUS ONE, REDUCE
C ACCEL. COEFF. BY HALF AND COMPARE AGAIN.
C *********************************************************************
C
  572 IF((ABS(DIFF)/FF).LE.1.E-3) GO TO 444
      STEPLH=0.5*STEPLH
      ACCEF=ACOEF*0.5
      INOCON=INOCON+1
      IF(INOCON-(KIT+5))581,581,582
  581 DO 595 I=1,NUMNP
      IZ=3*I-1
      IR=IZ-1
      IN=IZ+1
      ALANDA(IN)=ALANDA(IN)-GVECTR(IN)*ACOEF
      UR(I)=UR(I)-GVECTR(IR)*ACOEF
  595 UZ(I)=UZ(I)-GVECTR(IZ)*ACOEF
      WRITE(6,1155) STEPLH,FSQR1,FF,DIFF,FSQRS,FFFF
      WRITE(6,1030) ACOEF
      DO 772 I=1,NUMNP
      IZ=3*I-1
      IR=IZ-1
      WRITE(6,1002)I,B(IR),B(IZ),UR(I),UZ(I)
  772 CONTINUE
      IF(ITCONT.EQ.1) GO TO 564
      DO 561 N=1,NUMEL
  561 YY(N)=TEPS(1,N)-TEPS(2,N)*0.5
      GO TO 564
C
C *********************************************************************
C IF CONTINUOUS REDUCING DECCEL. COEFF. OF FIVE TIMES, THE SOLUTION
C STILL NOT CONVERGENT, THEN PUNCH AND PRINT THE RESULT AND STOP THE
C PROGRAM.
C *********************************************************************
C
  582 WRITE(6,1135) STEPLH,FSQR1,FF,DIFF,FSQRS,FFFF
      WRITE(6,1056)
      ITST=2
      GO TO 600
C
C *********************************************************************
C CASE FOR SQUARE NORM OF NEW SOLUTION LESS THAN PREVIOUS ONE, IF
C CONVERFENCE CHARACTER IS IN GOOD SITUATION, THEN INCREASE STEP
C LENGTH FOR NEXT ITERATION.
C *********************************************************************
C
  571 FSQR2=(STEPOR/STEPLH)*(FSQR1-FF)+FF
      IF(FSQR2-0.965*FF) 574,574,575
  575 STEPLH=0.8*STEPLH
      GO TO 444
  574 IF(FSQR2-0.900*FF) 576,576,444
  576 STEPLH=1.2*STEPLH
  444 CONTINUE
      STEPOR=STEPLH
      WRITE(6,1155) STEPLH,FSQR1,FF,DIFF,FSQRS,FFFF
  788 CONTINUE
C
C *********************************************************************
C STOP ITERATIONS AND PUNCH RESULTS IF (ERROR NORM)/(SOLUTION NORM)
C REACH THE ASSIGNED ACCURACY.
C *********************************************************************
C
      IF(ESNORM.LE.FLIMIT) GO TO 600
C
C *********************************************************************
C PUNCH SOLUTIONS AT EVERY FIFTH ITERATION BUT DOES NOT STOP THE
C ITERATIONS. PUNCH SOLUTIONS AT FINAL ITERATION.
C *********************************************************************
C
      K1=KIT/5
      K2=K1*5
```

```
      IF(K2.GE.KIT) GO TO 600
      IF(KIT.EQ.ITER) GO TO 600
      GO TO 660
  600 PUNCH 1017, (UR(I),UZ(I), I=1, NUMNP)
      NN=3*NUMNP
      IF(NPUNCH .EQ. 0) GO TO 660
      PUNCH 1017, (TEPS(5,N),N=1,NUMEL)
      PUNCH 1017, ( (EPS(I,N),I=1,5), N=1,NUMEL)
      PUNCH 1017,((STS(I,N),I=1,6),N=1,NUMEL)
      DO 100 I=1,NBF
      K=NF(I)
  100 PUNCH 1012,K,UR(K),UZ(K),FR(I),FZ(I)
  660 CONTINUE
      IF(ITST.EQ.2) GO TO 2205
      IF(ESNORM.LE.FLIMIT) GO TO 2205
 2000 CONTINUE
C
C *********************************************************************
C  PRINT THE FINAL STRAIN-RATES, THE INCOMPRESSIBILITY AND THE
C  INTEGRATED EFFECTIVE STRAIN DISTRIBUTION.
C *********************************************************************
C
 2205 CONTINUE
      WRITE(6,1019) KIT
      DO 500 N=1,NUMEL
      SUM=EPS(1,N)+EPS(2,N)+EPS(3,N)
  500 WRITE(6,1003) N,(EPS(I,N),I=1,5),SUM,TEPS(5,N)
      WRITE(6,2222) STEPLH
C
 1002 FORMAT(I10,2F13.7,10X, 2F13.7, 10X, 2F13.7)
 1003 FORMAT(I7,11F11.6)
 1004 FORMAT(I7,12F10.6)
 1005 FORMAT(1H1,* STRAIN RATE-STRESS SOLUTION AT ITER.  NUMBER  =*,I4//
     1 * EL. NO..R-STRAIN..Z-STRAIN.TH-STRAIN.RZ-STRAIN.EF-STRAIN.TOT.E
     2FF....R-STRESS..Z-STRESS.TH-STRESS.RZ-STRESS.EF-STRESS.AVG-STRESS.
     3.*,/,11X,*RATE*,6X,*RATE*,6X,*RATE*,6X,*RATE*,6X,*RATE*,8X,*STRAIN
     4*/)
 1006 FORMAT(///  30X, * VELOCITY     SOLUTION AT ITERATION NUMBER =*,I4
     1/,30X,* DECELARATION COEFFICIENT=* F13.8,
     1/// 15X,*CORRECTED AMOUNT OF VEL.*,15X,*NEW SOLUTION*,21X,*COORDIN
     1ATES*/,24X,*IN..*,29X,*OF*
     2   /* NODAL NO.      R-VELOCITY    Z-VELOCITY                R-VELOCITY
     3   Z-VELOCITY            R-COORD              Z-COORD*)
 1007 FORMAT(1H1)
 1010 FORMAT( //   * NODAL POINT FORCE*//
     1*.......N.P.........R-FORCE.......Z-FORCE......SHEAR FORCE ON DIE
     2  SURFACE...*)
 1012 FORMAT(I9,4F17.5)
 1015 FORMAT( //   50X, * NORM OF SOLUTION VECTOR =*, F13.8
     1           /  50X, * NORM OF   ERROR  VECTOR =*, F13.8
     2           /  50X, * FRACTIONAL  NORM        =*, F13.8)
 1016 FORMAT(/// 65X, *    VELOCITY  SOLUTION AT ITERATION NUMBER =*,I4)
 1017 FORMAT(8F10.6)
 1019 FORMAT(1H1,*FINAL STRAIN RATE SOLUTION AT ITER.NUMBER = *,I4,//
     1 * EL. NO...R-STRAIN...Z-STRAIN..TH-STRAIN..RZ-STRAIN..EF-STRAIN..
     2......SUM.......TOT-EF-STRAIN*,/,12X,*RATE*,7X,*RATE*7X,*RATE*
     3,7X,*RATE*,7X,*RATE*/)
 1020 FORMAT(//,* THE INITINAL GUESS( OR INPUT DATA) OF VELOCIT DISTRIBU
     1TION*,/,*      FROM FIRST NODAL POINT(R-VEL., Z-VEL.) TO LAST NODAL
     2 POINT(R-VEL., Z-VEL.)*)
 1030 FORMAT(///,25X,*THE ABOVE VELOCITY DISTRIBUTION DOES NOT CONVERGE*
     1/,25X,*REDUCE DECCELARATION COEFF. WITH THE FOLLOWING VELOCITY DIS
     1TRIBUTIONS*/,25X,*AND CALCULATE ALL NORMS AGAIN*
     1/,25X,*NEW DECCELARATION COEFFICIENT=*,F13.8,
     1 // 15X,*CORRECTED AMOUNT OF VEL.*,15X,*NEW SOLUTION*/,24X,*IN..*,
     129X,*OF*,/,
     2     * NODAL NO.      R-VELOCITY    Z-VELOCITY                R-VELOCITY
     3   Z-VELOCITY*)
 1056 FORMAT(///,20X,*SOLUTION DOES NOT CONVERGENT*)
 1155 FORMAT(////,25X,*STEP LENGTH FOR NEXT ITERATION=*F13.8,
     1          /,25X,*TOTAL SQUARE NORM OF ALL EQUATIONS AT PRESENT SOL
     1UTION=*E16.8,
     1          /,25X,*TOTAL SQUARE NORM OF ALL EQUATIONS FROM PREVIOUS
     1SOLUTION=*E16.8,
     1      /,25X,*DIFFERENCE=*E16.8,
     1//,25X,*SQUARE NORM OF PRESENT VALUE IN VOL.CONSISTANCE=*E16.8,
     1 /,25X,*SQUARE NORM OF PREVIOUS VALUE IN VOL.CONSISTANCE=*E16.8)
 2222 FORMAT(//,20X,*FINAL STEPLH=* F14.6)
C
      RETURN
      END
```

```
      SUBROUTINE HARD(STRAIN,YIELD)
C
C ***********************************************************************
C SPECIFY THE MATERIAL PROPERTIES FOR WORK-HARDENING MATERIAL (STRESS-
C STRAIN RELATIONSHIP) FOR NON-HARDENING MATERIAL, REPLACE *YIELD* CARD
C AND SET YIELD=THE CONSTANT YIELD STRESS.
C ***********************************************************************
C
      B=0.262E-4
      AN=0.06
      YIELD=(1.+STRAIN/B)**AN
      RETURN
      END


      SUBROUTINE STIFF (R,Z,UR,UZ,CODE,IEL,YY,STS,EPS,NF,FPUR,FST,
     1IJBC,PSBC,A,B,NEL,NO,NPC,NB2,ALANDA,NWKHRD)
C
C ***********************************************************************
C CALCULATION STIFFNESS MATRIX FOR ENTIRE SYSTEM.
C ***********************************************************************
C
      COMMON/GENCON/NUMNP,NUMEL,HED(12),VOL,NEQ,NS,ITERNO,ISTOP,
     1YIELD,MBAND,TEST,MDIAG,NBF,NUMPC,ITER,NBF2,NSCALE,NPUNCH,NPRINT,
     2  NCHECK,ACFINI
      COMMON /WALL/ THETA,FT,TANTH
      COMMON /STFMAT/ P(9,9),H(9)
      DIMENSION ALANDA(1)
      DIMENSION R(1),Z(1),CODE(1),UR(1),UZ(1),IEL( NEL ,1),P(1),A( NO,1)
     1,EPS(5,1),STS(6,1),NF(1),FST( NB2 ,1),FPUR(1),IJBC( NPC ,1),
     2 PSBC(NPC,1),RR(4),ZZ(4),IXY(9),UU(8),YY(1),ID(2)
C
C ***********************************************************************
C INITIALIZED A AND B MATRICES (FOR EQUATION AX=B)
C BECAUSE BANDED SYMMETRIC PROPERTY OF THE STIFFNESS MATRIX A, THE
C STORAGE OF A IS IN A SQURE ARRAY.
C ***********************************************************************
C
      NSTOP=0
      DO 50 N=1, NEQ
      B(N)=0.
      DO 50 M=1, MBAND
   50 A(N,M)=0.
C
C ***********************************************************************
C CONSTRUCT ELEMENT LEVEL MATRICES FOR STIFFNESS
C IF ITERNO.GT.1 MEANS SUBROUTINE QUAD1 HAS BEEN PERFOMED ONCE BEFORE
C AND IS STORED IN TAPE 1.
C ***********************************************************************
C
      IF(ITERNO.GT.1) GO TO 20
      REWIND 1
      DO 510 N=1,NUMEL
      DO 100 I=1,4
      II=IEL(N,I)
      RR(I)=R(II)
  100 ZZ(I)=Z(II)
      CALL QUAD1(RR,ZZ,VOL)
   42 IF(VOL.GT.0.) GO TO 510
      WRITE(6,1005) N
      NSTOP=1
  510 CONTINUE
   20 REWIND 1
      IF(NSTOP .EQ. 1) STOP
C
C ***********************************************************************
C CONSTRUCT P AND H MATRICES AT ELEMENT LEVEL.
C ***********************************************************************
C
      DO 1000 N=1, NUMEL
      DO 60 I=1,4
      II=IEL(N,I)
      I2=2*I
      I1=I2-1
      IXY(I1)=3*II-2
      IXY(I2)=3*II-1
      UU(I2)=UZ(II)
   60 UU(I1)=UR(II)
      II=MAX0(IEL(N,1),IEL(N,2),IEL(N,3),IEL(N,4))
      IXY(9)=3*II
      CALL QUAD2(UU,IPLNAX,TEX,TEY,TEZ,TEXY)
```

```
C
C ***************************************************************************
C NWKHRD IS AN INDEX TO INDICATE WHETHER ONLY STRAIN RATE CALCULATION IS
C REQUIRED OR THE WHOLE STIFFNESS MATRIX NEED TO BE CONSTRUCTED.
C ***************************************************************************
C
      IF(NWKHRD.EQ.1) GO TO 201
C
C ***************************************************************************
C PERFORM THE ASSEMBLY OPERATION. BECAUSE MATRIX A IS SYMMETRIC, ONLY
C UPPER HALF OF THE MATRIX IS CREATED. AND THE STORAGE FOR MATRIX A IS
C A SQUARE ARRAY BECAUSE OF BANDED SYMMETRIC PROPERTY.
C ***************************************************************************
C
      DO 62 I=1,8
      H(I)=H(I)*YY(N)
      DO 62 J=1,8
   62 P(I,J)=P(I,J)*YY(N)
      DO 200 I=1, 9
      II=IXY(I)
      B(II)=B(II)-H(I)
      DO 200 J=1, 9
      JJ=IXY(J)-II+1
      IF(JJ .LT. 1) GO TO 200
      A(II,JJ)=A(II,JJ)+P(I,J)
  200 CONTINUE
  201 CONTINUE
      EPS(1,N)=TEX
      EPS(2,N)=TEY
      EPS(3,N)=TEZ
      EPS(4,N)=TEXY
 1000 CONTINUE
  563 DO 150 N=1,NUMEL
  150 EPS(5,N)=RBAR(EPS(1,N),EPS(2,N),EPS(3,N),EPS(4,N))
      IF(NWKHRD.EQ.1) RETURN
C
C ***************************************************************************
C     PREPARATION FOR FORCE CALCULATION
C ***************************************************************************
C
      IF(NBF .LE. 0) GO TO 402
      MBAND2=2*MBAND-1
      DO 330 I=1, NBF
      IZ=2*I
      IR=IZ-1
      DO 330 J=1, MBAND2
      FST(IR,J)=0.
  330 FST(IZ,J)=0.
      DO 400 I=1, NBF
      II=NF(I)
      IZ=3*II-1
      IR=IZ-1
      IIZ=2*I
      IIR=IIZ-1
      DO 401 J=MBAND, MBAND2
      JJ=J-MBAND+1
      FST(IIR,J)=A(IR,JJ)
  401 FST(IIZ,J)=A(IZ,JJ)
      DO 403 J=1, MBAND
      NR=IR-J+1
      NZ=IZ-J+1
      JJ=MBAND-J+1
      IF(NR .LE. 0) GO TO 404
      FST(IIR,JJ)=A(NR,J)
  404 IF(NZ .LE. 0) GO TO 403
      FST(IIZ,JJ)=A(NZ,J)
  403 CONTINUE
      FPUR(IIR)=B(IR)
  400 FPUR(IIZ)=B(IZ)
  402 CONTINUE
C
C ***************************************************************************
C ADD PRESSURE BOUNDARY CONDITION. (FOR CONSTANT FRICTIONAL STRESS DIES.
C THE SHEAR TRACTIONAL STRESS (FRICTIONAL STRESS) IS ADDING HERE).
C ***************************************************************************
C
      IF ( NUMPC .EQ. 0 ) GO TO 410
      ID(1)=2
      ID(2)=1
      RI=1.0
      RJ=1.0
      DO 420 L=1,NUMPC
      I=IJBC(L,1)
      J=IJBC(L,2)
      DR=R(I)-R(J)
      DZ=Z(I)-Z(J)
```

```
      DO 290 M=1,2
      N=ID(M)
      I=IJBC(L,M)
      J=IJBC(L,N)
      RI=R(I)
      RJ=R(J)
      I2=3*I-1
      I1=I2-1
      PI=PSBC(L,M)
      PJ=PSBC(L,N)
      SI=PSBC(L,M+2)
      SJ=PSBC(L,N+2)
      PM=(RI*(3.0*PI+PJ)+RJ*(PI+PJ))/12.0
      SM=(RI*(3.0*SI+SJ)+RJ*(SI+SJ))/12.0
      R1=DZ*PM+DR*SM
      R2=-DR*PM+DZ*SM
      B(I1)=B(I1)+R1
      B(I2)=B(I2)+R2
  290 CONTINUE
  420 CONTINUE
  410 CONTINUE
C
 1005 FORMAT(// 29H ELEMENT WITH NEGATIVE AREA =, I5)
C
      RETURN
      END
```

```
      SUBROUTINE QUAD1(RR,ZZ,VOL)
C
C ***********************************************************************
C CONSTRUCT B MATRIX AND K MATRIX (K=(TRANPOSE(B))(D)(B)), AND Q VECTOR
C AT ELEMENT LEVEL FOR ALL ELEMENTS AND WRITE THESE MATRIX ON TAPE 1.
C ***********************************************************************
C
      COMMON /QUAD/ B(4,8),XX(8,8),Q(8)
      DIMENSION RR(4),ZZ(4),SS(4),TT(4)
      DATA SS/-1.,+1.,+1.,-1./, TT/-1.,-1.,+1.,+1./
      SQRT2=1.414213562373092
      DO 1 I=1,8
      Q(I)=0.
      DO 1 J=1,4
    1 B(J,I)=0.
      R1=RR(1)
      R2=RR(2)
      R3=RR(3)
      R4=RR(4)
      Z1=ZZ(1)
      Z2=ZZ(2)
      Z3=ZZ(3)
      Z4=ZZ(4)
      R12=R1-R2
      R13=R1-R3
      R14=R1-R4
      R23=R2-R3
      R24=R2-R4
      R34=R3-R4
      Z12=Z1-Z2
      Z13=Z1-Z3
      Z14=Z1-Z4
      Z23=Z2-Z3
      Z24=Z2-Z4
      Z34=Z3-Z4
      VOL=R13*Z24-R24*Z13
      IF(VOL.LE.0.) RETURN
C
C ***********************************************************************
C CALCULATION OF TOTAL VOLUME PER RADIAN OF THE ELEMENT.
C ***********************************************************************
C
      VOL1=(Z1-Z4)*(R1*R1+R4*R4+R1*R4)
      VOL2=(Z3-Z2)*(R3*R3+R2*R2+R3*R2)
      VOL3=(Z2-Z1)*(R1*R1+R2*R2+R1*R2)
      VOL4=(Z4-Z3)*(R3*R3+R4*R4+R3*R4)
      VOLL=(VOL1+VOL2+VOL3+VCL4)/6.
C
C ***********************************************************************
C THE FOLLOWING CONSTRUCT B AND K MATRIX BY TAKING FOUR INTEGRATION
C POINTS OF THE ELEMENT.
C ***********************************************************************
C
```

```
      DO 15 II=1,4
      S=SS(II)*0.577350269189626
      T=TT(II)*0.577350269189626
      XJ8=VOL+S*(R34*Z12-R12*Z34)+T*(R23*Z14-R14*Z23)
      XJ=XJ8/8.
C
      SMM=1.-S
      SP=1.+S
      TM=1.-T
      TP=1.+T
      H1=0.25*SMM*TM
      H2=0.25*SP*TM
      H3=0.25*SP*TP
      H4=0.25*SMM*TP
      R=H1*R1+H2*R2+H3*R3+H4*R4
      G1=H1/R
      G2=H2/R
      G3=H3/R
      G4=H4/R
C
C ***********************************************************************
C CONSTRUCT B MATRIX AT EACH POINT
C ***********************************************************************
C
      X1=(-R24+R34*S+R23*T)/XJ8
      X2=(R13-R34*S-R14*T)/XJ8
      X3=(R24-R12*S+R14*T)/XJ8
      X4=(-R13+R12*S-R23*T)/XJ8
      Y1=(Z24-Z34*S-Z23*T)/XJ8
      Y2=(-Z13+Z34*S+Z14*T)/XJ8
      Y3=(-Z24+Z12*S-Z14*T)/XJ8
      Y4=(Z13-Z12*S+Z23*T)/XJ8
      B(1, 1)=Y1
      B(1, 3)=Y2
      B(1, 5)=Y3
      B(1, 7)=Y4
      B(2, 2)=X1
      B(2, 4)=X2
      B(2, 6)=X3
      B(2, 8)=X4
      B(3, 1)=G1
      B(3, 3)=G2
      B(3, 5)=G3
      B(3, 7)=G4
      B(4, 1)=X1/SQRT2
      B(4, 2)=Y1/SQRT2
      B(4, 3)=X2/SQRT2
      B(4, 4)=Y2/SQRT2
      B(4, 5)=X3/SQRT2
      B(4, 6)=Y3/SQRT2
      B(4, 7)=X4/SQRT2
      B(4, 8)=Y4/SQRT2
C
C ***********************************************************************
C CONSTRUCT K MATRIX AT EACH POINT (IE. XX(I,J))
C ***********************************************************************
C
      DO 6 I=1,8
      DO 6 J=I,8
      DUM1=0.
      DO 5 K=1,4
    5 DUM1=DUM1+B(K,J)*B(K,I)
      XX(I,J)=DUM1
      XX(J,I)=DUM1
    6 CONTINUE
C
C ***********************************************************************
C  CONSTRUCT Q VECTOR AT EACH POINT, AND ADD ALL FOUR INTEGRATION POINTS
C ***********************************************************************
C
      XJR=XJ*R
      Q(1)=Q(1)+(Y1+G1)*XJ*R
      Q(2)=Q(2)+    X1   *XJ*R
      Q(3)=Q(3)+(Y2+G2)*XJ*R
      Q(4)=Q(4)+    X2   *XJ*R
      Q(5)=Q(5)+(Y3+G3)*XJ*R
      Q(6)=Q(6)+    X3   *XJ*R
      Q(7)=Q(7)+(Y4+G4)*XJ*R
      Q(8)=Q(8)+    X4   *XJ*R
C
C ***********************************************************************
C WRITE K AND B MATRICES AT EACH INTEGRATION POINT ON TAPE 1
C ***********************************************************************
C
```

```
      WRITE(1) XJR
      WRITE(1)((XX(I,J),J=1,8 ),I=1,8 )
      WRITE(1)((B(I,J),J=1,8 ),I=1,4)
   16 CONTINUE
C
C ********************************************************************
C WRITE Q VECTOR (AFTER INTEGRATION, I.E. ADDING FOUR POINTS) AND THE
C TOTAL VOLUMN OF THE ELEMENT ON TAPE 1.
C ********************************************************************
C
      WRITE(1)(Q(I),I=1,8)
      VOL=VOLL
      WRITE(1) VOL
C
      RETURN
      END


      SUBROUTINE QUAD2(UU,IPLNAX,TEX,TEY,TEZ,TEXY)
C
C ********************************************************************
C READ INFORMATION FROM TAPE1 REGARDING B, K AND Q, AND CONSTRUCT P AND
C H MATRICES AT ELEMENT LEVEL (I.E.P(I,J) AND H(I))
C ********************************************************************
C
      COMMON /QUAD/ B(4,8),XX(8,8),BZERO(8)
      COMMON /STFMAT/ P(9,9),H(9)
      DIMENSION E(4),UU(8)
      DO 1 I=1,9
      H(I)=0.
      DO 1 J=I,9
    1 P(I,J)  =  0.
      SQRT2  =  1.414213562373092
      SQRT1  =  1.224744871391586
C
C ********************************************************************
C TEX= R-STRAIN RATE
C TEY= Z-STRAIN RATE
C TEZ= TH-STRAIN RATE
C TEXY= RZ-STRAIN RATE
C ********************************************************************
C
      TEX  =  0.
      TEY  =  0.
      TEZ  =  0.
      TEXY=0.
      DO 16 II=1,4
      READ(1)XJR
      READ(1)((XX(I,J),J=1,8 ),I=1,8 )
      READ(1) ((B(I,J),J=1,8 ),I=1,4)
      DO 8 I=1,8
      DUM1=0.
      DO 7 J=1,8
    7 DUM1=DUM1+XX(I,J)*UU(J)
    8 BZERO(I)=DUM1
      PZERO=0.
      DO 9 I=1,8
    9 PZERO=PZERO+UU(I)*BZERO(I)
C
C ********************************************************************
C PZERO=(3/2) * SQUARE OF (EFF. STRINT RATE).
C IF PZERO IS TOO SMALL CORRESPONDING TO RIGID ELEMENT, SET PZERO AS A
C LIMITING VALUE IN ORDER NOT TO BREAK THE STIFFNESS MATRIX
C P1=(2/3)/(SQUARE OF (EFFECTIVE STRAIN RATE))
C P2=(2/3)/(EFFECTIVE STRAIN RATE)
C ********************************************************************
C
      IF(PZERO.LE.1.E-08) PZERO=1.E-08
      P1=1./PZERO
      PZERO=SQRT(PZERO)
      P2=PZERO*SQRT1
      DO 13 I=1,8
      DO 12 J=I,8
   12 P(I,J)=P(I,J)+(XX(I,J)-P1*BZERO(I)*BZERO(J))*XJR/P2
   13 H(I)=H(I)+BZERO(I)*XJR/P2
      DO 14 I=1,4
      E(I)=0.
      DO 14 J=1,8
   14 E(I)=E(I)+B(I,J)*UU(J)
      TEX=TEX+E(1)*XJR
      TEY=TEY+E(2)*XJR
      TEZ=TEZ+E(3)*XJR
      TEXY=TEXY+E(4)*SQRT2*XJR
   16 CONTINUE
```

```
C
      READ(1)(P(J,9 ),J=1,8 )
      DO 17 J=1,8
   17 H(9 )=H(9 )+P(J,9 )*UU(J)
      READ (1) VOL
      DO 18 I=1,9
      DO 18 J=I,9
   18 P(J,I)=P(I,J)
      TEX=TEX/VOL
      TEY=TEY/VOL
      TEZ=TEZ/VOL
      TEXY=TEXY/VOL
C
      RETURN
      END
```

```
      FUNCTION RBAR (RX,RY,RZ,RXY)
C
C ****************************************************************************
C CALCULATE THE EFFECTIVE STRAIN RATE
C ****************************************************************************
C
      RBAR=(RX-RY)**2+(RY-RZ)**2+(RZ-RX)**2
      RBAR=2.*SQRT(0.5*RBAR+3.*RXY**2/4.)/3.
C
C ****************************************************************************
C IF THE EFFECTIVE STRAIN RATE IS TOO SMALL CORRESPONDING TO A RIGID
C ELEMENT, SET IT TO A LIMITING VALUE.
C ****************************************************************************
C
      IF(RBAR.LT.1.E-04) RBAR=1.E-04
      RETURN
      END
```

```
      FUNCTION EFSTRS(SR,SZ,ST,SRZ)
C
C ****************************************************************************
C CALCULATION OF EFFECTIVE STRESS.
C ****************************************************************************
C
      EFSTRS=(SR-SZ)**2+(SZ-ST)**2+(ST-SR)**2
      EFSTRS=SQRT(0.5*EFSTRS+3.*SRZ**2)
      RETURN
      END
```

```
      SUBROUTINE MODIFY (CODE,A,B,NUMNP,NEQ,MBAND)
C
C ****************************************************************************
C  DETERMINE THE POINTS FOR WHICH CORRESPONDING COMPONENT OF X IS
C  SPECIFIED EQUAL TO ZERO IN AX=B, AND CALL CONDEN FOR MATRIX
C  CONDENSATION
C ****************************************************************************
C
      COMMON /WALL/ THETA,FT,TANTH
      DIMENSION CODE(1),A(NEQ,1),B(1)
      DO 121 I=1, NUMNP
      IL=3*I
      IZ=IL-1
      IR=IZ-1
      C=CODE(I)
C
C ****************************************************************************
C  CHECK IF THIS POINT CONTAINS NO INFORMATION ABOUT MEAN STRESS
C ****************************************************************************
C
      IF(C.LT.10.) CALL CONDEN(A,B,NEQ,MBAND,IL,0.)
C
C ****************************************************************************
C  CHECK IF THE R-VELOCITY IS SPECIFIED
C ****************************************************************************
C
      IF(C.EQ.1..OR.C.EQ.11..OR.C.EQ.3..OR.C.EQ.13.)
     1 CALL CONDEN(A,B,NEQ,MBAND,IR,0.)
```

```
C
C ***********************************************************************
C  CHECK IF THE Z-VELOCITY IS SPECIFIED
C ***********************************************************************
C
      IF (C.EQ.2..OR.C.EQ.12..OR.C.EQ.3..OR.C.EQ.13.)
     1  CALL CONDEN(A,B,NEQ,MBAND,IZ,0.)
C
C ***********************************************************************
C  CHECK IF THE POINT IS ALONG THE INCLINED BOUNDARY
C ***********************************************************************
C
      IF(C.EQ.5..OR.C.EQ.15.) CALL BCMIX(A,B,NEQ,MBAND,I,THETA)
  121 CONTINUE
C
      RETURN
      END
```

```
      SUBROUTINE CONDEN(A,B,NEQ,MBAND,N,U)
C
C ***********************************************************************
C PERFORM THE MATRIX CONDENSATION WHEN THE VALUE OF A COMPONENT X IN
C AX=B IS SPECIFIED EQUAL TO ZERO.
C ***********************************************************************
C
      DIMENSION B(NEQ),A(NEQ,1)
      DO 235 M=2,MBAND
      K=N-M+1
      IF(K) 235,235,230
  230 A(K,M)=0.0
  235 A(N,M)=0.0
      A(N,1)=1.0
      B(N)=U
      RETURN
      END
```

```
      SUBROUTINE BCMIX(A,B,NEQ,MBAND,N,THETA)
C
C ***********************************************************************
C  THIS SUBROUTINE IS TO ENSURE THAT THE VELOCITY ALONG THE DIE IS
C  TANGENTIAL TO THE DIE FOR CONICAL DIES
C ***********************************************************************
C
      DIMENSION B(NEQ),A(NEQ,1)
C
C ***********************************************************************
C  SINCE UR=UZ*TAN(THETA) ALONG THE DIE, A CORRESPONDING CHANGE IS MADE
C  IN THE STIFFNESS EQUATIONS FOR ROWS AND COLUMNS CORRESPONDING TO
C  THESE COMPONENTS...THEN THE EQUATIONS CONTAINING UR ARE ELIMINATED
C ***********************************************************************
C
      NZ=3*N-1
      NR=NZ-1
      ALPA= TAN(THETA)
      DO 350 M=1,MBAND
  350 A(NR,M)=A(NR,M)*ALPA
      A(NR,1)=A(NR,1)*ALPA
      A(NR,2)=A(NR,2)*2.
      DO 340 M=2,MBAND
      KR=NR-M+1
      IF(KR.LE.0) GO TO 341
  340 A(KR,M)=A(KR,M)*ALPA
  341 CONTINUE
      B(NR) = B(NR)*ALPA
      DO 351 M=2,MBAND
      KZ=NZ-M+1
      IF(KZ.LE.0) GO TO 352
      A(KZ,M)=A(KZ,M)+A(KZ,M-1)
  352 CONTINUE
      IF(M.EQ.MBAND) GO TO 353
      KZ=NZ+M-1
      IF(KZ.GT.NEQ) GO TO 353
      A(NZ,M)=A(NZ,M)+A(NR,M+1)
  353 CONTINUE
  351 CONTINUE
      A(NZ,1)=A(NZ,1)+A(NR,2)
      A(NR,1)=1.0
```

```
      DO 355 M=2,MBAND
      KR=NR-M+1
      IF(KR.LE.0) GO TO 360
      A(KR,M)=0.0
  360 CONTINUE
      A(NR,M)=0.0
  355 CONTINUE
      B(NZ)=B(NR)+B(NZ)
      B(NR)=0.0
C
      RETURN
      END
```

```
      SUBROUTINE TRIA(NN,MM,A)
C
C ****************************************************************************
C TRIANGULARIZATION OF GUASSIAN ELIMINATION FOR THE SOLUTION OF BANDED
C SYMMETRIC MATRIX.
C ****************************************************************************
C
      DIMENSION A(NN,1)
 1000 N=0
  100 N=N+1
      IF(N.EQ.NN)RETURN
      IF(A(N,1).EQ.0.0)GO TO 100
      I=N
      MB=MIN0(MM,NN-N+1)
      DO 260 L=2,MB
      I=I+1
      C=A(N,L)/A(N,1)
      IF(C.EQ.0.0)GO TO 260
      J=0
      DO 250 K=L,MB
      J=J+1
  250 A(I,J)=A(I,J)-C*A(N,K)
      A(N,L)=C
  260 CONTINUE
      GO TO 100
      END
```

```
      SUBROUTINE BACKS(NN,MM,A,B)
C
C ****************************************************************************
C BACK SUBSTITUTION FOR SOLUTION OF BANDED SYMMETRIC MATRIX
C ****************************************************************************
C
      DIMENSION A(1),B(1)
      MMM=MM-1
      N=0
  270 N=N+1
      C=B(N)
      IF(A(N).NE.0.0)B(N)=B(N)/A(N)
      IF(N.EQ.NN)GO TO 300
      IL=N+1
      IH=MIN0(NN,N+MMM)
      M=N
      DO 285 I=IL,IH
      M=M+NN
  285 B(I)=B(I)-A(M)*C
      GO TO 270
  300 IL=N
      N=N-1
      IF(N.EQ.0) RETURN
      IH=MIN0(NN,N+MMM)
      M=N
      DO 400 I=IL,IH
      M=M+NN
  400 B(N)=B(N)-A(M)*B(I)
      GO TO 300
C
      END
```

```
      SUBROUTINE CFORCE(NF,FR,FZ,FST,FPUR,B,MBAND,NBF,NBF2)
C
C ********************************************************************
C CALCULATION OF FORCES ON BOUNDARY NODAL POINTS
C ********************************************************************
C
      DIMENSION NF(1),FST(NBF2,1),FPUR(NBF2),FR(1),FZ(1),B(1)
      IF(NBF .LE. 0) GO TO 124
      MBAND2=2*MBAND-1
      DO 121 I=1, NBF
      IZ=3*NF(I)-1
      IR=IZ-1
      IIZ=2*I
      IIR=IIZ-1
      SUMR=0.
      SUMZ=0.
      DO 122 J=1, MBAND2
      JR=IR+J-MBAND
      JZ=JR+1
      IF(JR .LE. 0) GO TO 126
      SUMR=SUMR+FST(IIR,J)*B(JR)
  126 IF(JZ .LE. 0) GO TO 122
      SUMZ=SUMZ+FST(IIZ,J)*B(JZ)
  122 CONTINUE
      FR(I)=SUMR-FPUR(IIR)
  121 FZ(I)=SUMZ-FPUR(IIZ)
  124 CONTINUE
      RETURN
      END

      SUBROUTINE INTRPOL (X,Y,U,XX,YY,UU,IFLAG)
C
C ********************************************************************
C  INTERPOLATE THE VALUE OF UU AT COORDINATES (XX,YY) BY KNOWING THE
C  VALUES OF U AT FOUR SURROUNDING POINTS.
C ********************************************************************
C
      DIMENSION X(4),Y(4),U(4),A(4,4),COEF(4)
C
C ********************************************************************
C  DETERMINE THE MATRIX A, THE INVERSE OF THE INTERPOLATION MATRIX...
C  IF IFLAG=1, THE A MATRIX IS ALREADY KNOWN
C ********************************************************************
C
      IF(IFLAG.EQ.1) GO TO 100
      X1=X(1)
      X2=X(2)
      X3=X(3)
      X4=X(4)
      Y1=Y(1)
      Y2=Y(2)
      Y3=Y(3)
      Y4=Y(4)
      X12=X1-X2
      X13=X1-X3
      X14=X1-X4
      X23=X2-X3
      X24=X2-X4
      X34=X3-X4
      Y12=Y1*Y2*X12
      Y13=Y1*Y3*X13
      Y14=Y1*Y4*X14
      Y23=Y2*Y3*X23
      Y24=Y2*Y4*X24
      Y34=Y3*Y4*X34
      A(1,1)=+X2*Y34-X3*Y24+X4*Y23
      A(1,2)=-X1*Y34+X3*Y14-X4*Y13
      A(1,3)=+X1*Y24-X2*Y14+X4*Y12
      A(1,4)=-X1*Y23+X2*Y13-X3*Y12
      A(2,1)=-Y23+Y24-Y34
      A(2,2)=+Y13-Y14+Y34
      A(2,3)=-Y12+Y14-Y24
      A(2,4)=+Y12-Y13+Y23
      Z11=Y1*X23
      Z12=Y1*X24
      Z13=Y1*X34
      Z21=Y2*X13
      Z22=Y2*X14
      Z23=Y2*X34
      Z31=Y3*X12
      Z32=Y3*X14
      Z33=Y3*X24
      Z41=Y4*X12
      Z42=Y4*X13
      Z43=Y4*X23
```

```
      A(3,1)=+X2*Z23-X3*Z33+X4*Z43
      A(3,2)=-X1*Z13+X3*Z32-X4*Z42
      A(3,3)=+X1*Z12-X2*Z22+X4*Z41
      A(3,4)=-X1*Z11+X2*Z21-X3*Z31
      A(4,1)=-Z23+Z33-Z43
      A(4,2)=+Z13-Z32+Z42
      A(4,3)=-Z12+Z22-Z41
      A(4,4)=+Z11-Z21+Z31
      DETER=A(1,1)+A(1,2)+A(1,3)+A(1,4)
  100 CONTINUE
      IFLAG=0
      IF(DETER.EQ.0.) GO TO 150
      DO 130 J=1,4
      COEF(J)=0.
      DO 120 I=1,4
  120 COEF(J)=COEF(J)+A(J,I)*U(I)
  130 COEF(J)=COEF(J)/DETER
      UU=COEF(1)+COEF(2)*XX+COEF(3)*YY+COEF(4)*XX*YY
      RETURN
  150 UU=(U(1)*(YY-Y(2))+U(2)*(Y(1)-YY))/(Y(1)-Y(2))
      RETURN
      END


      SUBROUTINE STRAINS (R,Z,UR,UZ,IEL,EPS,TEPS,STR,X,Y,XARB,U,V,XX,YY,
     1  A,B,AA,BB,C,EE,NI,NJ,NTIMES,NEL,NNP,NMAX)
C
C ******************************************************************
C  SUBROUTINE FOR DETERMINATION OF FLOW PATTERN, NETWORK OF GRID
C  DISTORTIONS, THE EFFECTIVE STRAIN DISTRIBUTION AND THE VALUES OF
C  EFFECTIVE STRAIN FOR EACH ELEMENT.
C ******************************************************************
C
      DIMENSION R(1),Z(1),UR(1),UZ(1),IEL(NEL,1),EPS(5,1),TEPS(5,1),
     1  STR(NI,1),X(NI,1),Y(1),XARB(1),U(NI,1),V(NI,1),XX(NTIMES,1),
     2  YY(NTIMES,1),A(1),B(1),AA(NI,1),BB(1),C(1),EE(NTIMES,1)
      DIMENSION RR(4),ZZ(4),URR(4),UZZ(4)
      COMMON /STRPATH/ STEP,YSTART,YDIE,YEXIT,YMIN,RENTER,REXIT,VEXIT
      COMMON /WALL/ THETA,FT,TANTH
      NIM1=NI-1
      NJM1=NJ-1
C
C ******************************************************************
C  FIRST ARRANGE THE AVAILABLE INFORMATION IN PROPER FORM
C ******************************************************************
C
      K=1
      L=0
  100 L=L+1
      Y(L)=Z(K)
      DO 110 I=1,NIM1
      X(I,L)=R(K)
      U(I,L)=UR(K)
      V(I,L)=UZ(K)
  110 K=K+1
      X(NI,L)=X(NIM1,L)
      U(NI,L)=U(NIM1,L)
      V(NI,L)=V(NIM1,L)
      IF (K.GE.NNP) 150,100
C
C ******************************************************************
C  DETERMINE THE COORDINATES OF THE CENTERS OF THE ELEMENTS
C ******************************************************************
C
  150 DO 160 N=1,NEL
      I1=IEL(N,1)
      I2=IEL(N,2)
      I3=IEL(N,3)
      I4=IEL(N,4)
      A(N)=(R(I1)+R(I2)+R(I3)+R(I4))/4.
  160 B(N)=(Z(I1)+Z(I2)+Z(I3)+Z(I4))/4.
C
C ******************************************************************
C  ARRANGE THE NEWLY DETERMINED VALUES IN A PROPER FORM
C ******************************************************************
C
      K=1
      L=0
  165 L=L+1
      BB(L)=B(K)
      AA(1,L)=0.
      STR(1,L)=EPS(5,K)
      DO 170 I=2,NIM1
      AA(I,L)=A(K)
      STR(I,L)=EPS(5,K)
```

```
  170 K=K+1
      AA(NI,L)=REXIT+BB(L)*TANTH
      IF(BB(L).GT.VDIE) AA(NI,L)=1.
      IF(BB(L).LT.VEXIT) AA(NI,L)=REXIT
      STR(NI,L)=EPS(5,K-1)
      IF(K.LT.NEL) GO TO 165
C
C *********************************************************************
C  NOW DO THE INTERPOLATION AND DETERMINE THE FLOW PATTERN
C *********************************************************************
C
      DO 500 N=1,NTIMES
C
C *********************************************************************
C  SET THE COORDINATES OF THE STARTING POINT
C *********************************************************************
C
      XX(N,1)=C(N)
      YY(N,1)=YSTART
C
C *********************************************************************
C  DETERMINE THE LOCATION OF THE PRESENT COORDINATES OF THE POINT IN
C  TERMS OF THE FOUR SURROUNDING NODAL POINTS
C *********************************************************************
C
      IFLAG=0
      NCOUNT=0
      MOLD=1
      LOLD=1
  210 NCOUNT=NCOUNT+1
      XXX=XX(N,NCOUNT)
      YYY=YY(N,NCOUNT)
      IF(N.EQ.NTIMES.AND.YYY.LE.YEXIT) GO TO 300
      IF(YYY.LE.YMIN) GO TO 300
      DO 220 I=MOLD,NJM1
  220 IF(YYY.LE.Y(I).AND.YYY.GE.Y(I+1)) M=I
      DO 230 I=1,NI
  230 XARB(I)=X(I,M)-(X(I,M)-X(I,M+1))*(Y(M)-YYY)/(Y(M)-Y(M+1))
      DO 240 I=1,NIM1
  240 IF(XXX.GE.XARB(I).AND.XXX.LE.XARB(I+1)) L=I
      IF(NCOUNT.EQ.1) GO TO 250
      IF(M.EQ.MOLD.AND.L.EQ.LOLD) GO TO 260
  250 RR(1)=X(L,M)
      RR(2)=X(L,M+1)
      RR(3)=X(L+1,M+1)
      RR(4)=X(L+1,M)
      ZZ(1)=ZZ(4)=Y(M)
      ZZ(2)=ZZ(3)=Y(M+1)
      URR(1)=U(L,M)
      URR(2)=U(L,M+1)
      URR(3)=U(L+1,M+1)
      URR(4)=U(L+1,M)
      UZZ(1)=V(L,M)
      UZZ(2)=V(L,M+1)
      UZZ(3)=V(L+1,M+1)
      UZZ(4)=V(L+1,M)
      GO TO 270
C
C *********************************************************************
C  THE POINT IS LOCATED IN THE SAME ELEMENT AS IT WAS FOR THE LAST STEP.
C  HENCE THE INVERSE OF THE INTERPOLATION MATRIX IS ALREADY KNOWN
C *********************************************************************
C
  260 IFLAG=1
C
C *********************************************************************
C  DETERMINE U AND V AT THE POINT ON FLOW LINE BY INTERPOLATION.
C *********************************************************************
C
  270 CALL INTRPOL(RR,ZZ,URR,XXX,YYY,UU,IFLAG)
      IFLAG=1
      CALL INTRPOL(RR,ZZ,UZZ,XXX,YYY,VV,IFLAG)
C
C *********************************************************************
C  DETERMINE THE NEXT LOCATION OF POINT ON FLOW LINE
C *********************************************************************
C
      XX(N,NCOUNT+1)=XXX+UU*STEP
      YY(N,NCOUNT+1)=YYY+VV*STEP
      LOLD=L
      MOLD=M
      IF(N.NE.NTIMES) GO TO 310
      XXX=REXIT+YY(N,NCOUNT+1)*TANTH
      IF(XXX.LT.XX(N,NCOUNT+1)) XX(N,NCOUNT+1)=XXX
      IF(XX(N,NCOUNT+1).GT.1.) XX(N,NCOUNT+1)=1.
      GO TO 310
```

```
C
C ***********************************************************************
C  THE POINT IS MOVING WITH EXIT VELOCITY
C ***********************************************************************
C
  300 XX(N,NCOUNT+1)=XXX
      YY(N,NCOUNT+1)=YYY+VEXIT*STEP
  310 IF(NCOUNT.LT.NMAX-1) GO TO 210
C
C ***********************************************************************
C  DETERMINE THE VALUES OF EFFECTIVE STRAIN AT EACH POINT FOR ALL FLOW
C  LINES
C ***********************************************************************
C
      NCOUNT=0
      EE(N,1)=0.
      MOLD=LOLD=1
  400 NCOUNT=NCOUNT+1
      YYY=YY(N,NCOUNT)
      XXX=XX(N,NCOUNT)
      IF(YYY.LE.VEXIT) GO TO 480
C
C ***********************************************************************
C  DETERMINE THE LOCATION OF FOUR SURROUNDING ELEMENT CENTERS.
C ***********************************************************************
C
      NJM11=NJM1-1
      DO 410 I=MOLD,NJM11
  410 IF(YYY.LE.BB(I).AND.YYY.GE.BB(I+1)) M=I
      DO 420 I=1,NI
  420 XARB(I)=AA(I,M)-(AA(I,M)-AA(I,M+1))*(BB(M)-YYY)/(BB(M)-BB(M+1))
      DO 430 I=1,NIM1
  430 IF(XXX.GE.XARB(I).AND.XXX.LE.XARB(I+1)) L=I
      IF(NCOUNT.EQ.1) GO TO 450
      IF(M.EQ.MOLD.AND.L.EQ.LOLD) GO TO 460
C
C ***********************************************************************
C  INTERPOLATE THE VALUES OF STRAIN-RATES.
C ***********************************************************************
C
  450 RR(1)=AA(L,M)
      RR(2)=AA(L,M+1)
      RR(3)=AA(L+1,M+1)
      RR(4)=AA(L+1,M)
      ZZ(1)=ZZ(4)=BB(M)
      ZZ(2)=ZZ(3)=BB(M+1)
      URR(1)=STR(L,M)
      URR(2)=STR(L,M+1)
      URR(3)=STR(L+1,M+1)
      URR(4)=STR(L+1,M)
      GO TO 470
  460 IFLAG=1
  470 CALL INTRPOL(RR,ZZ,URR,XXX,YYY,ESTEP,IFLAG)
C
C ***********************************************************************
C  ADD THE INTERPOLATED STRAIN-RATE INCREMENTALLY TO THE VALUE OF
C  EFFECTIVE STRAIN AT PREVIOUS LOCATION TO DETERMINE THE EFFECTIVE
C  STRAIN AT NEW LOCATION.
C ***********************************************************************
C
      EE(N,NCOUNT+1)=EE(N,NCOUNT)+ESTEP*STEP
      LOLD=L
      MOLD=M
      GO TO 490
  480 EE(N,NCOUNT+1)=EE(N,NCOUNT)
  490 IF(NCOUNT.LT.NMAX-1) GO TO 400
  500 CONTINUE
C
C ***********************************************************************
C  INTERPOLATE THE EFFECTIVE STRAIN DISTRIBUTION FOR ELEMENTS FROM VALUE
C  OF EFFECTIVE STRAINS ALONG FLOW LINES.
C ***********************************************************************
C
      DO 700 N=1,NEL
      IF(B(N).GT.YY(1,1)) GO TO 550
      DO 550 J=2,NTIMES
      DO 520 I=1,NMAX
      IF(B(N).LT.YY(J,I)) GO TO 520
      L=I
      GO TO 530
  520 CONTINUE
  530 IF(XX(J,L).LT.A(N)) GO TO 550
      K=J
      GO TO 540
  550 CONTINUE
```

```
  560 IFLAG=0
      RR(1)=XX(K-1,L)
      RR(2)=XX(K-1,L-1)
      RR(3)=XX(K,L-1)
      RR(4)=XX(K,L)
      ZZ(1)=YY(K-1,L)
      ZZ(2)=YY(K-1,L-1)
      ZZ(3)=YY(K,L-1)
      ZZ(4)=YY(K,L)
      URR(1)=EE(K-1,L)
      URR(2)=EE(K-1,L-1)
      URR(3)=EE(K,L-1)
      URR(4)=EE(K,L)
      CALL INTRPOL (RR,ZZ,URR,A(N),B(N),TEPS(5,N),IFLAG)
      GO TO 700
  650 TEPS(5,N)=0.
  700 CONTINUE
C
      RETURN
      END
```


★U.S.Government Printing Office: 1977 — 757-080/204